Characterization of CDK14-18 as therapeutic targets in hepatocellular carcinoma

DIEGO MARTÍNEZ ALONSO

Universidad Autónoma de Madrid
Programa de Doctorado en Biociencias Moleculares

Departamento de Bioquímica
Facultad de Medicina
Universidad Autónoma de Madrid

Characterization of CDK14-18 as therapeutic targets in hepatocellular carcinoma

Diego Martínez Alonso
Graduado en Biología (UAM)

Thesis Directors:
Dr. Marcos Malumbres Martínez
Dr. Guillermo de Cárcer Díez

Centro Nacional de Investigaciones Oncológicas (CNIO)

Madrid, 2021

A mis padres

''Desde el espacio con su hermano el tiempo, bajo la gravedad insistente, con una luz para ver como no veo, entre el ya no y el todavía no fui colocado. El asombro ante lo que desconozco fue mi maestro. Escuchando su inmensidad. He tratado de mirar, no sé si he visto''

Eduardo Chillida

Acknowledgements

A lo largo de estos años de doctorado he tenido la inmensa suerte de conocer a gente única y presenciar como cada día crean el entorno de creatividad, saber científico y pensamiento crítico que caracteriza el CNIO. Me gustaría reflejar brevemente mi agradecimiento a algunas de estas personas, aunque de muchas más he aprendido durante mi tesis.

Marcos sin duda te llevas el agradecimiento más grande que tengo que hacer, por darme la que hasta ahora ha sido mi mejor oportunidad. También por ser el jefe que eres, creo que cualquiera que ha trabajo contigo se lleva no solo una forma excelente de hacer ciencia, sino una manera de transmitir creatividad y motivación que nos impulsa a darlo todo para llegar lejos en el proyecto que tenemos entre manos. También tengo que agradecerte que te hayas preocupado no solo de lo relativo al proyecto en el que trabajaba sino también de mi formación científica general, dándome la oportunidad de participar en otros proyectos y artículos, respetando mis tiempos, aportando reconocimiento a mi trabajo y creyendo en mis ideas.

Quiero agradecer al resto del equipo de Marcos todo el apoyo personal y técnico que he recibido durante estos años. Me llevo un aprendizaje científico y personal de gran valor, ¡gracias a todos vosotros CDCs! Guille, gracias por formar con vocación a los que venimos incautos e ignorantes, y gracias por haber estado ahí en los momentos difíciles con palabras de apoyo, y en los buenos momentos con palabras de recompensa. También quiero hacer un agradecimiento particular a Luis y a Senn por toda su ayuda colaborando en este proyecto, que ha sido esencial, y por los buenos ratos.

Me gustaría agradecer también a los colaboradores del proyecto todo su apoyo profesional y personal. A Paco Real, por todo lo que aprendí de él cuando colaboramos estudiando la ciclina Y, y por sus consejos y apoyo. A Amaia Lujambio, por su enorme disposición para ayudar asesorándonos en experimentos que han sido esenciales para la tesis y facilitándonos los reactivos y la información que necesitábamos.

Finalmente, quiero agradecer a mis abuelos Manolo y Mª del Carmen haber sido una inspiración para mí, en tantos sentidos, desde bien temprano en mi vida. A mi Ana, a mi hermana Blanca, María, Adri, Cris y Pepe. También a Miguelete, desde el colegio siendo compañeros de fatigas y ahora en la ciencia también. Si los anteriores agradecimientos han ido para gente que fue importante en el laboratorio, este va para vosotros porque habéis sido, y sois, los más importantes fuera de él.

Summary/Resumen

Multifold molecular events allow proliferating cells adapt to environmental signals and ensure fidelity in DNA replication and chromosome segregation. Cyclin-dependent kinases (CDKs) are cell cycle master regulators, integrating a complex signaling network to drive cell division and modulate transcription. These protein kinases are activated by a separate subunit named cyclin, which provides domains essential for enzymatic activity. Connected to their central implications in cell division, alterations in cyclins and CDKs are frequently associated to human disease, and particularly to cancer. Despite CDK4,6 pharmacological inhibition represents a major breakthrough in oncology, scientific and medical community aim to overcome resistance to available treatments, and to accelerate drug discovery to increase the number of treatable tumor types. In this context, delineation of the implication in human cancer of alternative CDK family members that remain uncharacterized could help uncover novel therapeutic opportunities.

CDK14-18 are classified as cell cycle-related CDKs and belong to CDK5 subfamily. They present structural, biochemical, and functional singularities, which hindered clarification of their roles. Similar to CDK5, their expression is mainly restricted to well-differentiated post-mitotic cells, suggesting they may be dispensable for the viability of most mammalian cell types.

Alterations in CDK14-18 expression and activity correlate with poor prognosis in tumors from different origin. Their implications in molecular pathways related to metastasis and sustained cancer progression (e.g., WNT signaling), suggest a spectrum of patients could benefit from CDK14-18 inhibition. However, the specific tumor types in which their inhibition could improve patient outcome, and the precise mechanisms underlying an eventual good clinical response, await experimental demonstration.

In the present work, we sought to identify susceptibilities to CDK14-18 depletion in human cancer. We demonstrate how ablation of these genes induces DNA damage reducing hepatocellular carcinoma (HCC) cell proliferation, an effect significantly improved with certain combinations due to functional redundancy between these kinases. Moreover, our results highlight a cooperative effect between CDK16 implications in WNT signaling and CDK18 roles in DNA repair, as alterations in either arm hinder replication stress control. Preliminary data of CDK14-18 inhibition in murine liver tumors evidences a promising therapeutic effect, whereas genetic ablation of these genes did not lead to major physiological abnormalities, suggesting minor toxicity could be expected to associate to their inhibition in human patients.

Numerosos eventos moleculares permiten a las células en proliferación adecuarse a las señales del ambiente y asegurar fidelidad en los procesos que definen el ciclo celular y en última instancia su división. Las quinasas dependientes de ciclina (CDKs), son reguladores centrales de estos procesos al integrar diversos módulos de señalización para ejercer control sobre el ciclo celular y la transcripción. Éstas son activadas por una subunidad llamada ciclina, que proporciona dominios esenciales para la actividad enzimática

Ciclinas y CDKs se encuentran frecuentemente alteradas en cáncer. Superar la resistencia a los tratamientos disponibles y aumentar el espectro actual de terapias dirigidas y tipos de tumores susceptibles es un objetivo prioritario de la comunidad científica y médica. En este contexto, delinear las implicaciones y la función de CDKs alternativas que permanecen sin caracterizar puede representar nuevas oportunidades terapéuticas.

CDK14-18 presentan singularidades estructurales, bioquímicas y funcionales, lo que ha dificultado la aclaración de sus implicaciones fisiológicas. De forma similar a CDK5, su expresión se restringe a células post-mitóticas bien diferenciadas, lo que sugiere que pueden ser prescindibles para la viabilidad de la mayoría de tejidos y tipos celulares. Alteraciones asociadas a CDK14-18 correlacionan con mal pronóstico en tumores de diferente origen. Su proximidad a CDK4,6 en la evolución y su implicación en vías moleculares relacionadas con la metástasis y la progresión tumoral (e.g., señalización por WNT), sugieren que un espectro de pacientes podría beneficiarse de la inhibición de CDK14-18. Sin embargo, el contexto para observar un efecto terapéutico y la explicación molecular subyacente aún requieren de demostración experimental.

En el presente trabajo, hemos caracterizado la susceptibilidad a la depleción de CDK14-18 para células tumorales de diferente origen. Hemos demostrado cómo la depleción de estos genes induce daño en ADN reduciendo así la supervivencia de células de carcinoma hepatocelular. Además, nuestros datos demuestran la cooperación entre las implicaciones de CDK16 en señalización por WNT y el papel de CDK18 en reparación de ADN. Finalmente, datos preliminares en modelos experimentales para tumores de hígado, sugieren que la inhibición farmacológica de CDK14-18 tiene un alto potencial terapéutico, mientras que modelos genéticos para la depleción de CDK14-18 no mostraron efectos fisiológicos relevantes asociados, sugiriendo que podría esperarse baja toxicidad asociada a su inhibición en pacientes humanos.

Index

Abbreviations

ATCC American Type Culture Collection

BAT Brown Adipose Tissue

CDK Cyclin-Dependent Kinase

CKI Cyclin-dependent Kinase Inhibitor

Ctrl Control

cKO conditional-knockout

DAPI 4',6-diamino-2-phenylindole

DMEM Dulbecco's Modified Eagle Medium

EdU 5-Ethynyl-2'-deoxiuridine

FBS Fetal Bovine Serum

FDR False Discovery Rate

GFP Green Fluorescent Protein

GSEA Gene Set Enrichment Analysis

HCC Hepatocellular Carcinoma

HEK Human Embryonic Kidney (cells)

IF Immunofluorescence

IHC Immunohistochemistry

IP Immunoprecipitation

KO knockout

MEF Mouse Embryonic Fibroblast

ORF Open Reading Frame

Padj p-adjusted value

PCR Polymerase chain reaction

PCTK PCTAIRE

PFA Paraformaldehyde

PFTK PFTAIRE

ROS Reactive Oxygen Species

RPMI Roswell Park Memorial Institute medium

RT Room Temperature

SD Standard Deviation

SDS-PAGE Sodium dodecyl sulfate Polyacrylamide Gel Electrophoresis

sgRNA single guide RNA

shRNA short hairpin RNA

TAM Tamoxifen

TGCA The Cancer Genome Atlas

WAT White Adipose Tissue

WT Wild Type

1. Introduction

1.1. Cyclins and CDKs: key drivers of cell division and cancer

1.1.1. Cyclin and CDK discovery, evolution and classification

All organisms rely on cell division for building, organizing and maintaining their structures from embryonic development until their death. The coordination of cell growth, chromosome duplication, separation, and distribution in two daughter cells is known as cell cycle. Mechanisms underlying cell cycle progression are conserved through evolution from unicellular to multicellular eukaryotic organisms, where their complexity has increased in the number of genes and regulatory mechanisms implicated [1].

The fundamental conserved machinery controlling cell cycle transitions consists in two types of genes, cyclin-dependent kinases (CDKs) and their activating subunits, named cyclins. Cyclin discovery dates back to the observation by Tim Hunt of a protein that was degraded after each division cycle in sea urchin embryos [2]. The demonstration of the requirement of these genes for cells to enter mitosis [3][4] accompanied the identification of CDKs by Leland H. Hartwell and Paul M. Nurse in yeast [5][6]. The three researchers received the Nobel prize in physiology and medicine ‘’for their discovery of key regulators of the cell cycle’’ in 2001.

Although the experimental organisms used in these initial studies present a simplified version of the mammalian cell cycle machinery, as previously mentioned the principles governing cell division are conserved in higher organisms. In fact, most yeast cyclins and CDKs meet one or more orthologs in mammals [1]. Like their yeast counterparts, mammalian cyclins have conserved their capacity to bind multiple CDK partners. This promiscuity forms the basis for the dynamic regulation they exert over different CDK substrates, thus controlling the cell-division cycle in response to different cellular cues [1][7].

Over the course of evolution, cyclin and CDK families have independently undergone extraordinary levels of divergence and functional specialization, which is reflected in the variety of compartmentalized and general functions for which cyclin-CDK complexes are required. The promiscuity of cyclins to bind multiple CDK partners burdens the functional diversity these gene families can display and hinders the clarification of their physiological relevance.

The human cyclin family contains at least 30 genes that share homology within the cyclin box domain, whereas the human CDK family comprises 20 genes classified

according to the homology they share in the kinase domain [1][7][8]. The evolutionary expansion of the CDK family in mammals led to the functional and sequence homology division of CDKs into three cell-cycle-related (CDK1, CDK4 and CDK5) and five transcriptional (CDK7, CDK8, CDK9, CDK11 and CDK20) subfamilies [1] (**Fig.1.1**).

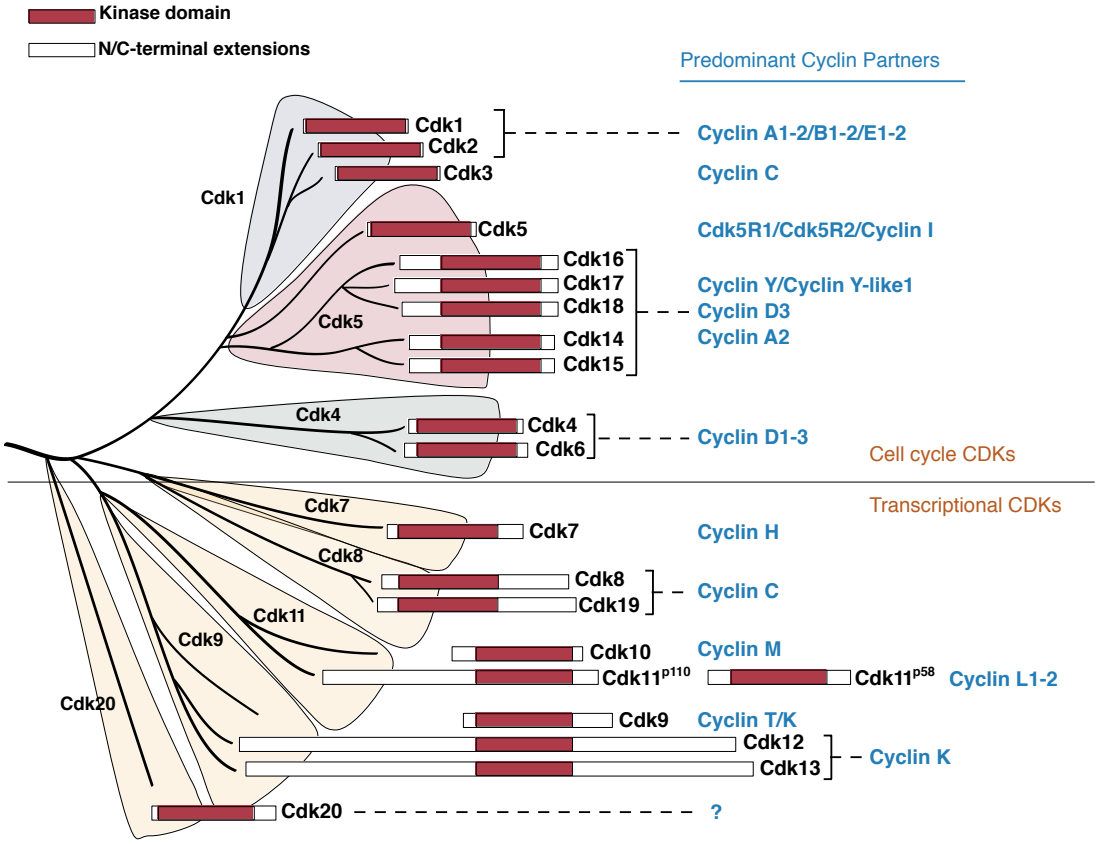

Figure 1.1. Evolutionary relationships between mammalian CDK subfamilies and their cyclin partners. The name of the different CDK subfamilies functioning in the cell cycle or transcription are shown in orange, and the domain structure of the individual proteins is depicted. The conserved protein kinase domain (red) and some additional domains (white) are indicated for each CDK. Alternative cyclin binding partners reported for each CDK subfamily are indicated in blue (indistinct from evidence support of a relevant physiological function). The phylogenetic tree is based on the comparison of the human kinase domains. Modified from [1].

1.1.2. Fundamentals of cell cycle progression control: roles of cyclins and CDKs

CDKs are defined as serine-threonine kinases activated by a separate subunit - a cyclin - that provide domains essential for enzymatic activity and confer substrate specificity [1]. CDKs play essential roles in the control of cell cycle progression, cell division and transcription modulation in response to several extra- and intracellular stimuli [1] (**Fig.1.2**).

Only a few cyclins adjust to the features initially used to define these genes: cyclic oscillations in their protein levels and direct implications in cell cycle progression (**Figure 1.2**). Whereas CDK protein levels are relatively constant throughout cell cycle, cyclin expression can be controlled at different levels to ensure CDK activation control. Cyclin transcription activation in G_1 relies on mitogen sensing, connecting cell cycle progression with the cellular environment [9]. Transcriptional repression of cyclin promoters is another mechanism to prevent premature CDK activation, ensuring sequential progression through cell cycle phases [1] (**Fig.1.2**).

Cyclin-CDK heterodimers are formed at certain points in the cell cycle ensuring temporal and spatial specificity for CDK activity. Subsequently, these complexes phosphorylate a wide variety of substrates required for transcriptional activation during G_1, DNA replication during S phase, centrosome duplication during S/G_2 and chromosome alignment and separation during mitosis [7].

Post-translational modification by phosphorylation of specific residues is a common mechanism to target cyclins for ubiquitin-dependent degradation as cells progress through cell cycle [7][10]. On the contrary, phosphorylation of alternative critical residues by cyclin-CDK complexes commonly leads to CDK activation. The CAK complex (composed by cyclin H, CDK7 and Mat1) control CDK activation through their direct phosphorylation [11], and other cyclin-CDK complexes (i.e., cyclin K-CDK12) regulate cyclin capacity to associate with its cognate CDK [12]. CDK inhibitors (e.g., INK4 family), other proteins that mediate CDK phosphorylation (e.g., PLK1) and their counteracting phosphatases (e.g., CDC25) also regulate CDK activation, localization and stability [1] (**Fig.1.2**). In addition, several checkpoints prevent CDK activation by different molecular means in the presence of unduplicated DNA regions, DNA damage, or chromosome misalignment [13][14][15]. Taken together, the multiple mechanisms of cyclin/CDK expression and stability control allow cells to progress through cell cycle in a concerted manner preventing premature or sustained CDK activation, features commonly associated with chromosomal instability [16][17][18].

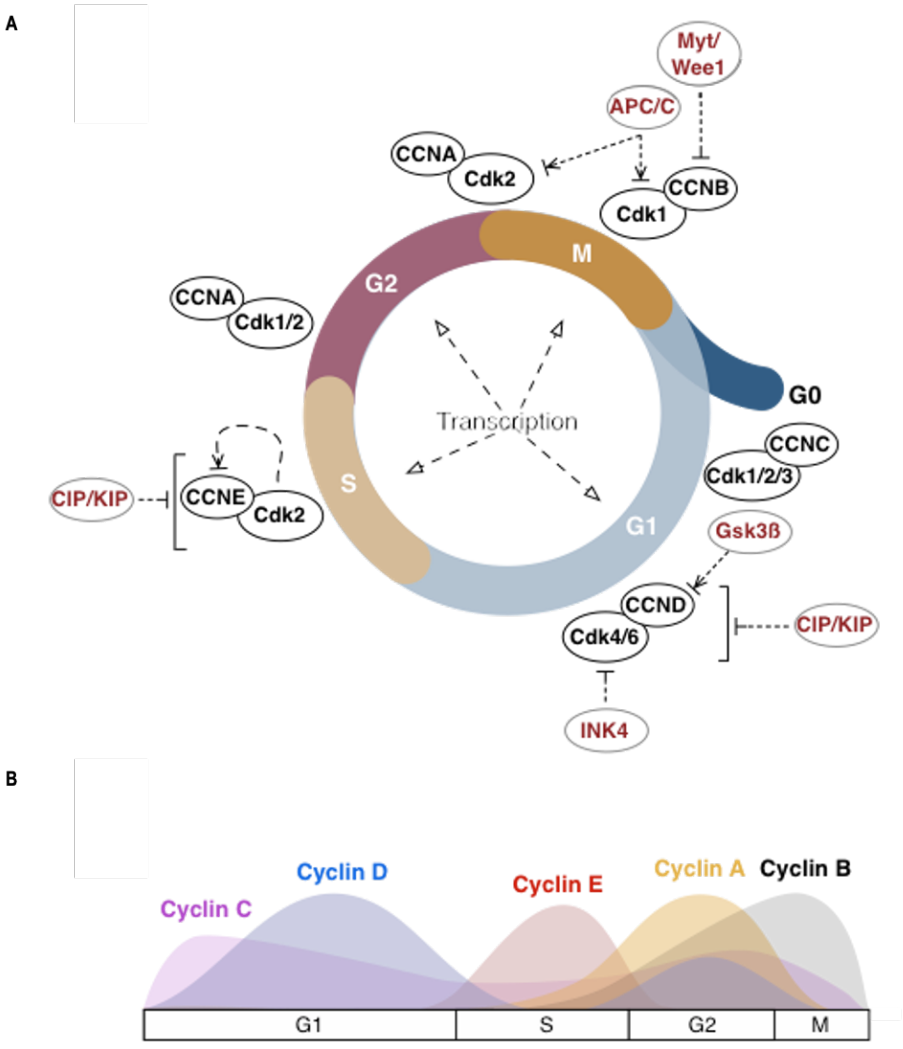

Figure 1.2. Temporal control of cell cycle progression by regulatory interactions between its key players and their transcriptional regulation. **A**) Schematic representation of mammalian mitotic cell cycle phases and regulators. Cyclin Y and cyclin F, whose protein levels oscillate in a cell cycle-dependent manner and have been proposed to activate cell cycle-CDKs, have not been included to represent only the most universal (regarding cell types) and evolutionary-conserved interactions. CIP/KIP class of inhibitors, CKIs and proteins controlling their stability are depicted in red. Dashed bottom lines: inhibition; dashed arrow bottom lines: degradation induction. **B**) Expression levels of most relevant cyclins related to cell cycle progression and their oscillations in proliferating mammalian cells.

Cyclins and CDKs have been extensively studied for decades contributing to our understanding of cell cycle and human disease. In this line, generation of mouse models for the genetic ablation of these genes helped characterize relevant cyclin/CDK features:

1. Functional redundancy between CDKs and promiscuity of cyclins to bind alternative CDK partners explain why CDK1 is the only essential CDK that can drive alone cell division [19][20].

2. Compensatory roles exerted by alternative cyclins-CDKs in the context of genetic ablation can be dependent on changes in the expression pattern of these surrogate genes [21].
3. Several cyclins and CDKs play essential, non-redundant roles in specific tissues during adulthood or at certain development stages [22].
4. Concomitant with CDK1 essential functions and the requirement of specific CDK activity in certain tissues or development stages, co-depletion of some cyclins or CDKs and their surrogates can result in embryonic lethality [23][24][25].
5. Alterations in the expression of cyclins and CDKs associates with increased susceptibility to tumor onset and progression, defects in development and tissue homeostasis and reduced lifespan [26][27].

1.1.3. Alterations and therapeutic relevance of cyclins and CDKs in cancer

Uncontrolled cell proliferation in human cancer is sustained by alterations in the expression levels, localization or accumulation of key cell cycle regulators. Not surprisingly, changes in cyclin and CDK activity is a common hallmark of all tumor types.

Genomic alterations in cyclin loci, or oncogenic pathways controlling their expression, can be detected in all tumors [7]. These alterations assist sustained activation of CDKs, leading to unrestrained cell cycle entry and defects in DNA replication and chromosome segregation fidelity [7]. Concomitantly, these defects associate with poor prognosis in many tumor types, and mouse models for cyclin overexpression are tumor-prone [7].

CyclinD-CDK4/6 central role in cell cycle entry explains why CDK4,6-RB1 axis is virtually altered in all tumor cells and constitute one of the best characterized CDK-related alterations in cancer [26][28][29][30]. D-type cyclins are typically upregulated by multiple mechanisms including amplification or translocations [26], or in response to oncogenic alterations in major oncogenic pathways controlling their expression or activity (Ras, PI3K-AKT, WNT) [26]. Targeting D-type cyclin overlapping roles through pharmacological inhibition of CDK4,6 has been a successful strategy for improving clinical outcome of hormone positive-breast cancer patients [28][29], and other tumor types are currently under evaluation [29][31].

Side effects associated to CDK4,6 inhibition are well tolerated thanks to a combination of the compensatory plasticity with other CDKs in normal cells [24][32][33] and the target specificity achieved with currently approved selective inhibitors (*Palbociclib/ PD-0332991*, *Abemaciclib/LY2835219* and *Ribociclib/LE011*) [29]. On the contrary, it was challenging to find a therapeutic window for other cell cycle-related CDKs given the toxicity associated to their inhibition in most contexts [29]. However, CDK5 subfamily implications in cancer remain elusive and recent reports evidence CDK16 and CDK18 are emerging as putative anti-cancer targets [34][35][36]. Furthermore, targeted therapies against transcriptional CDKs such as CDK8/19 or CDK12,13 are currently under evaluation [37][38][39][40].

Despite CDK4,6 inhibitors represent one of the major breakthroughs in cancer therapeutics, some tumors appear to be resistant or show modest clinical effect even though molecular alterations would suggest a robust response [29]. Although monotherapy benefits can be improved through potent combination strategies, as recently shown in pre-clinical trials [31][41] and in the combinations with endocrine therapy in the clinic [28], the factors that determine whether other CDKs can compensate for CDK4 and CDK6 inhibition in these tumors are poorly understood [29].

In conclusion, further characterization of human CDK family represents an opportunity to increase our understanding of resistance mechanisms to available treatments and a source of unexplored therapeutic opportunities.

1.2. CDK14-18: ‘’atypical CDKs’’

1.2.1. CDK14-18 subfamily discovery, evolution and structural features

Murine *Cdk16* and *Cdk18* cDNAs were the first identified sequences corresponding to members of CDK14-18 subfamily, and human *CDK16*, *CDK17* and *CDK18* were simultaneously identified using probes specific for Cdc2-related genes in a screening with a human cDNA library [42][43]. Whereas murine *Cdk16* mRNA was more ubiquitously expressed, *Cdk18* detection was mainly restricted to brain, intestine and kidney tissue [43]. Soon after, analysis of rat *Cdk17* expression evidenced it was restricted to brain tissues, peaking during brain development but associated to terminally differentiated post-mitotic neurons [44].

L63 or Eip63E, the ortholog for CDK14 in *Drosophila*, was first identified looking for Cdc2-related sequences by PCR screen. Like CDK5, it was expressed during embryogenesis [45]. Later on, murine *Cdk14* sequence was also identified using

Cdc-2 cDNA probes and its expression was found to be predominantly associated to postmitotic and differentiated cells in the postnatal nervous system [46]. Subsequently, *Cdk14* mRNA was also identified by screening a testis cDNA library for new serine/threonine kinases [47]. In that report, the authors showed *Cdk14* mRNA was detected, like *Cdk16*, at low levels in all tissues with the exception of embryo, brain and testis, suggesting a role for these kinases during development and in differentiated tissues [47].

After their discovery, CDK14-18 kinases were considered "orphan CDKs", because their cyclin partners were unknown. They were named according to a characteristic alpha-helical sequence that corresponds to the cyclin-interaction "PSTAIRE" helix in CDK1, i.e., PFTAIRE (CDK14-15) and PCTAIRE (CDK16-18) [48]. It was not until the demonstration of *Drosophila* cyclin Y (CycY) capacity to interact with Eip63E that these orphan CDKs finally found a cyclin partner [49][50]. Nevertheless, additional regulators have been proposed for these genes as described below.

Human CDKs range in size from ~300 amino acid residues, which just encompass the catalytic domain, to proteins of more than 1,500 residues with N- and/or C-terminal extensions of variable lengths, that contain sequences essential for their function, regulation and localization [1]. CDK14-18 are closely related to CDK5, and therefore are included in the cell cycle-related CDKs group [1] (**Fig.1.1**). Whereas most cell cycle-related CDKs are mainly composed by the kinase domain, CDK14-18 present additional sequences that provide residues critical for their activation by cyclins and other kinases (**Fig.1.3**). The core catalytic domain of PCTAIRE kinases represents their most conserved region (~50% homology to Cdk1), whilst most of their differences are located within the N- (37% identity) and C-terminal (17% identity) extensions (**Fig.1.3**). These extensions, however, show hot spot regions of conservation that harbor essential domains for cyclin binding and enzymatic activation, that can be also found in PFTAIRE genes [1][48].

CDK14, CDK16 and CDK17 are the most conserved members of the subfamily, whereas CDK15 and CDK18 appeared later in evolution [48]. Although cyclin Y is highly conserved and its conservation degree is only comparable to that of CDK1 or cyclin C [48][51], CDK14-18 appeared later on during the expansion of eumetazoans [48]. ''PCTAIRE'' sequences are detected in many species of eumetazoans but are missing in insects [48]. Primitive ''PCTAIRE''-containing kinases are more closely

related to CDK5 than to CDK16, evidencing the origin of the first true CDK16 homologs can be tracked in evolution to kinetoplastids and amoebozoa divergence [48]. However, although collared flagellate and parazoan genomes contain genes ~40% similar to CDK16, they lack the above-mentioned N- and C-terminal extension conserved domains essential for human CDK16 enzymatic activity [48]. Thus, sequence

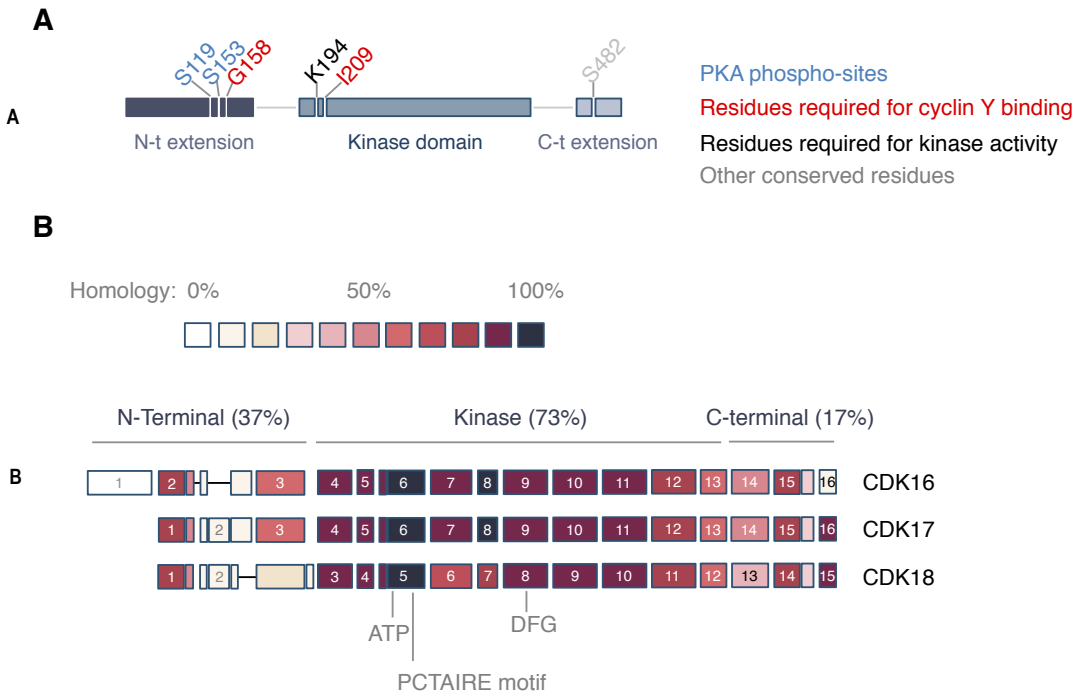

Figure 1.3. Structural features and sequence alignment of human PCTKs. A) Schematic representation of Cdk16 domains and residues with functional annotation. **B)** Structural domains of human PCTKs and their sequence homology, obtained from aminoacidic sequence alignment. Domains interacting with cyclin Y and ATP/proton acceptor (DFG) motifs, and exon numbers are indicated. Protein alignment was made with T-Coffee [52].

analyses suggest real CDK16 homologs arose with the development of a nervous system and can only be found in animals, with the notable exception of insects [48], supporting an important role for these kinases in neurons.

In spite of sequencing and functional studies that suggest the mammalian homolog of yeast Pho85 is CDK5, it also clusters with CDK14-18. In fact, yeast Pho85 can interact with cyclins of the Pcl1/Pcl2 group, proteins closely related to cyclin Y, and Pho80 group, the yeast ortholog for p35 [1]. Whereas mammalian CDK5 main activators are non-cyclin proteins, named CDK5R1 (p35) and CDK5R2 (p39), CDK14 and CDK16 are activated by cyclin Y, suggesting both CDK5 and CDK14-18 may have arisen from a common ancestor gene.

1.2.2. Regulation of CDK14-18 activity and localization

A potential CDK partner for CycY was originally identified in a yeast two-hybrid screen with *Drosophila* proteins. The identified kinase was Eip63E, which had not been previously associated to any cyclin partner [49]. Years later, CDK16 binding to cyclin Y was also demonstrated in nematodes and mice [53][54], and the characterization of CDK16 expression at the protein level showed it was cytoplasmic and predominant in testis and brain, showing low expression levels in other tissues [55][56][57]. After the isolation of human *CDK14* cDNA and its fusion to a GFP tag, analysis of ectopically expressed CDK14 in Hela cells showed its expression pattern was cytoplasmic [58][59][60], and same results were obtained for a CDK18 fusion with GFP [61]. Although CDK17 cyclin partners remain unknown, its expression pattern is also cytoplasmic and, interestingly, was found to localize to mitochondria in COS7 cells [44][62].

As previously mentioned, CDK activity is dictated by the temporal and spatial control of cyclin expression and localization, and their association acts as a major determinant of substrate specificity. Cyclin Y bound CDK14-18 are the only known membrane-targeted CDKs, with the exception of the closely related CDK5, which is targeted to cellular membranes by its activators P35 and P39 in a similar fashion [60]. In fact, CDK16 is also able to interact with P35 and can be phosphorylated by P25-CDK5 complexes [63], evidencing the complex functional relationship between members of the subfamily.

In contrast to conventional cyclins, cyclin Y contains an N-myristoylation signal (responsible for its capacity to associate with membranes) and only a single cyclin fold, which harbor critical, conserved residues required for its capacity to bind and activate CDK14 and CDK16. Both the cyclin box in cyclin Y and the PFTAIRE/PCTAIRE motifs of CDK14 and CDK16, respectively, are essential for their interaction [54][59][64]. It has been suggested that the structure of cyclin Y resembles that of P25, a proteolytic fragment of P35, which adopts a cyclin fold-like structure and alleviates the need of T-loop activating phosphorylation in CDK5 [48].

Two residues in cyclin Y (S100 and S326) are required for 14-3-3 protein binding, which enhances its association to CDK14 and CDK16 [65][66][67][68]. Similarly, PKA-mediated phosphorylation of CDK16 in S119 generates a 14-3-3 binding site [69][70]. On the contrary, PKA-mediated phosphorylation of S153 has been shown to inhibit cyclin Y-dependent targeting of CDK16 to the cell membrane by

blocking their interaction [54][70]. Mutation of the nearby residue G158 also disrupts interaction between cyclin Y and CDK16, suggesting phosphorylation or mutation of conserved residues within the N-terminal extension of CDK16 induce conformational changes that ultimately block cyclin binding [54] (**Fig.1.3**). Moreover, PKA is able to phosphorylate CDK18 in several residues, and S12 phosphorylation was shown to be critical for CDK18 activation [71]. Additional reports have shown other phosphorylation sites important for CDK16 activity. For example, P25-CDK5 phosphorylation of S95 in CDK16 enhances its activity [63].

Although S153 is conserved in both CDK14 and CDK16, S119 is only present in CDK16, and there is no evidence of S153 phosphorylation of CDK14. CDK16 S95 is conserved in CDK17 and CDK18, but the surrounding residues are thought to prevent CDK5 phosphorylation given its substrate specificity [72]. Therefore, even though cyclin Y shows promiscuity towards both PFTAIRE and PCTAIRE kinases, distinct modes of regulation might confer specificity to their functions.

CDK14 can control cyclin Y stability in a negative feedback loop by phosphorylating two critical residues (S71 and S73), which creates a phospho-degron that targets cyclin Y for ubiquitin-dependent proteolysis [73]. This resembles the negative feedback loop triggered by other CDKs over their activators, such as CDK5-mediated phosphorylation of P35 that negatively regulates their interaction and P35 stability [74][75]. Similarly, CDK16 has been shown to phosphorylate cyclin Y (S336), although the functional relevance of this phosphorylation remains unknown [67][68].

1.2.3. CDK14-18 functions

1.2.3.1. Cyclin Y-dependent functions of CDK14-18 and cooperation with Cdk5

The above-mentioned cyclin Y-CDK interactions have been confirmed functionally relevant and, for CDK16, translated to *in vivo* mouse models [54]. Early studies of the function of *Drosophila* CDK14 ortholog evidenced cyclin Y binding was essential to rescue developmental defects associated to Eip63E null mutants [49]. Davidson et al. showed cyclin Y-CDK14 interaction mediates LRP6 receptor priming prior to WNT ligand binding. In particular, CDK14 phosphorylates LRP6 S1490 in cells from different organisms, including human cells [76]. Since WNT signaling is well known to be essential for multiple developmental and homeostatic processes [77], this interaction provided a molecular explanation for the developmental defects linked to

Eip63E ablation, and the authors further demonstrated cyclin Y-CDK14 implications in development using a different organism model (*Xenopus laevis*) [76].

Cyclin Y expression peaks during the G2/M phase of the cell cycle, and so does its interaction with CDK14 [76], thus providing a link between WNT signaling and cell division. The consequences of transcriptional activation of WNT-responsive genes at late stages of cell cycle are not clear, and non-dividing cells such as liver cells and neurons also show WNT activation [78][79]. Nevertheless, other reports have demonstrated ß-catenin stabilization is important for centrosome separation in mitosis [80]. Moreover, hyperactivation of WNT signaling in cells in which is absent or controlled under normal conditions can act as a driver of proliferation and oncogenic transformation [81][82].

Although there are not examples in the literature of studies analyzing the crosstalk between cyclinY-CDK14 and CDK5, both kinases have been shown to regulate WNT signaling. CDK5 implications in WNT pathway in healthy tissues are related to the activation of Axin and Neuregulin, leading to GSK3ß inhibition in developing and adult mouse brains, respectively [83][84], whereas its activator P25 has been shown to induce GSK3ß activation [85]. Additionally, CDK5 has been shown to phosphorylate ß-catenin and regulate its activity [86], thus providing additional examples of WNT signaling regulation at different levels by members of the subfamily.

Recent reports have started to clarify the molecular implications of cyclin Y-CDK16 complexes in human cells. Hernández-Ortega et al. have identified PRC1 as a cyclin Y-CDK16 substrate, a protein essential for cell division that organizes microtubules during mitosis [87]. Another study has shown cyclin Y-CDK16 complexes control autophagy and their activity is directly induced by AMPK [68]. Interestingly, a different study screened a library of activated kinases for their ability to stimulate autophagy and found CDK17 and CDK18 as putative inhibitors of the process [88]. CDK5 has also been linked to this signaling pathway [89], hence supporting important implications for several members of the subfamily in autophagy.

The relevance of the interactions between P25-CDK5 and cyclinY-CDK16 complexes has been mainly demonstrated in the nervous system. Studies in *C. elegans* showed both complexes cooperate and are partially redundant in the regulation of polarized trafficking of presynaptic components by inhibiting dynein-mediated retrograde transport [53]. Furthermore, studies in mouse evidenced they cooperate in dendrite development, neurite outgrowth and neural migration, and provided the basis

for linking CDK16 with actin dynamics. Concomitantly, cyclin Y-CDK16 and P35-CDK5 activities are essential for brain development [69][90][91]. The implications of cyclin Y-CDK16 in vesicle trafficking in the brain have been confirmed in a chemical genetic screen using an engineered cyclin Y-CDK16 complex and mouse brain extracts. In that report, Sehata et al. identified AAK1, Dynamin 1 and Synaptojanin 1 as CDK16 substrates. These genes have been demonstrated to regulate crucial steps of receptor endocytosis and to control neuronal synaptic transmission [92], and therefore their results provided a link between the suggested physiological function of CDK16 in the brain and CDK16 regulation. Not surprisingly, *CDK16* has been proposed as a novel X-linked intellectual disability (XLID) gene, and loss-of-function mutations have been identified in human patients [93].

1.2.3.2. Other CDK14-18 functions without cyclin partner annotation and Cdk5 overlapping roles

There are examples of additional implications of CDK16 in vesicle transport beyond that exerted at the synapse. First, CDK16 has been shown to interact with P11/ANX2L, a protein involved in cell cycle progression, differentiation and endocytosis/exocytosis [94]. Another report showed CDK16 mediates NSF phosphorylation to regulate its membrane fusion activity and exocytosis [95], although other authors have questioned NSF is a *bona fide* CDK16 target given its substrate specificity [64]. In addition, it has been suggested that both CDK16 and CDK18 participate in COPII mediated vesicle transport between the endoplasmic reticulum and the Golgi [96]. Moreover, CDK14 and CDK16 were identified in a siRNA screen as potential regulators of glucose uptake in adipocytes by regulating transport of the cell surface receptors Glut1 and Glut4 [97]. Finally, CDK18 is a key regulator of the localization and abundance of aquaporin-2 (AQP2) in the plasma membrane [98]. Taken together, these studies indicate PCTKs play important roles related to vesicle trafficking, protein secretion and translocation of transmembrane receptors at the cell surface.

Although CDK16 has been shown to interact with P35, there is no evidence of this interaction leading to CDK16 kinase activity induction [63]. Nevertheless, it would be important to consider CDK5 functions because, as stated above, they have been shown to cooperate and CDK5 regulates CDK16 activity [63][90][91]. The best demonstrated role of CDK5 is the regulation of the cytoarchitechture of the central

nervous system by the regulation of processes such as actin dynamics, cadherin-mediated adhesion, secretion, membrane transport or dopamine signaling. Additionally, CDK5 has been implicated in myogenesis, haematopoietic cell differentiation and spermatogenesis [99][100], and recent reports demonstrated it is implicated in the control of circadian clock [101]. Interestingly, many of these functions and physiological implications are shared with CDK16 and CDK18, and possibly with other members of the subfamily (**Table 1.1**). As previously mentioned, the expression pattern of CDK16 in differentiated post-mitotic tissues suggested a role of this kinase in differentiation [55]. Beyond the commented cyclin Y-dependent roles of CDK5/CDK16 axis in dendrite development and neural differentiation [90], other reports have shown additional CDK16 functions that overlap CDK5 roles (**Table 1.1**): one study have demonstrated CDK16 plays a role in myogenic differentiation by promoting myoblast migration and fusion [102], and the generation of mouse models for the genetic ablation of *Cdk16* evidenced CDK16 regulates spermatogenesis in mice [54], as detailed in the following sections. In addition, CDK18 has been also implicated in differentiation in the nervous system, as it has been shown to promote oligodendrocyte precursor cell differentiation [103]. Other CDK18 functions shared with CDK5 include the phosphorylation of Tau [61]. Together with its expression status in patient samples, along with that of CDK17, explains why these genes have been proposed as novel players contributing to the pathogenesis of Alzheimer's disease [61][104].

Despite increasing evidence of the implications of this subfamily in differentiation in and outside the nervous system, and with the exception of CDK16 roles in spermatogenesis, these physiological functions lack cyclin partner annotation.

1.2.3.3. Alternative cyclin interactions with CDK14-18 and their functional relevance

The first evidence that suggested existence of alternative cyclin partners for CDK14-18 was found in rodent brain extracts, where CDK16 expression was cytoplasmic in most cells, but associated to the nucleolus in Pukinje and pyramidal cells of the hippocampus [105]. Precisely, there are not reports describing alternative interactions for CDK16, and attempts of finding interactions with cyclins D1, E, A, B1, B2, G and F failed in co-immunoprecipitation experiments [72].

To date, there are only two examples confirmed as functionally relevant of alternative cyclins binding CDK14-18 members. First, CDK14 has been shown to

interact with cyclin D3, but not cyclin D1, in mammalian cells and is able to phosphorylate RB1 *in vitro*. Moreover, ectopically expressed CDK14 is able to form a ternary complex with $p21^{CIP1}$ and cyclin D3, which enhances cyclin D3-CDK14 interaction [106]. Although the relevance of this interaction has not been confirmed in other reports, CDK14 capacity to interact with cyclin D3 and phosphorylate G_1 cell cycle regulators suggest these CDKs may play roles during other phases of the cell cycle apart from G_2/M, at least in the analyzed cell types (bone marrow and osteosarcoma cell lines).

Second, cyclin A2 and cyclin E1 were shown to interact with ectopically expressed strep-tagged CDK18 in HEK293T cells, in contrast to other tested cell cycle cyclins (B1, D1, E2). Interestingly, cyclin Y also failed to co-immunoprecipitate with CDK18 in these experiments [71]. Cyclin A2 association with CDK18 or PKA-mediated phosphorylation of CDK18 S12 results in CDK18 kinase activity and has a direct impact in actin cytoskeleton dynamics through the regulation of cofilin phosphorylation [71]. Remarkably, cyclin A2-CDK18 complexes concentrate in the cytoplasm, in contrast to cyclin A2-CDK2 complexes that co-localized in the nucleus of HEK293T cells [71]. Importantly, for the *in vitro* kinase assays RB1 was used as kinase substrate. Although cyclin E1-CDK18 complexes showed no kinase activity against this substrate, it should not be discarded as functionally relevant without further evaluation.

Additionally, cyclin K has been shown to interact with CDK18 in a large proteomic analysis [107], but the relevance of this interaction remains to be confirmed in any context, and this cyclin failed to co-immunoprecipitate with CDK18 in pull down experiments [71].

1.2.4. Mouse models of Y-cyclins and Cdk16

It was not until 2012, twenty years after their discovery, that the first mouse model of CDK14-18 kinases was generated. In that report, Mikolcevic et al. showed mice lacking *Cdk16* developed normally, but males were infertile [54]. Concomitant with its expression pattern, showing a marked increase in protein levels in brain and testis, the authors demonstrated a role of CDK16 in spermatogenesis [54].

Although this initial report suggested CDK16 functions in spermatogenesis were CCNY-dependent, a different study showed it was not cyclin Y, but its ortholog, cyclin Y-like 1, the regulator of CDK16 in this process [108]. In spite of the demonstration by Mikolcevic et al. of the interaction between cyclin Y and CDK16 in mouse brain and

testis, the generation of cyclin Y and cyclin Y-like 1 null animals clarified the regulation of spermatogenesis exerted by CDK16 was dependent on the latest, thus suggesting cyclin Y-CDK16 complexes might mediate additional roles in testis [54][108].

Recently, another report demonstrated cyclin Y-like 1 regulates spermatogenesis impacting WNT post-transcriptional function independently of ß-catenin (WNT/STOP). *Ccnyl1*$^{-/-}$ animals show reduced WNT signaling, leading to GSK3ß hyperactivation with the consequent impact in protein ubiquitylation levels and proteome stability [109]. The authors provided a mechanistic explanation for the sperm maturation defects but did not report the CDK partner mediating this function, raising important questions: it is surprising to find a connection to WNT signaling because the phenotype overlaps with that found in CDK16 null animals, and CDK14, but not CDK16, has been implicated in WNT signaling. Determining CDK16 roles in WNT signaling, or further clarification of the compensatory roles of Y-cyclins and CDK14-18 would help to understand their implications in this process and likely many others.

Zeng et al. showed double *Ccny*$^{-/-}$;*Ccnyl1*$^{-/-}$ mutants had severe developmental defects leading to premature death at E16.5 [110]. The demonstration of an overlapping function during development was accompanied by the observation of high expression levels of Ccnyl1 in mammary terminal end buds during pubertal development. By using tissue specific promoters, they were able to show both cyclins have an overlapping role in keeping the properties of dividing mammary stem/progenitor cells, through WNT signaling enhancement and in a ß-catenin dependent manner [110]. Importantly, CCNYL1 expression is cell cycle dependent like that of CCNY [76], therefore providing additional links between cell cycle, Y-cyclins and WNT signaling.

Ccny$^{-/-}$ mice show lower weight and fat content as a consequence of a reduced adipocyte differentiation and higher metabolic rates [111]. Cyclin Y plays a role in adipogenesis, as cyclin Y ablation suppresses adipocyte differentiation both in vitro and in vivo. At the same time, it promotes BAT metabolic activity, yielding an explanation for the reduced body weight. Furthermore, cyclin Y depletion impairs insulin signaling in the liver but not in WAT or muscle, indicating that CCNY is involved in regulating the hepatic insulin signaling pathway [111].

Taken together, these studies increased the evidence of the implications of these genes in differentiation. The generation of knockout alleles for other PCTKs and PFTKs will likely clarify their functional redundancy or cooperation in these physiological

processes. Furthermore, it would also determine if their physiological relevance is restricted to their interaction with Y-cyclins and differentiation.

Table 1.1. Functions of Cdk5 subfamily in mammalian healthy tissues and non-tumoral cells. Overlapping functions are depicted in blue, and unique functions are in black. The references for their function are indicated in the text body. References for published mouse models are indicated in the table.

Gene	Function	Mouse models	Phenotype	References
Cdk5	Vesicle transport and fusion Neurite outgrowth Brain development Myogenesis Spermatogenesis Actin cytoskeleton dynamics Regulation of circadian clock WNT signaling Oligodendrocyte differentiation	*Cdk5*$^{fl/fl}$	Perinatal death. Developmental defects in brain.	[112], [113], [114]
Cdk14	Regulation of glucose uptake WNT signaling in mitosis	*Cdk14*$^{tm1a(KOMP)Wtsi}$	Viable. Decreased magnesium circulating levels.	Unpublished (Source: IMPC)
Cdk15	Unknown	*Cdk15*$^{tm1a(KOMP)Wtsi}$	Viable.	Unpublished (Source: IMPC)
Cdk16	Vesicle transport and fusion Neurite outgrowth Regulation of glucose uptake Cell division Brain development Myogenesis Spermatogenesis Autophagy Regulation	*Cdk16*$^{fl/fl}$	Viable. Infertile males -defects in spermatogenesis	[54]
Cdk17	Putative autophagy regulator	*Cdk17*$^{em1(IMPC)J}$	Pre-weaning lethality, incomplete penetrance. Decreased body length.	Unpublished (Source: IMPC)
Cdk18	Actin cytoskeleton dynamics Putative autophagy regulator Oligodendrocyte differentiation	*Cdk18*$^{em1(IMPC)J}$	Viable. Abnormal behavior in response to light.	Unpublished (Source: IMPC)

1.3. CDK14-18 as therapeutic targets in cancer

1.3.1. Rationale for CDK14-18 evaluation as putative cancer targets

Despite recent functional and biochemical characterization of CDK14 and CDK16 evidence increased interest in these atypical CDKs, very little is known about their molecular functions, physiological relevance and implications in human disease.

Furthermore, there is a lack of knowledge about the compensatory roles these CDKs can exert over the other members of the subfamily in almost any context, as they have been studied individually in most cases. One of few examples would be the study by Davidson et al. that demonstrates CDK14 implications in WNT signaling, which evidenced individual CDK14 knockdown had no effect in vitro (MEFs and HEK cells), whereas cyclin Y/cyclin Y-like 1 knockdown effectively impaired LRP6 phosphorylation and WNT signaling [76]. These results, together with the independently discovered overlapping roles shared by members of the subfamily and the cooperation between them in different pathways, suggest individual inhibition of these CDKs might have a narrow effect. Luckily, ATP competitors bind them all with comparable efficacy [115], given their high homology sequence in the kinase domain. Moreover, FDA-approved compounds (e.g., Dabrafenib) can inhibit CDK16 at clinically achievable concentrations [116][117]. Thus, to ensure safety and efficacy of these compounds in their clinical application, it would be essential to understand the potential implications of CDK14-18 inhibition.

Similar to CDK5, CDK14-18 are mainly expressed in brain tissue and specific cell types in mammals, in most cases well-differentiated post-mitotic cells [64]. This suggests they may be dispensable for the viability of many adult tissues, as demonstrated for CDK16 in mice [54]. Thus, it is reasonable to think side effects associated to CDK14-18 inhibition might be well tolerated.

On the other hand, de-regulation of their expression and activity has been reported in human diseases such Alzheimer's [61][104], coronary artery disease associated to diabetes type 1 [118] and cancer [35]. Their proximity to CDK4,6 in evolution, their requirement for tumor cell proliferation and migration and their implication in molecular pathways of great impact in cancer, make CDK14-18 subfamily an attractive source to evaluate new cancer targets.

1.3.2. CDK14-18 alterations and roles in cancer

CDK15 and CDK17 remain unexplored and, with few exceptions that will be mentioned, there is a lack of evidence in the literature of implications of these genes in cancer. However, in the recent years several reports have started to characterize *CDK14*, *CDK16* and *CDK18* implications in human cancer cells.

First reports on CDK14 implications in human cancer are related to hepatocellular carcinoma (HCC). Alterations in *CDK14* expression correlate with advanced metastatic HCCs and tumor grading, microvascular invasion, and early age onset [119][120]. Knockdown or overexpression of *CDK14* does not have effect in cell viability, whereas both alterations have a direct impact in the motility, migration and invasion capacity of HCC cell lines [119][120]. Like CDK18, which as previously mentioned has been related to actin cytoskeleton dynamics in tumoral and non-tumoral cell lines [71][121], *CDK14* overexpression resulted in marked filamentous actin polymerizations [119]. Conversely, *CDK14* ablation was causative of actin depolymerizations in HCC cells [120][122]. Mass-spectrometry analysis revealed changes in ß-actin (*ACTB*) and *TANGLN2* phosphorylation upon *CDK14* knockdown [120]. Therefore, this data further evidenced the implications of this subfamily in control of actin cytoskeleton dynamics (**Fig.1.4**). Moreover, CDK14 kinase activity was shown to influence the motility of HCC cell lines, providing a mechanistic explanation for the correlations found in human HCC patients. Similarly, another study demonstrated *CDK14* overexpression promotes proliferation, migration and invasion of gastric cancer cells, indicating the above-mentioned results could be extended to other tumor types [123].

Surprisingly, CDK15 expression has been recently suggested to impair migration and invasion capacity of breast cancer cell lines [124]. This work demonstrates PA28α/β repress CDK15 expression and promotes cell migration, invasion and metastasis. Importantly, CDK15 expression is absent in tumoral tissue specimens in contrast to their normal tissue counterparts, although its mRNA was detected in human breast cancer cell lines.

The same study showed either *CDK15* knockdown or overexpression did not influence breast cancer cell line proliferation [124]. Nevertheless, another report found CDK15 contributes to TRAIL-induce apoptosis resistance via survivin phosphorylation in breast cancer cell lines [125], thereby having a direct effect in cell viability. Remarkably, CDK16 knockdown was also shown to sensitize prostate cancer cell lines

to TRAIL-induced apoptosis [126], once again suggesting crosstalk or overlapping functions between members of the subfamily may exist.

Skin cancer seems to be another niche to explore the relevance of CDK14 and CDK16 in metastasis and tumor progression. Recent genomic analysis that took advantage of TCGA data suggested *CDK14* could be used as a marker for cutaneous melanoma metastasis [127]. Another report identified CDK16 and Nek9 as unique targets of the BRAF inhibitor Dabrafenib. The authors showed *CDK16* and *NEK9* are highly expressed in specimens of advanced melanoma, and their overexpression correlates with worse overall survival. Combined inhibition of both genes in the absence of *BRAF* mutations was shown to inhibit melanoma cell growth [128]. Interestingly, knockdown of CDK16 increased P27 expression, an effect that could be phenocopied by Dabrafenib [128]. The relationship between *CDK16* and *P27* was established in earlier studies that showed CDK16 phosphorylate P27 at S10 during S and M phases of the cell cycle [129]. These results were confirmed precisely in melanoma cell lines, were the knockdown of CDK16 was shown to inhibit proliferation [130].

Recent reports have shown CDK16 is highly expressed in lung cancer cells and tissues, and there is a correlation between CDK16 overexpression with lymph node stage and poor prognosis in lung cancer patients [131]. Another study has proposed *CDK16* can be used as a diagnostic biomarker, as it was found to be abundant in the plasma of lung cancer patients as a circulating mRNA, a its high abundance correlated with poor-progression free survival [132]. Moreover, CDK16 has been shown to phosphorylate p53 at S315 in lung cancer cells. This modification inhibits TP53 transcriptional activity and promotes its ubiquitin-dependent degradation. CDK16 control of TP53 stability has been proposed as a mechanism of radioresistance in lung cancer cells through the suppression of reactive oxygen species (ROS) production, DNA damage response and TP53-dependent induction of cell death [133].

Links between this subfamily of CDKs and DNA damage have become more evident in the recent years. CDK18 has been implicated in radioresistance in breast tumors [134], and also seems to be related to TP53, influencing cell growth and reactive oxygen species (ROS) formation in glioblastoma cell lines [135]. Several reports also found CDK18 influences DNA damage response and replication stress signaling [134][136]. Interestingly, whereas CDK16 has been identified as an off target of some clinically relevant PARP inhibitors, CDK18 has been suggested as a mediator of

resistance to PARP inhibition in glioblastoma through ATR activation and the induction of homologous recombination (**Fig.1.4**) [137].

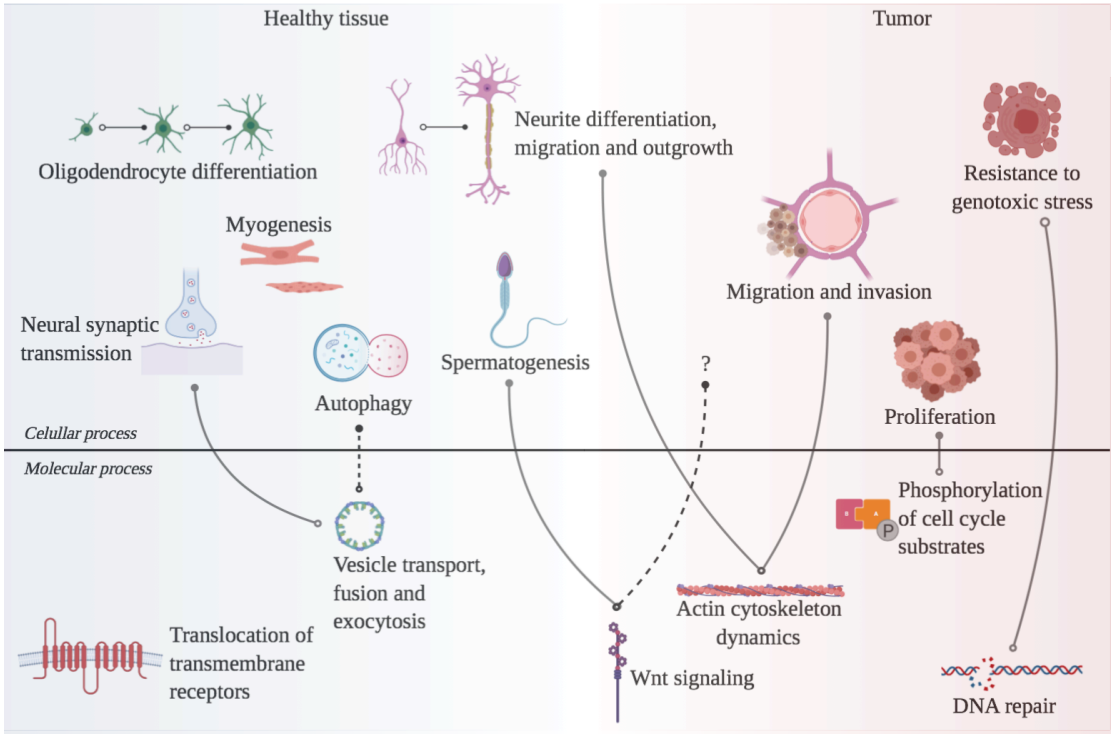

Figure 1.4. Schematic representation highlighting described roles of Y-cyclins and CDK14-18 subfamily in healthy tissues and tumor cells. Some CDK14-18 implications in healthy tissues were demonstrated to be events exploited by cancer cells. Control of actin cytoskeleton dynamics connects differentiation in the nervous system and migration of neural lineages with the metastatic capacity of tumor cells from different tissue of origin. Connections lacking robust experimental demonstration are represented with dashed lines.

Importantly, CDK18-mediated resistance to PARP inhibitors was shown to be dependent on MYC and MYCN, which mediate transcriptional repression of *CDK18*. Since CDK18 depletion was shown to sensitize cells to PARP inhibition by inducing defects in homologous repair signaling, this allows the distinction between responders and non-responders depending on *MYC* amplification status and CDK18 expression [137]. Interestingly, a previous report had already identified CDK16 in a kinome-wide RNA interference screening to find novel kinases that may be targeted to inhibit the proliferation of c-Myc-overexpressing medulloblastoma (MB) [138]. Given that MYC amplification characterizes a subgroup of MB with very poor prognosis, this result provides another link between PCTAIRE kinases, MYC amplification and therapeutic potential of their inhibition.

Altogether, CDK14-18 data in human cancer indicate they may play important roles in several tumor types of different oncogenic backgrounds and in particular of

those related to *MYC* amplification. Whereas cyclin Y has been mainly related to differentiation, CDK14-18 roles in cancer cells suggest additional partners may regulate their activity in these contexts. Finally, expression of these genes is frequently deregulated in human cancer and associated to resistance to several current clinical treatments and poor prognosis, indicating their activity is required for sustained cancer progression and their inhibition could represent novel therapeutic opportunities.

2. Objectives

CDK14-18 is the less characterized subfamily of human cell cycle-related CDKs. The discovery of their interaction with cyclin Y set the basis for several studies that aimed to characterize their implications in differentiation. However, over the years it has become clear that they display wider functional diversity, and data suggests their activity may be induced by different interactions. It is also evident that these kinases are altered in different tumors and mediate resistance to available clinical treatments. Characterization of the requirement of CDK14-18 for cancer progression and identification of tumor types susceptible to their inhibition is the main aim of this project. Thus, we sought to demonstrate their potential as therapeutic targets by proposing the following objectives:

1. Comparative analysis of the requirement of CDK14-18 for cancer cell line proliferation and selection of susceptible tumor types.
2. Biochemical analysis of molecular alterations following CDK14-18 depletion in cancer cells.
3. In vivo studies of the physiological requirement of CDK14-18 for normal tissue viability.
4. In vivo validation of CDK14-18 as new cancer targets in HCC.

3. Materials and Methods

3.1. Cell culture and cellular biology

3.1.1. Cell culture and proliferation analyses

All human cancer cell lines were grown in DMEM supplemented with 10% FBS, or alternatively in RPMI 10% FBS at 37ºC; 5% CO2. Huh7, HepG2, SNU449, SNU475, JHH2, PLC5 and Hep3B HCC cell lines were kindly provided by Dr. N. Djouder (Growth factors, metabolism and cancer group, CNIO, Spain) and Dr. A. Lujambio (Icahn School of Medicine at Mount Sinai, USA). Human embryonic kidney (HEK) 293-T cell line was obtained from American Type Culture Collection (ATCC). All cell lines were checked to be mycoplasma-free. Single cell clones of the Huh7 cell line stable for the CRISPR-Cas9 system for CDK14, CDK16, CDK17 and CDK18 ablation, and control Cas9 empty vector, were *de novo* generated from the parental cell line. Unless otherwise indicated, Huh7 cell line was used for most experiments.

For cell cycle analysis, western blot and RNAseq experiments, cells were seeded into 60 mm plates at an initial density of 300,000 cells per well for 48h samples and decreasing concentrations for longer time points and infected simultaneously in suspension.

For proliferation analyses, optimal non-confluent densities were determined for each cell line. For colony formation and growth curve assays with single cell clones, cells were plated at an initial density of 8000 cells per well in 6-well plates, and cultured for 9 days, until colonies were visible. When colonies were visible, cells were fixed in methanol and stained with Giemsa. Colony number/area was automatically measured using ImageJ software, plugin ‘’colony area’’.

To analyze the requirement of CDK14-18 for the proliferation in a panel of human cancer cell lines, cells were seeded on µCLEAR bottom 96-well plates (Greiner Bio-One) in lentivirus-CRISPR/Cas9 containing medium. 6 days after infection cells were fixed in paraformaldehyde 4% and stained for Hoechst. Nuclei counting was performed using OPERA high content screening (Perkin Elmer).

3.1.2. Cell cycle analysis by flow cytometry

For quantification of S- phase entry, cells were incubated with 10 µM EdU for 30 minutes before harvesting. Cells were trypsinized and split in complete media containing 10% FBS for the indicated time points and DNA replication was analyzed by flow cytometry. Fixation was performed in cold 70% ethanol at 4ºC for at least 12 h. For EdU staining we followed the classical azide-based EdU Click-iT protocol

(Invitrogen) plus an additional step for signal amplification using biotin-azide and streptavidin-Alexa fluor. For cell cycle profile analysis, DNA was stained with DAPI (Sigma). Samples were run on a LSR Fortesa flow cytometer (BD, San Jose), and 10,000 single events were acquired. Data were analyzed using the analyzer FlowJo v10 (Treestar, Oregon).

3.2. Molecular biology tools and constructs

3.2.1. sgRNA design, selection and cloning and RNAi-mediated knockdown

For sgRNA selection, CDK14-18 were queried in ChopChop v3 [139]. sgRNAs were selected according to the consensus criteria of absent/low off-target sites and high efficiency. Off-target sites, when present, were checked in the human (hg38/GRCh38) and murine (mm10/GRCm38) reference genomes to discard disruption of annotated exonic sequences. In all cases, sgRNAs with off-target sites with three or less mismatches were discarded.

Table 3.1. sgRNAs against human and murine genes used in this work. Target loci (gene), and position in gene of target sequence (exon), as well as PAM sequence required for Cas9 function are indicated. T7E1 primers are listed, with forward primer in the top row and reverse sequence in bottom row.

Gene	Position	sgRNA target sequence	PAM	T7E1 primers
		Homo sapiens		
CDK14	Exon 8	TGACACGGGGGAGTTAAAGC	TGG	TGGAGTACAGATCTCTCTGGC
				AAAGACTCTAACAAGCAGTCTGAAT
CDK15	Exon 7	GTTTCAACTTTTGCGGGGCC	TGG	TGTCAGGAAAAGCAGAATCCC
				ATGTTCTTGGGCCTCCAGTT
CDK16	Exon 9	CGAGAGGGGAGAGCTCAAGC	TGG	CAGGAAGCAGGGGCACAAG
				AGGCCTGGAAATCAGAGAAAGG
CDK17	Exon 3	ACATAGACGGATCTCAATGG	AGG	GTGATTTTTACTCGTTGGCCT
				AGTAACTTTCTTACAAGTGTCACG
CDK18	Exon 8	ACCACCGCAAGATCCTGCAC	CGG	CCACACTCACTGCGTCCTCTG
				GTCACCACCTCATTGGAGTAAGTC
		Mus musculus		
Cdk15	Exon 1	CTACCACCGTTCGGAGGGAG	GGG	GGGTGGGAAGAGGTTCAAGG
				AAGTCAAAAGCGGCCAAACC
Cdk17	Exon 6	GGCATTAAAAGAGATCCGCT	TGG	TTAGCAGCTGTCACATCTTAAAAA
				GTCACCATGGTCTCTCCATAAC
Cdk18	Exon 5	GGCCCTGAAGGAGATCCGGC	TGG	AGGGAGAGTGTGAGCAGGAT
				GAGGTCATGCAGGGTCACAA

Selected sgRNAs were subcloned into pLentiCRISPRv2 (Addgene #56921), or alternatively pLentiCRISPRv2GFP (Addgene #82416), by restriction enzyme digestion of the vector (BsmBI, New England Biolabs) and oligonucleotide annealing and

ligation. Oligonucleotides containing the sgRNA target sequence were designed with 5'- and 3'-overhangs complementary to the BsmBI restriction site cut.

For MYC knockdown, cells were transfected in suspension (400.000 cells) with scramble (Quiagen) or human MYC siRNA (Horizon) in OPTIMEM medium and using RNAiMax lipofectamine (Invitrogen). Cells were incubated with transfection mix for 4 hours and then fresh medium was added. 24-48 hours after transfection cells were collected for subsequent analyses.

3.3. Biochemical analyses

3.3.1. Protein overexpression

As previously mentioned, for transient overexpression of proteins, cDNAs were subcloned into pcDNA3.1 (+) (Thermofisher Scientific #V79020). pcDNA3.1 (+) vector was transfected in OPTIMEM medium into Huh7 cells using Lipofectamine 2000 (Invitrogen) for 4 hours, and then fresh medium was added. For MYC overexpression we purchased pcDNA3.1-MYC (Addgene #16011). 24-48 h later, cells stably expressing the cDNA were collected for subsequent analyses and experiments.

3.3.2. sgRNA validation and protein knockout

For virus production, pLentiCRISPR v2 plasmids were co-transfected into HEK293-T cells in suspension along with packaging pMDL, pREV and envelope (VSVG) expression plasmids using Lipofectamine 2000 (Invitrogen) and following manufacturer's instructions. Lentiviral supernatants were collected 48 hours after transfection and target cells were infected in suspension in the presence of 4 µg/mL polybrene and selected in puromycin for 48 h. Efficiency of edition for selected sgRNAs was primarily assessed by T7E1 assay (**Figure 3.1**), using specific primers for PCR amplification step (**Table 3.1**) and T7E1 for digestion of PCR products (New England Biolabs).

3.3.3. Single cell clones

pLentiCRISPR v2-GFP plasmid was used to infect Huh7 and sort GFP+ cells (Influx Citopeia-Becton Dickinson) into µCLEAR bottom 96-well plates (Greiner Bio-One). Single cell clones were grown in the presence of puromycin and validated for Cas9 expression and protein knockout by western blot.

For sequence analysis, genomic region corresponding to the targeted site was amplified by PCR with specific primers (**Table 3.1**), and PCR product was subcloned in pGEM (Promega) for transformation of competent bacteria. Six colonies were picked

from ampicillin containing LB-agar plates and grown in LB medium at 37ºC. after 24 hours DNA was extracted and sequenced using PCR primers (**Figure 3.1**).

Same procedure was followed for CDK16 and CDK18 KO clones and their combinations. In all cases, only when both alleles contained an insertion/deletion (indel) leading to disruption of the ORF (or when WT sequence was not found), clone was selected.

Knockout efficiencies were additionally examined by immunoblot analysis using specific antibodies against target proteins (see below). In all cases, lentiviral vectors contained puromycin resistance gene, used for selection of infected cells, for 48h, at the optimal concentration (2 μg/mL for Huh7, Hela, HepG2, Hep3B and SNU475; 3 μg/mL for SNU449).

3.3.4. Immunobloting

For immunoblot analysis, cells were extracted on ice in cold lysis buffer (50 mM Tris-HCl pH 7.5, 1 mM EDTA, 1 mM EGTA, 0.1% Triton X-100, protease inhibitors, 1 mM sodium orthovanadate, 50 mM sodium fluoride, 20 mM β-glycerophosphate, 0.1% 2-mercaptoethanol), or alternatively in Laemmli buffer 1X at room temperature (RT). Cell lysates were cleared by centrifugation at 13.2K rpm for 15 min at 4ºC and protein was quantified using the Bradford method when resuspended in cold lysis buffer, or at 13.2K rpm for 15 min at RT and quantified by the BCA method when resuspended in Laemmli. Protein extracts were mixed with sample buffer (350 mM Tris-HCl pH 6.8, 30% glycerol, 10% SDS, 0.6 M DTT, 0.1% bromophenol blue), boiled for 10 min and subjected to electrophoresis using the standard SDS-method. Proteins were then transferred to a nitrocellulose membrane, blocked in PBS 0.1% Tween-20 buffer containing 3% non-fat dried milk, and probed overnight with primary antibodies (1:500-1:10.000 dilution) (**Table 3.3**) at 4ºC and for 1 h at room temperature with peroxidase-conjugated secondary antibodies. Blots were developed using enhanced chemiluminiscence reagent (Western Lightning Plus-ECL; Perkin Elmer), exposed to an autoradiograph film and developed using standard methods. Films were scanned and quantifications were performed using ImageJ.

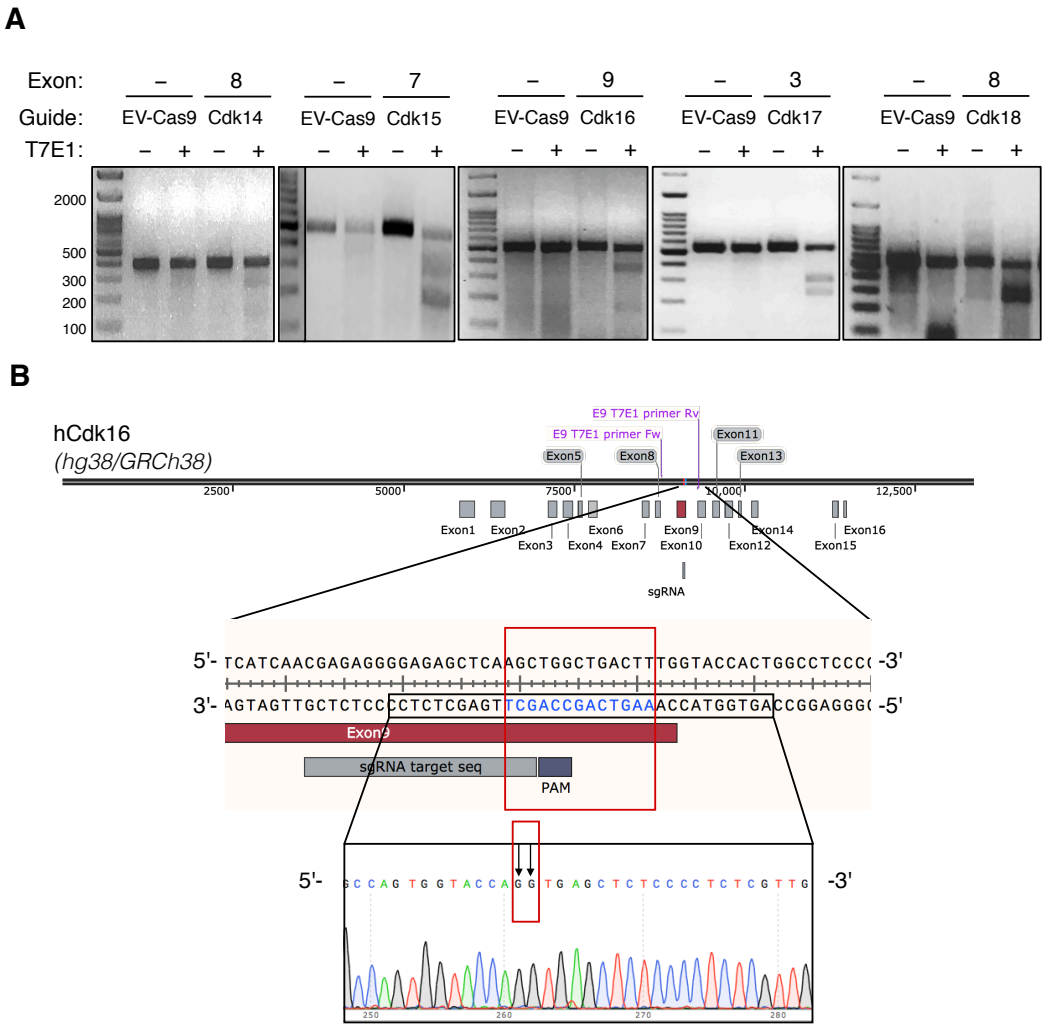

Figure 3.1. In vitro validation of CDK14-18 genetic ablation. A) T7E1 assay for sgRNAs against human genes. Endonuclease cut activity was used as a read-out of edition by the CRISPR/Cas9 system as previously described [140]. Hela cells were infected with lentiCRISPRv2 and selected in puromycin. DNA was extracted from the pool of resistant cells, PCR performed, and T7 endonuclease digestion executed. Empty vector (EV-Cas9) was used as a control. **B)** Schematic map of *CDK16* genomic sequence, primers for amplification of edited genomic region (named T7E1 forward and reverse) and validated sgRNA target site. As an example, edited sequence found in one CDK16 KO single cell clone is depicted. Indels (red box) are highlighted (blue and red letters), and their corresponding position in PCR-amplified sequence is shown (black box).

Table 3.3. Antibodies used for immunoblot and immunofluorescence analyses.

Protein symbol	Residue	Reference	Company	Dilution (IF/WB)
Western blot/IF				
CDK14	–	sc-376366	Santa Cruz	1:500
CDK15	–	TA811932	ThermoFisher	1:500
CDK16	–	HPA001366	Sigma Aldrich	1:1000
CDK17	–	NBP1-87316	Novus Biologicals	1:1000
CDK18	–	NBP1-92249	Novus Biologicals	1:1000
RB1	–	554136	BD Pharmigen	1:1000
CCNY	–	NBP1-88542	Novus Biologicals	1:1000
pß-catenin	S33/37/Thr41	9561	Cell Signaling	1:1000
H2AX	S139	07-164	Millipore	1:200
		2577	Cell Signaling	1:500
Cas9	–	14697	Cell signaling	1:5000
pCHK1	S280	2347	Cell Signaling	1:1000
	S345	2348		
c-MYC	–	sc-40	Santa Cruz	1:1000
pMYC	T58	ab185655	Abcam	1:500
pMYC	S62	Ab185656	Abcam	1:500
MIZ1	–	14300	Cell Signaling	1:1000
SP1	–	5931	Cell Signaling	1:1000
pRPA32	S8	54762	Cell Signaling	1:1000
53BP1	–	NB100-304	Novus Biologicals	1:200
pLRP6	S1490	2561	Cell Signaling	1:1000
LRP6		2568	Cell Signaling	1:1000
VCL	–	V91-31	Sigma Aldrich	1:20000
Immunohistochemistry/WB				
CDK14	–	sc-376366	Santa Cruz	1:500
CCNY	–	NBP1-88542	Novus Biologicals	1:1000
c-MYC	–	sc-54	Santa Cruz	1:1000
ß-catenin	–	610153	BD Biosciences	1:500

3.3.5. Immunohistochemistry

For histological analysis tissues were fixed in 10%-buffered formalin (Sigma) and embedded in paraffin wax. Sections of 3- or 5-µm thickness were stained with haematoxylin and eosin (HE) or Periodic Acid Schiff (PAS) staining. Additional immunohistochemical (IHC) examination was performed using specific antibodies against Cyclin Y, Cdk14, proliferation and DNA damage markers and oncogenes used for the induction of tumors (**Table 3.3**).

3.3.6. Immunofluorescence

Cells were cultured in coverslips and fixed in 4% buffered paraformaldehyde (PFA) for 10 min at room temperature (RT). When performed, EdU staining was done following de Click-iT EdU specifications (Invitrogen; C10086) and followed by immunofluorescence (IF) staining of proteins of interest at a concentration of 1:100-1:500 (**Table 3.3**). Briefly, after EdU detection, cells were permeabilized with 0.5% Triton X-100 for 10 min and blocked with 10% FBS for 1h at RT, antibodies were incubated overnight at 4ºC and nuclei were stained with DAPI. Images were captured using a laser scanning confocal microscope TCS-SP5 (AOBS) Leica. Image analysis was done using ImageJ software.

3.3.7. Luciferase reporter assays

Hela cells were infected in suspension in p100 dishes with LentiCRISPR viruses containing either an empty vector (EV-Cas9) or sgRNAs against human CDK14-18. 72h after infection cells were trypsinized and $7.5x10^5$ cells were seeded in 6-well plates (n=3). pRL-CMV-Renilla luciferase (200ng/well), pGL3 control (2µg/well), pBv-Luc wt MBS 1-4 (2µg/well), pBv-Luc mut MBS 1-4 (2µg/well), pGL2 HBM Luc (2µg/well), pCDNA3 human MYC (1µg/well) plasmids were cotransfected using Lipofectamine 2000 (Invitrogen). 6h after transfection medium was removed and replaced with DMEM low glucose, 10% FBS supplemented with 1µg/ml of Puromycin for selection of infected cells. 24h after transfection of reporter plasmid, cells were harvested and seed over 96-well plates in 75µL of complete medium. 75µL/well of Dual-Glo® Luciferase Reagent (Dual-Glo® Luciferase Assay System E2920, Promega) was added. After 30 minutes of incubation at RT, protected from light, Firefly luminescence was measured (550 nm). Finally, 75µL/well Dual-Glo® Stop & Glo® reagent was added. Following 30 minutes of incubation at RT protected from light,

Renilla luminescence was measured (481 nm). For background luminescence removal ratio between Firefly luminescence/ Renilla luminescence was calculated. Fold change values were normalized to pGL3-Luc control vector.

3.3.8. Treatments

For cell culture treatment, inhibitors were added at the indicated concentrations and times (see table 3.4).

Table 3.4. Compounds used in this work and their working concentration.

Compound	Target (Gene name)	Concentration	Time	Supplier
Palbociclib	CDK4,6	0.5 µM	48h	Selleckchem
Olaparib	PARP	10 µM	48h	Selleckchem
Cis-platin	-	1 µM	48h	Selleckchem
ATRi	ATR	0.3 µM	48h	CNIO
FMF-04-159-2	CDK14-18	0.2-1 µM	24-48h	Tocris
EndoIWR1	Axin2	10 µM	8-24h	Sigma Aldrich
iCrT3	ß-catenin	75 µM	8-24h	Sigma Aldrich
CHIR99021	Gsk3ß	10 µM	8-24h	Tocris

3.4. Bioinformatic analysis

3.4.1. In silico and RNAseq/proteomics analyses

For cell line information Broad Cancer Institute Cancer Cell Line Encyclopedia (CCLE) was consulted. To assess the correlation between expression levels of CDK14-18 and patient survival, Kaplan-Meier Plotter was used [141]. Oncomine was employed to analyze alterations at the expression level (mRNA) of these genes in specific tumor types. Pre-processing of RNAseq data (obtained by using QuantSeq expression profiling library prep kits) involved BAM files conversion to FASTQs files using Lexogene Quantseq pipeline at BlueBee Genomics platform, which was also used to ibtain differential expression analyses. RNAseq and proteomics data processing involved use of several publicly available databases and tools (Enrichr, DAVID, Venny) [142][143][144]. Additionally, specific software for gene enrichment analysis was used (GSEA 4.1.0). Gene enrichment analyses were carried out at a number of permutations

of 1000, with no collapse to gene symbols, using several gene set databases and the Chip platform NCBI_Entrez_Gene_ID_MSigDB.v.7.2.chip.

3.5. Studies in vivo in CDK14-18 mutant mice

3.5.1. Generation of *Cdk14*, *Cdk15*, *Cdk17* and *Cdk18* KO mice

Constitutive loss-of-function knockout mouse models were generated for all members of CDK14-18 subfamily with the exception of *Cdk16*-null mice (previously reported by [54]). For *Cdk14*, targeting vector carrying a neomycin resistance gene flanked by frt sites in *Cdk14* intron 4 and loxP sites flanking exon 4, was electroporated in mouse embryonic stem cells (mESCs). Once homozygous clones were selected, they were used for the generation of chimeric mice by microinjection in developing blastocysts. The resulting chimeric mice $Cdk14^{+/loxfrt}$ were crossed with C57BL6/J mice. Subsequently, the neo cassette was removed by mating with mice expressing the Flp recombinase (Tg.pCAG-Flp), generating the *Cdk14* cKO allele, termed $Cdk14^{lox}$. To obtain a ubiquitous and constitutive depletion of Cdk14, $Cdk14^{+/lox}$ mice were crossed with animals expressing DNA recombinase Cre (Cre) under control of a human cytomegalovirus minimal promoter (CMV). Excision of exon 4 of the *Cdk14* gene leads to a frame shift in the mRNA generating several new premature stop codons that results in loss of CDK14 protein and renders the $Cdk14^{\Delta}$ allele.

For *Cdk15*, *Cdk17* and *Cdk18*, specific sgRNAs were validated (**Table 3.1**) and microinjected along with Cas9 protein for the generation of chimeric mice. Genomic DNA of edited mice was analyzed by pGEM cloning and sequencing to detect mutations. Mice with frame-shift mutations were selected and crossed with C57BL6/J mice to fix the mutant alleles. $Cdk15^{-/-}$ mice with 31 base pair deletion, $Cdk17^{-/-}$ with 16 base pair deletion and $Cdk18^{-/-}$ mice with 17 base pair deletion were expanded and used in subsequent experiments.

Mice were housed in the pathogen-free animal facility of the CNIO (Madrid) and maintained under a standard 12-h light-dark cycle, at 23ºC with free access to food and water. All animal work and procedures were approved by the ISCIII committee for animal care and research and were performed in accordance with the CNIO Animal Care program.

Routine genotyping of the $Cdk14^{lox}$, $Cdk16^{lox}$ *and* $Cdk14^{-}$, $Cdk15^{-}$, $Cdk17^{-}$ *and* $Cdk18^{-}$ alleles was done by PCR using DNA from the tail of the mice. All PCRs were done using a standard Taq Polymerase (Promega), and the following protocol with

specific primers in each case (**Table 3.5**): i) 5 minutes at 95ºC to denaturalize the DNA; ii) 35 cycles of denaturing 30 s at 95ºC, annealing 30 s at the specific temperature for each primer pair, and elongation 60 s at 72ºC; and iii) final elongation step 10 min 72ºC.

Table 3.5. Primers used for genotyping *CDK14-18* mutant alleles.

Allele	Product amplified	Primer sequence	Annealing Tº
Cdk14(lox)	*Cdk14(+)/Cdk14(lox)*	CTTTATTTTGGTCCCTCCCCAACT GTACACTGTTGCATAAGATCCTTCCCCCA	58ºC
Cdk16(lox)	*Cdk16(+)/Cdk16(lox)*	GGGTACCTATGCCACTGTCT GGCCTTGTTCTAAACCTAAG	58ºC
Cdk14(-)	*Cdk14(+)/Cdk14(-)*	CTTTATTTTGGTCCCTCCCCAACT GCCCAATATATACTAAAGCACCATGAGG	55ºC
Cdk15(-)	*Cdk15(+)/Cdk15(-)*	GGGTGGGAAGAGGTTCAAGG AAGTCAAAAGCGGCCAAACC	61ºC
Cdk17(-)	*Cdk17(+)/Cdk17(-)*	CTATAGGGTACATATGCAACAG CCAAAAGTTCTATGTAAACACTG	51ºC
Cdk18(-)	*Cdk18(+)/Cdk18(-)*	GTACCTATGCCACCGTCTTCAAG CATTGTACCCTCTCGAATAGC	51ºC

PCR products were run in 2% agarose gels for all alleles and 4% gels for CRISPR-generated indels and interpreted as follows: PCR products for $Cdk14^{lox}$ were 1200 bp for $Cdk14^{lox}$, 950 bp for $Cdk14^{+}$ allele and 362 bp for $Cdk14^{-}$ allele. PCR products for $Cdk16^{lox}$ were 530 bp for $Cdk16^{lox}$ and 590 bp for $Cdk16^{+}$ allele. $Cdk15^{-}$ PCR gave a band of 150 bp for $Cdk15^{+}$ allele and 110 bp for $Cdk15^{-}$. $Cdk17^{-}$ PCR produced a band of 147 bp for $Cdk17^{+}$ allele and 131 bp for $Cdk17^{-}$. $Cdk18^{-}$ PCR produced a band of 122 bp for $Cdk18^{+}$ allele and 105 bp for $Cdk18^{-}$.

3.5.3. Hydrodynamic injection for the generation of liver tumors

For the generation of liver tumors, we followed standard protocols for the hydrodynamic injection technique [145]. Different combinations of oncogenes were tested for their capacity to generate liver tumors in our mice at different concentrations and injected in saline solution (10% of body weight) in the lateral tail vein in a rapid injection (6s), along with sleeping-beauty transposase (SB13) for stable oncogene expression, according to standard protocols. Luciferase reporter signal (SB13 vector) was assessed one week after injection in an IVIS Spectrum In Vivo Imaging System (Perkin Elmer). Mice status was monitored during 30 minutes after injection and every day until the end of the experiment, according to EU and CNIO's good care practices.

DNA vectors containing SB13 transposase and oncogenes were kindly provided by Dr. Amaia Lujambio (Icahn School of Medicine at Mount Sinai, USA).

3.5.4. Treatment with FMF-04-159-2

The CDK14-18 inhibitor FMF-04-159-2 [115] was administered to luciferase-positive mice 3 weeks after hydrodynamic injection. FMF-04-159-2 was administered by tail vein injection in a dose of 15 mpk, twice a week for 1 week. FMF-04-159-2 was dissolved in DMSO and control mice, which received only vehicle (DMSO; triton 0.01%), were included in the study to discard any effect indirect to the inhibitor.

3.6. Statistics

Statistical analysis was carried out using Prism 5 (GraphPad). Statistical tests were performed using either two-sided, unpaired Student's t-test, paired Student's t-test, 1- or 2-way ANOVA (Dunnet's multiple test) according to specifications in the figures. Data with $p>0.05$ were considered not statistically significant (ns); *, $p<0.05$; **, $p<0.01$; ***, $p<0.001$, ****, $p<0.0001$.

4. Results

4.1. Identification of susceptibilities to CDK14-18 depletion

4.1.1. Unbiased selection of susceptible cancer types

To determine which tumor types may benefit from CDK14-18 inhibition, we performed *in silico* analyses taking advantage of publicly available databases searching for association between alterations in these genes and specific tissues. Alterations such

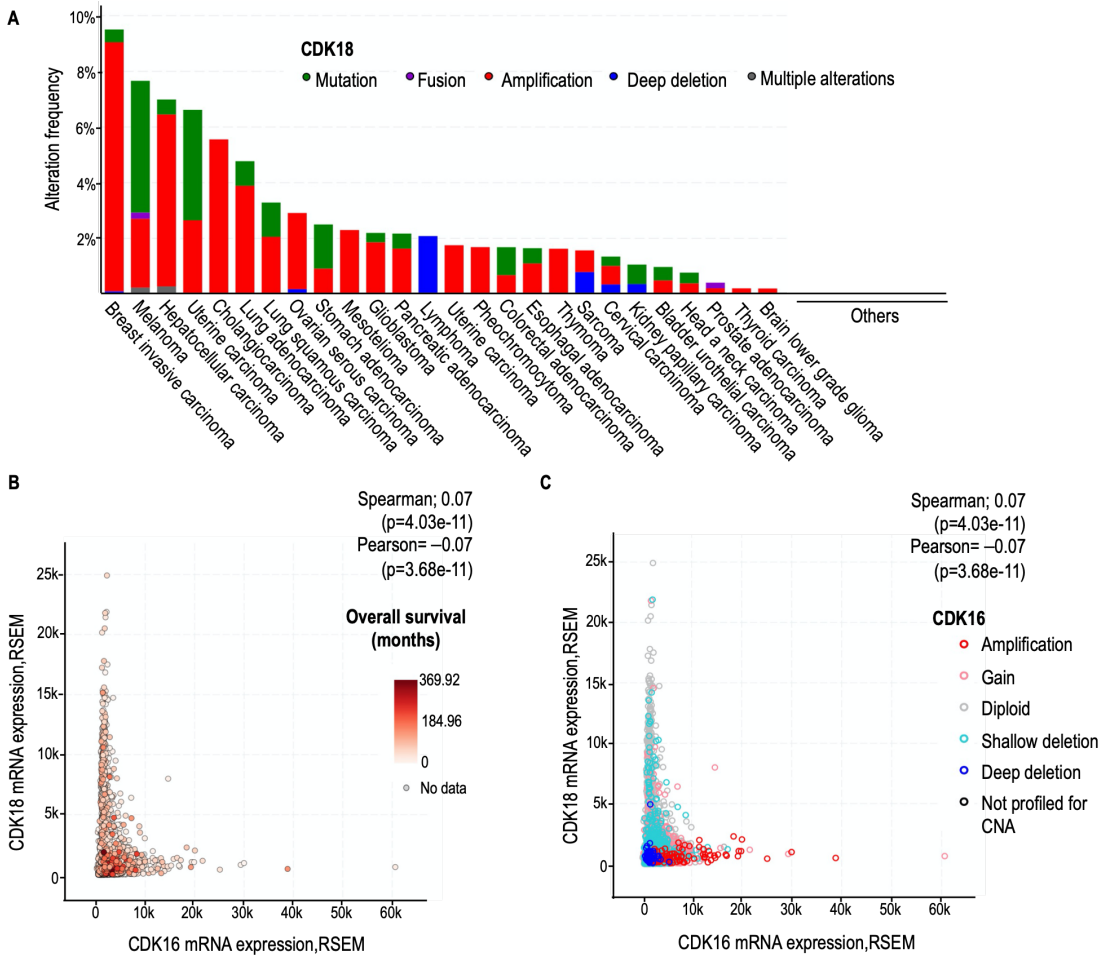

Figure 4.1. *In silico* analysis reveals CDK18 amplification in breast and liver tumors and a positive correlation in expression with CDK16 shallow deletion. **A)** CDK18 genomic alterations in human cancer (TGCA). Samples were distributed by studies and different colors correspond to mutation types, as indicated in the legend. **B)** CDK16 and CDK18 mRNA expression (batch normalized from Illumina RNAseq), and the corresponding overall survival (months) for each patient, in studies representative of all tumor types (TGCA). **C)** Same samples as in B) with the corresponding CDK16 genomic alterations with a specific color code, as indicated in the legend. Modified from cBioportal [146][147].

as amplifications or deletions were widespread with similar incidence across several tumor types, and therefore this information did not allowed selection of any specific tissue (data not shown). Nonetheless, when genes were queried individually, we found that CDK18 amplification was present in approximately 6-9% of breast, HCC and

cholangiocarcinoma tumors, but in a notably smaller fraction of all other tumor types (**Fig.4.1a**).

Because CDK16 is a close relative to CDK18 in terms of homology sequence, we sought to analyze the correlation in expression of these genes. As shown in **Fig.4.1b,c**, samples with low CDK16 expression tend to express high levels of CDK18, and conversely, although less numerous, samples with high CDK16 express low levels of CDK18 mRNA. Interestingly, samples with lower expression values correlated with better overall survival (**Fig.4.1b**). Samples with CDK16 shallow deletion had significantly higher levels of CDK18 mRNA, whereas those with CDK16 deep deletion showed a marked tendency towards low expression values for CDK18 (**Fig.4.1c**). None of these correlations were found for any other pair of genes in the subfamily, and individual analysis of other members showed their alterations were present in a markedly lower proportion of tumor types (data not shown).

Seeking to translate these observations into experimental data, we analyzed association between CDK14-18 expression and tissue origin in human cancer cell lines. Expression at the protein level of these kinases does not collectively associate to human cell lines of any particular tumor type, thereby correlating with the results from our *in-silico* analyses regarding genomic alterations (**Fig.4.2a,b**). Nevertheless, these analyses suggested certain positive correlation with MYC expression in the case of CDK16 and CDK18 (**Fig.4.2a,b**).

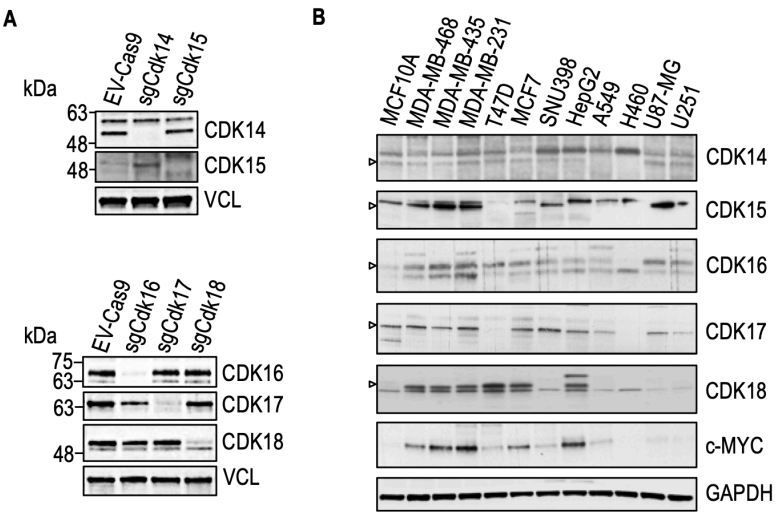

Figure 4.2. CDK14-18 antibody and sgRNA validation and expression analysis in human cancer cell lines.
A) CDK14-18 antibody and sgRNA validation, in Hela cells, 96 hours after infection with lenti-viruses expressing Cas9-sgRNAs targeting indicated genes. **B)** CDK14-18 and MYC expression in human cancer cell lines representative of different tissue origins. Bands of specific molecular weights in which intensity was reduced upon sgRNA expression were considered specific of each gene and indicated with arrows in B).

Following our initial analyses, we became interested in Hepatocellular carcinoma (HCC), since liver tumors appeared as positive hits for CDK16,18 alterations. We

confirmed that high CDK16 expression predicts worse overall survival in HCC patients as reported by the database *Kaplan-Meier Plotter* [141] (**Fig.4.3a**), and that *CDK16* mRNA expression can be found significantly up regulated in HCC samples compared to their normal tissue counterparts, according to data reported from *Oncomine* portal (**Fig.4.3b**). Furthermore, CDK14-18 expression in human HCC cell lines revealed that CDK16-18 could be detected in all cases, whereas CDK14-15 levels were more variable (**Fig.4.3c**).

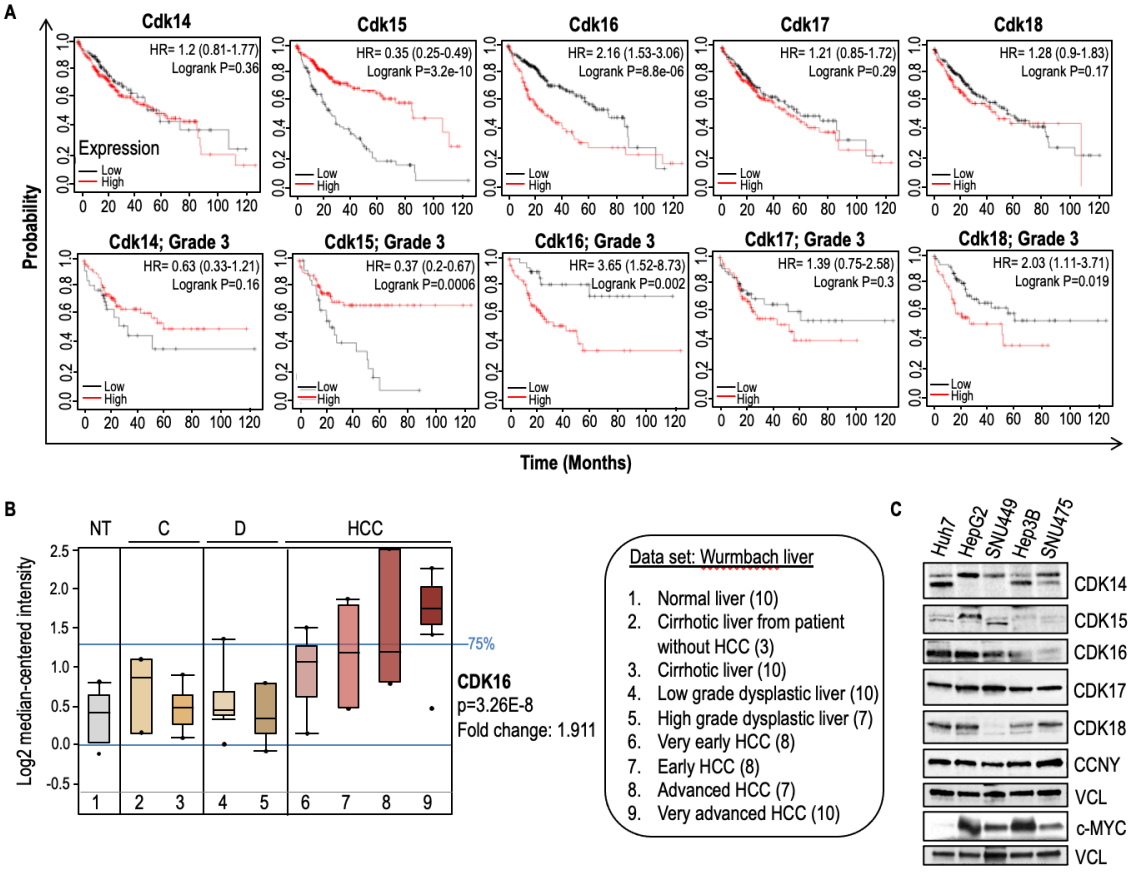

Figure 4.3. Analysis of CDK14-18 expression in human cancer reveals a correlation of CDK16 alterations with survival and disease progression in liver cancer. A) Kaplan-Meier plots of HCC patients stratified according to their CDK14-18 expression status, including all stages or only patients corresponding to HCC grade III [141]. **B)** CDK16 expression in normal liver versus samples representative of disease stages as indicated in the legend. Adapted from Oncomine. **C)** CDK14-18, Cyclin Y and MYC expression analysis in human HCC cell lines.

Although these correlations with survival and disease stage were rarely found in other tumor types and helped us narrow tissue selection, we decided to evaluate the impact of the depletion of these genes in a panel of human cancer cell lines which included liver cancer cells and several others randomly selected from different tissue of origin. This allowed us to identify susceptible tumor types and gather a comparative view of HCC susceptibility compared to others. We targeted CDK16,18 loci in these

cell lines with specific sgRNAs (**Fig.4.2a**), and CDK1 locus in a similar fashion as a positive control of reduced proliferation [20].

We initially focused in CDK16 and CDk18 to evaluate their requirement for proliferation/survival because we could expect positive hits, as previously reported [128][134], and because our *in-silico* analysis suggested a therapeutic value for these genes. We assayed the combination of the depletion of both genes based on two additional observations. First, CDK14-18 alignment revealed high sequence homology between CDK14 and CDK15 and between CDK16, CDK17 and CDK18 (**Fig.4.4a**). Second, CDK16 depletion leads to an up-regulation of CDK18 expression (**Fig.4.4b**), suggesting the existence of compensatory mechanisms. Concomitantly, single depletion of CDK16 or CDK18 did not render significant reduction in proliferation/survival in most of the cell lines evaluated, whereas combined depletion of both genes revealed significant differences in cell lines belonging to all tumor types evaluated (**Fig.4c**). Remarkably, all lung and liver cancer cells evaluated were susceptible (**Fig.4.4c**).

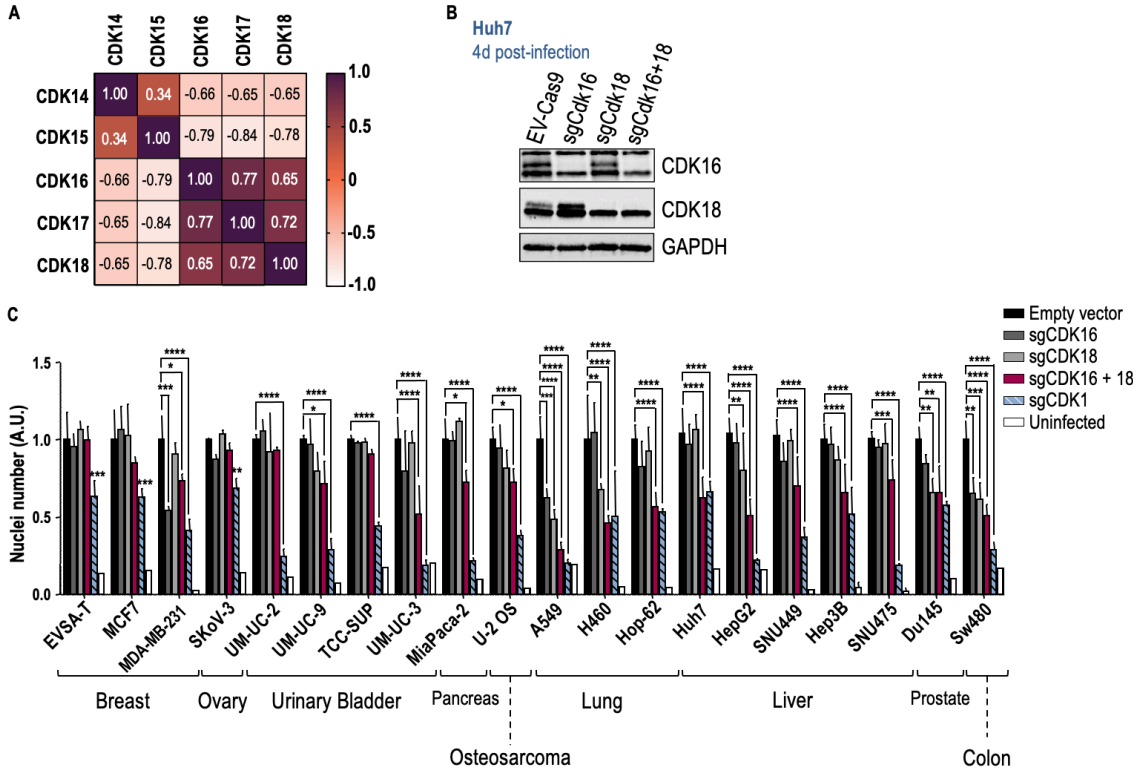

Figure 4.4. Rationale for CDK16,18 co-depletion and identification of susceptible human cancer cell lines. **A)** CDK14-18 kinase domain sequence alignment ('Pearson r' coefficient correlation; CI: 95%). **B)** CDK16 and CDK18 protein levels 96h after infection. **C)** CRISPR-Cas9 screening for the identification of human cancer cell lines susceptible to CDK16,18 depletion. Nuclei number (Hoechst) was normalized to Empty vector (EV) negative control. Histogram represents median ± SD of 3 technical replicates and 1-2 biological replicates. One-way anova: ns p>0.05; *p<0.05; **p<0.005; ***p<0.0005; ****p<0.0001.

4.1.2. Evaluation of susceptibilities to CDK14-18 depletion in human HCC cell lines

To further evaluate the requirement of other members of the subfamily and different combinations in HCC cell lines, we followed the same experimental approach used in the initial CRISPR/Cas9 screening. As in previous experiments, individual CDK14-18 depletion did not affected proliferation (**Fig.4.5a-c**). However, depleting all PCTAIRE subfamily members (CDK16-18) revealed a significant reduction in proliferation in most of the cell lines analyzed, whereas depletion of PFTAIRE kinases (CDK14-15) did not induce significant variations (**Fig.4.5a-c**).

Remarkably, two ‘’minimal combinations’’ lead to a significant reduction in cell number in a higher proportion of cell lines: CDK14,16 and CDK16,18 dKO (**Fig.4.5c**), hence suggesting that these CDKs share functional redundancy or cooperatively promote human HCC cell line proliferation and survival.

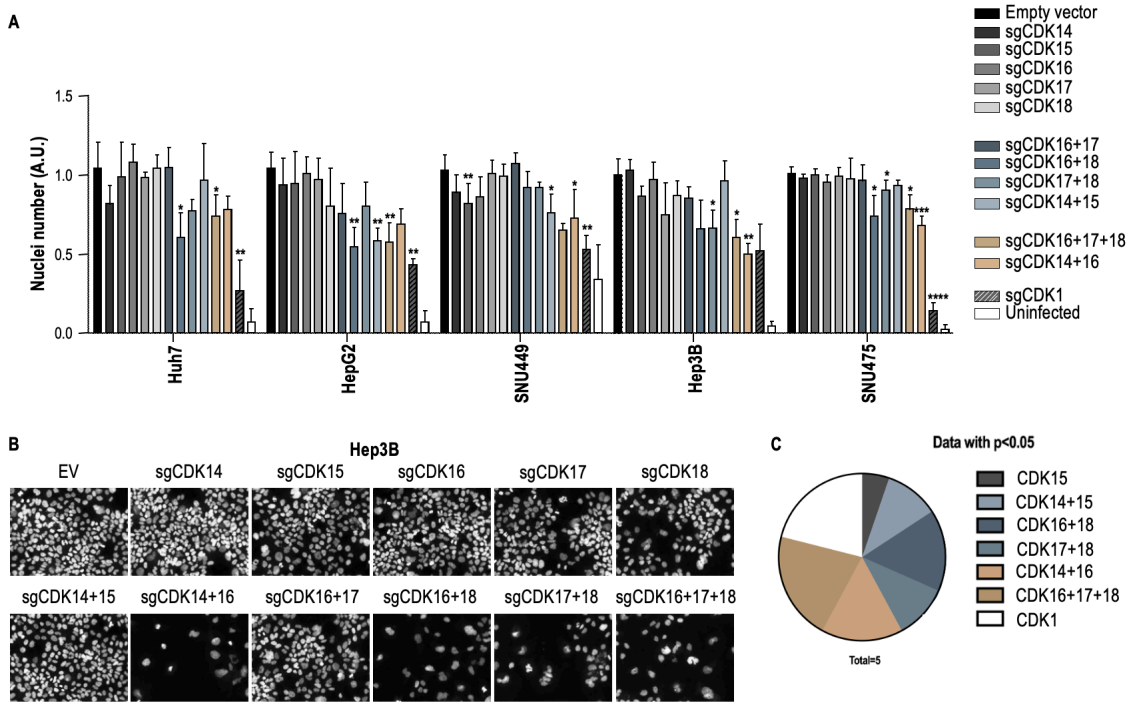

Figure 4.5. Evaluation of HCC cell line proliferation/survival after CDK14-18 depletion. **A)** CRISPR-Cas9 screen for CDK14-18 depletion in human HCC cell lines. Nuclei number was evaluated by Hoechst staining 6 days after infection with LentiCRISPR-Cas9 and normalized to Empty vector (EV) negative control. Histogram represents median ± SD of 3 biological replicates and a total number of 9 technical replicates. One-way anova: ns $p>0.05$; *$p<0.05$; **$p<0.005$; ***$p<0.0005$; ****$p<0.0001$. **B)** Representative images of fixed Hoechst-stained samples of control and CDK14-18 depleted Hep3B cells. **C)** Distribution of samples belonging to each group analyzed in the CRISPR-Cas9 screening with $p<0.05$.

4.2. Cell cycle and proliferative defects associated to CDK14, CDK16 and CDK18 depletion in HCC cell lines

4.2.1. Cell cycle alterations associated to CDK14-18 depletion

To better understand the above-mentioned reduction in cell number, we selected CDKs whose depletion induced a phenotype, to explore how their depletion affected cell cycle progression. We chose SNU475 and Huh7 cell lines because they express all members of the subfamily and therefore represent a good scenario to exclude functional redundancy in the evaluated phenotype (**Fig.4.3c**). CDK14, CDK16 and CDK18 individual knockout (KO) induced mild S and G_2/M increased cell populations six days after infection, compared to the lentiCRISPR-Cas9 empty vector (EV) control, in SNU475 cells (**Fig.4.6a**). This increase was more evident in CDK16,18 dKO and CDK14+CDK16,18 triple-knockout (tKO) cells (**Fig.4.6a,b)**, although, remarkably, there was no difference between the cell cycle profiles of these two groups (**Fig.4.6a**). Since CDK14,16 dKO combination did not improve cell cycle alterations compared to their single KO counterparts, we decided to further characterize CDK16,18 dKO combination.

These results were recapitulated using PAN-TAIRE inhibitor FMF-04-159-2 (hereafter referred as FMF), which inhibits all members of the subfamily with comparable efficacy [115], that induced a strong accumulation of cells in S/G_2/M phases (**Fig.4.6c**).

EdU incorporation was particularly affected in CDK18 KO cells, where we could observe an increase in S phase population with an observable dispersion of EdU+ cell cloud (**Fig.4.6d**). Similarly, CDK16,18 dKO cells accumulate in S phase and the cloud is not as discrete as in the control group (**Fig.4.6d**). These alterations in EdU incorporation and cell cycle progression in CDK18 KO cells suggest they undergo replicative stress, as supported by a recent publication [136]. To better understand defects in the transition throughout the cell cycle, we analyzed PCNA/γ-tubulin co-staining by immunofluorescence. Interestingly, CDK16,18 dKO cells were represented in a slightly higher proportion in S phase compared to control cells, but most strikingly, the earliest S phase fraction showed a prominent increase (**Fig.4.6e,f**). At later time points (6d), the most evident difference compared to control EV-Cas9 was the accumulation of cells in G_2 (**Fig.4.6e,f**), suggesting that CDK16,18 dKO induces S phase entry, replication stress and ultimately, G_2/M checkpoint activation.

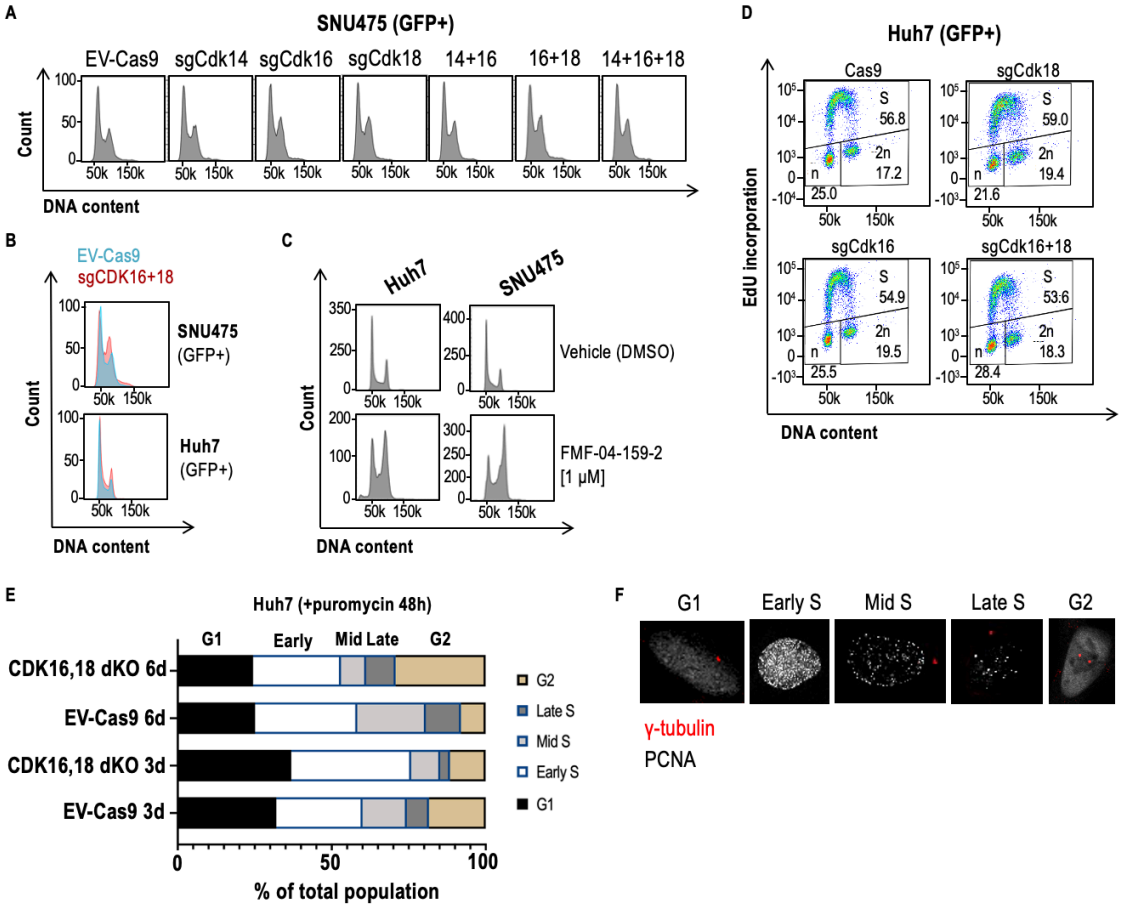

Figure 4.6. Evaluation of cell cycle progression after CDK14-18 depletion. A) DNA content analysis by flow cytometry of SNU475 cells infected with lentiCRISPR-Cas9 GFP, sorted for GFP+ cells and stained with DAPI. **B)** Comparison of control (EV-Cas9) and CDK16,18 dKO SNU475 and Huh7 GFP+ cells stained with DAPI for DNA content (n=3). **C)** Cell cycle profiles of SNU475 and Huh7 cells treated with DMSO or CDK14-18 inhibitor FMF-04-159-2, for 48 hours, and stained for DAPI. **D)** EdU/DAPI co-staining of Huh7 EV-Cas9 (Ctrl.) or CDK16/18 single and dKO GFP+ cells obtained as in A). **E)** Quantification of cell cycle phases in EV-Cas9 and CDK16,18 dKO Huh7 cells based on γ-tubulin and PCNA immunostaining. **F)** Representative images of PCNA/γ-tubulin immunostaining corresponding to indicated cell cycle phases.

4.2.2. Adaptation to CDK16 and CDK18 depletion is severely impaired in CDK16,18 dKO combination

Given CRISPR/Cas9 system introduces random indels, with *wild type-like* mutational events or affecting only one out of two alleles of the target loci, we speculated observed phenotypes were attenuated by these factors. Therefore, we sought to obtain single cell clones and evaluate the mutations introduced in each of the edited *CDK16-18* loci. Furthermore, analysis of stable KO clones would allow us to evaluate the adaption to depletion of CDK16/18 in the long term, for which we used Huh7 cell line that expresses all members of the subfamily (**Fig.4.3c**). After selecting cells edited

in both alleles and with frameshift mutations giving rise to premature stop codons, we tested proliferative capacity of these clones.

As expected, impact in proliferation was stronger compared to the lentivirus infection pools, and significant even for CDK16/18 single depleted cells (**Fig.4.7a-c**). Like previously, combination of CDK16,18 dKO was more efficient reducing growth over time and colony formation capacity, with its single KO counterparts rendering an intermediate effect between the WT and the dKO (**Fig.4.7a-c**).

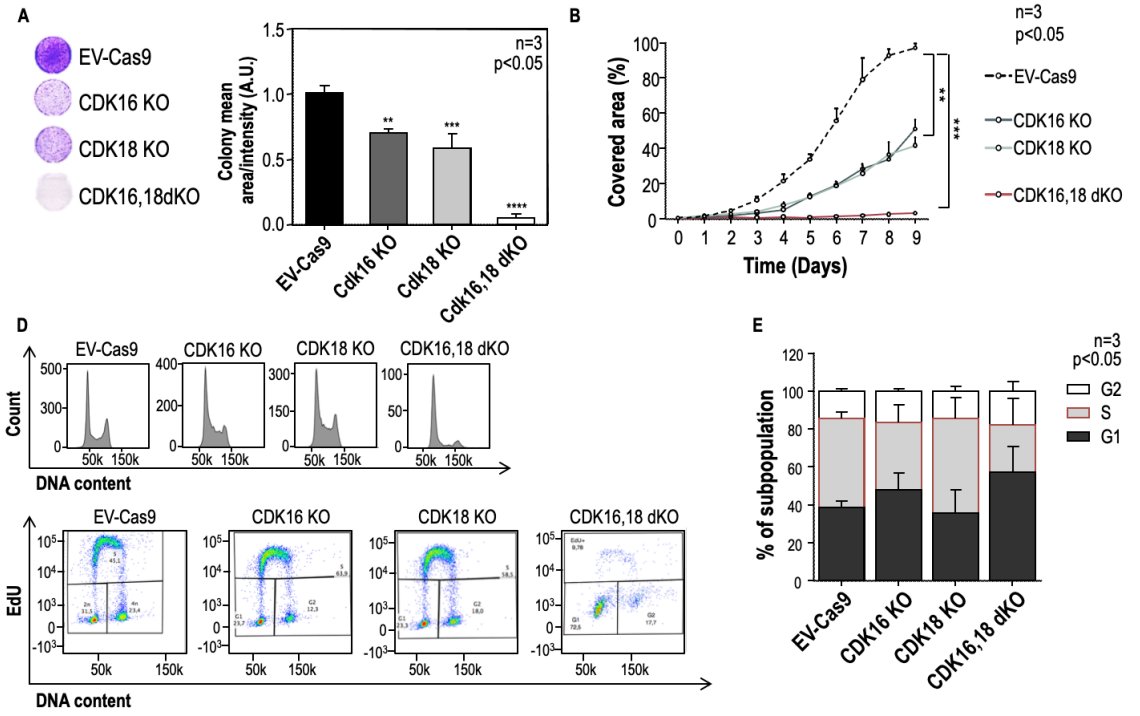

Figure 4.7. Characterization of CDK16,18 depletion effects in the proliferative behavior of Huh7 single cell clones. A) Representative images and quantification of colony formation assays and **B)** growth curve of CDK16,18 KO and dKO single cell clones. **C)** Representative images of FACS analysis of total DNA content histograms (DAPI) and EdU incorporation of CDK16,18 KO and dKO single cell clones. **E)** Quantification of EdU incorporation. All experiments included in this figure are representative of n=3 single cell clones ± SD. One-way anova: ns p>0.05; *p<0.05; **p<0.005; ***p<0.0005; ****p<0.0001.

Concomitant to reduced proliferative capacity and compromised tumoral properties, cell cycle analysis of these single cell clones denoted an tendency towards accumulation of cells in G_1 in CDK16 KO cells (p=0.072), which was intensified in some of the CDK16,18 dKO clones (p=0.163) (**Fig.4.7d,e**). Other CDK16,18 dKO clones, however, showed increased S phase populations (p=0.127), a re-distribution that was also observed in CDK18 KOs (**Fig.4.7d,e**). Hence, CDK16,18 dKO clones show mixed effects that reflect CDK16 and CDK18 individual KO alterations. To summarize, statistical analysis of cell cycle alterations in these clones revealed a clear, yet in many

cases non-significant ($p<0.05$) tendency towards variations in cell cycle progression, therefore suggesting that significantly reduced proliferation was also a consequence of compromised survival.

4.3. Transcriptomic and proteomic analysis of CDK14-18 depleted cells

4.3.1. CDK16,18 co-depletion improve enrichment in specific signatures associated to their single depletion

To explore gene expression alterations following CDK16,18 depletion, we analyzed transcriptomic profiles (bulk RNAseq) of individual CDK16 and CDK18 KOs, and CDK16,18 dKO Huh7 cells compared to controls infected with lentiCRISPR-Cas9 empty vector (EV). We initially focused in CDK16,18 dKO combination to ease the understanding of the additive/synergistic effects we encountered with their depletion.

Interestingly, individual CDK16 and CDK18 KOs induced almost identical alterations (**Fig.4.8a**). All significantly deregulated gene sets were found in common for the three groups or between the single KOs (**Fig.4.8b**), and CDK16,18 dKO unique hallmarks were also deregulated in single KOs to a lesser and non-significant extent (**Fig.4.8a**), thereby arguing in favor of functional redundancy between these genes. Therefore, we interpret that a combination of CDK16,18 depletion cooperates increasing the depth of transcriptomic alterations found in their single KO counterparts.

Given that CDK16,18 dKO cells elicited a stronger reduction in proliferation and cell cycle defects, we wanted to gain insight into the gene sets with stronger enrichment or uniquely deregulated in the combination of both genes. Based on FDR qValue difference, gene sets with more robust association to CDK16,18 dKO cells compared to their single KO counterparts were WNT signaling via ß-catenin (FDR=0.046; NES=1.42), DNA repair (FDR=0.063; NES=1.37) and MYC targets V2 (FDR=0.009; NES=1.63) (**Fig.4.8a,b**).

As shown in the following sections, JHH2 cell line is partially resistant to CDK16,18 depletion and CDK14-18 pharmacological inhibition. Further supporting that significant deregulation in the above-mentioned hallmarks may be responsible for the stronger phenotypes that associate to the combination, CDK16,18 depletion in JHH2 did not induced a significant enrichment in DNA repair or MYC targets V2 hallmarks, whereas WNT signaling via ß-catenin was also significantly deregulated (**Fig.4.8c**).

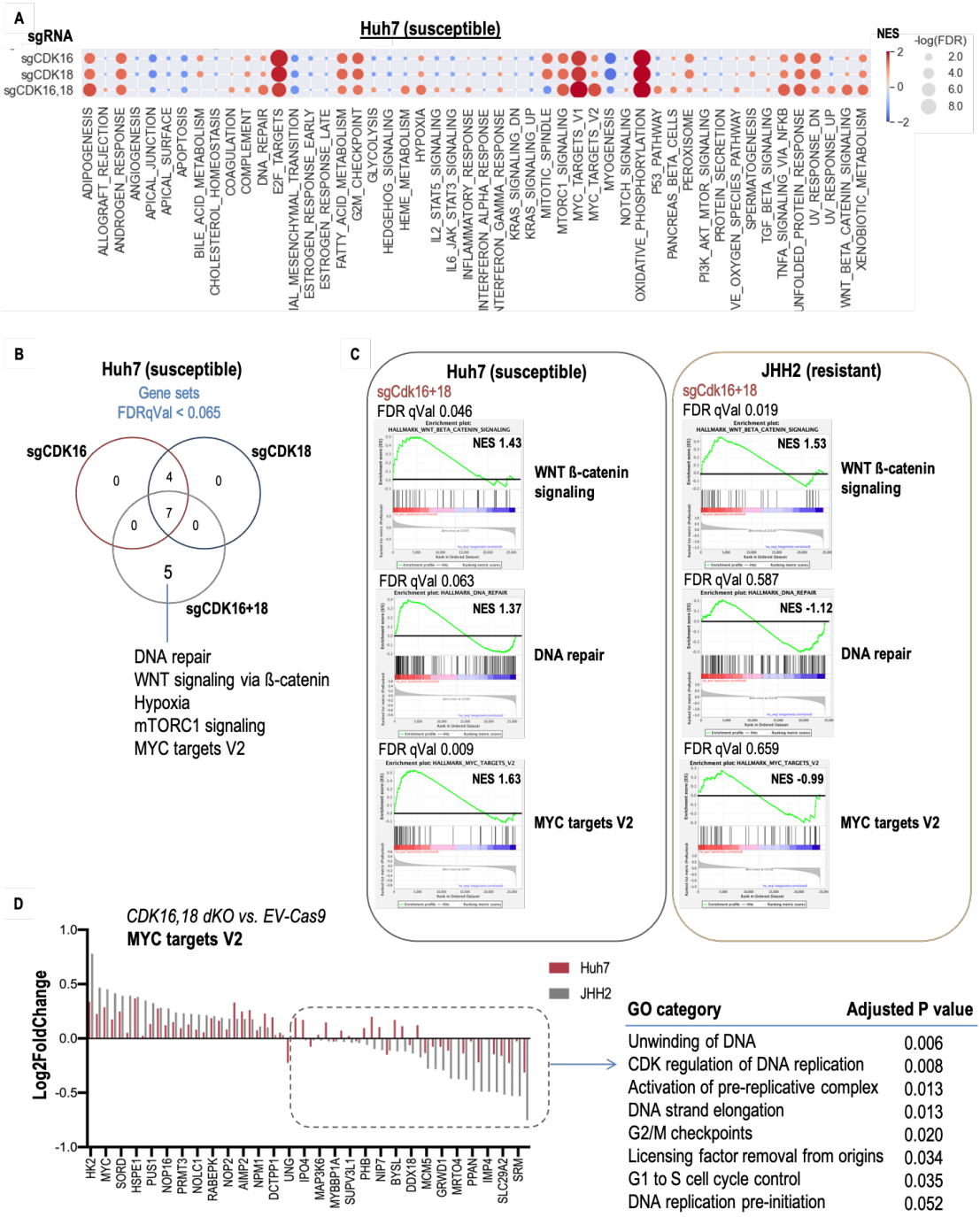

Figure 4.8. Expression profiling suggests MYC-driven replication is responsible of increased S-phase population in CDK16,18 dKO cells. A) Dot plot of up- and down-regulated gene sets (mRNA) according to their normalized enrichment score (NES) and FDR q-value in CDK16-18 depleted cells (3d post-infection). **B)** Venn diagram for the comparison of gene sets de-regulated in CDK16, CDK18 and CDK16,18 dKO cells. Gene sets were included in each group when FDRqVal<0.065. **C)** Comparative gene enrichment of indicated hallmarks in CDK16,18 dKO Huh7 and JHH2 cell lines. **D)** Comparison of log_2FoldChange of individual genes within MYC targets V2 gene set and associated GO categories for differentially expressed gene subset. GO categories were obtained from *Enrichr* [142][144].

MYC targets V1 hallmark was significantly deregulated in single KOs, and in CDK16,18 dKO in both resistant and susceptible analyzed cell lines. However, as previously stated, MYC targets V2 was not deregulated in single KOs (FDRqVal>0.05) and was only significantly deregulated after CDK16,18 depletion in Huh7 (susceptible) and not in JHH2 (resistant). Hence, these results suggest that specific genes or signaling modules linked to MYC are playing a critical role responsible for the phenotypic effects observed after CDK16,18 depletion. Analysis of differentially expressed genes in MYC targets V2 gene set in Huh7 and JHH2 revealed that a subset of genes related to DNA replication initiation were strongly downregulated in JHH2 but not in Huh7 (**Fig.4.8d**). Thus, a subset of MYC-dependent DNA replication-related genes might explain the differences in susceptibility and phenotypic strength associated to CDK16,18 depletion.

4.3.2. Changes in phosphorylation status of genes associated to DNA repair, cell cycle and cytoskeleton organization in CDK16,18 dKO cells

To further gain insight into the mechanisms leading to reduced proliferation in CDK16,18 dKO cells we explored the proteomic landscape of Huh7 cells at 2.5- and 4-days post-infection (lentiCRISPR-Cas9).

Analysis of genes with significant changes in their phosphorylation status and without changes in their protein expression levels (padj<0.05), revealed that most upregulated genes at day 4 were associated to actin cytoskeleton dynamics (pValue=1.9E-09) and DNA repair hallmarks, in particular to DBS break repair via non-homologous end joining (NHEJ) (pValue=4.6E-04) (**Table4.1**). Genes with significantly downregulated phosphosites were associated to mRNA export from nucleus, microtubule cytoskeleton dynamics and DNA repair (pValue=2.1E-04), according to our analysis in DAVID portal (**Table 4.1**).

We were particularly interested in the regulation of DNA repair given our previous results in transcriptomic analyses. Integrative analysis of up- and down-regulated phosphosites with the RNAseq data, revealed a signature possibly related to oncogene-induced replicative stress, which include the gene enrichment in oxidative phosphorylation hallmark (FDR=0.0; NES=2.04) (**Fig.4.8a**), and the alterations in the phosphorylation of genes (padj<0.05) implicated in purine nucleoside triphosphate metabolic process ($\log_{10}(q)$= -14.65) and proteins (pVal<0.05) linked to the regulation of DNA metabolic process ($\log_{10}(q)$= -6.40) (**Fig.4.9c,d**). Moreover, genes with downregulated phosphosites were significantly associated to G2/M transition ($\log_{10}(q)$=

-4.04), whereas genes with upregulated phosphosites were related to apoptosis execution (log_{10}(q): -3.53) on the report of our analysis in Metascape portal (**Fig.4.9d**).

Table 4.1. Gene ontology categories from phosphoproteomic analysis of CDK16,18 dKO cells. Genes with significant variations in their phosphorylation status (q<0.05) in Huh7 after Cdk16,18 depletion were queried for association with gene ontologies in DAVID portal [143][144]. Number of genes in each category and statistical significance for each association are indicated.

GO categories for genes with padj<0.05	Count	p-Value
Up-regulated		
Actin cytoskeleton organization	19	1.9E-09
Positive regulation of apoptotic process	9	3.2E-04
Double strand break repair via NHEJ	5	4.6E-04
DNA damage checkpoint	3	1.3E-02
ATM signaling pathway	3	2.6E-02
Lipid binding	7	6.8E-04
Intracellular transport	20	1.5E-03
Golgi organization	4	8.8E-03
mRNA metabolic process	12	1.5E-03
Down-regulated		
mRNA export from nucleus	8	7.9E-07
Microtubule cytoskeleton organization	13	1.8E-06
DNA damage	9	2.1E-04
DNA repair	10	1.5E-03
Double strand break repair	5	2.1E-02

We were also interested in the identification of potential CDK16/18 substrates. To obtain these candidates we analyzed genes with significant changes in their phosphorylation status (padj<0.05) at both day 2 and day 4. We obtained 13 candidate genes with downregulated phosphosites and 14 genes with upregulated phosphosites. Among these, it is worth highlighting SOX13 (logFC= -0.58; pVal= 7.7e-04 at 4d) (**Fig.4.9c**), implicated in WNT signaling through the inhibition of TCF1/TCF7 transcriptional activity [148]. Since we had previously observed increased expression of genes related to canonical WNT signaling and MYC (**Fig.4.8**), a downregulation in SOX13 phosphorylation provides a valuable observation that may indicate one possible underlying mechanism through one putative CDK16/18 substrate. Additionally, APC,

another critical regulator of WNT signaling, showed significant variations in the phosphorylation status of several of its residues, and one particularly was downregulated at day 2.5 (logFC= -0.53; pVal= 2.47e-03). Although attenuated at day 4, this serine residue still presented a tendency towards downregulation (logFC= -0.11; pVal= 0.34). Taken together, results from transcriptomic and proteomic analyses support our initial explanation for the antiproliferative effects observed in HCC cell lines after CDK16,18 depletion, indicative of a signature of defective DNA repair and possibly related to replication stress.

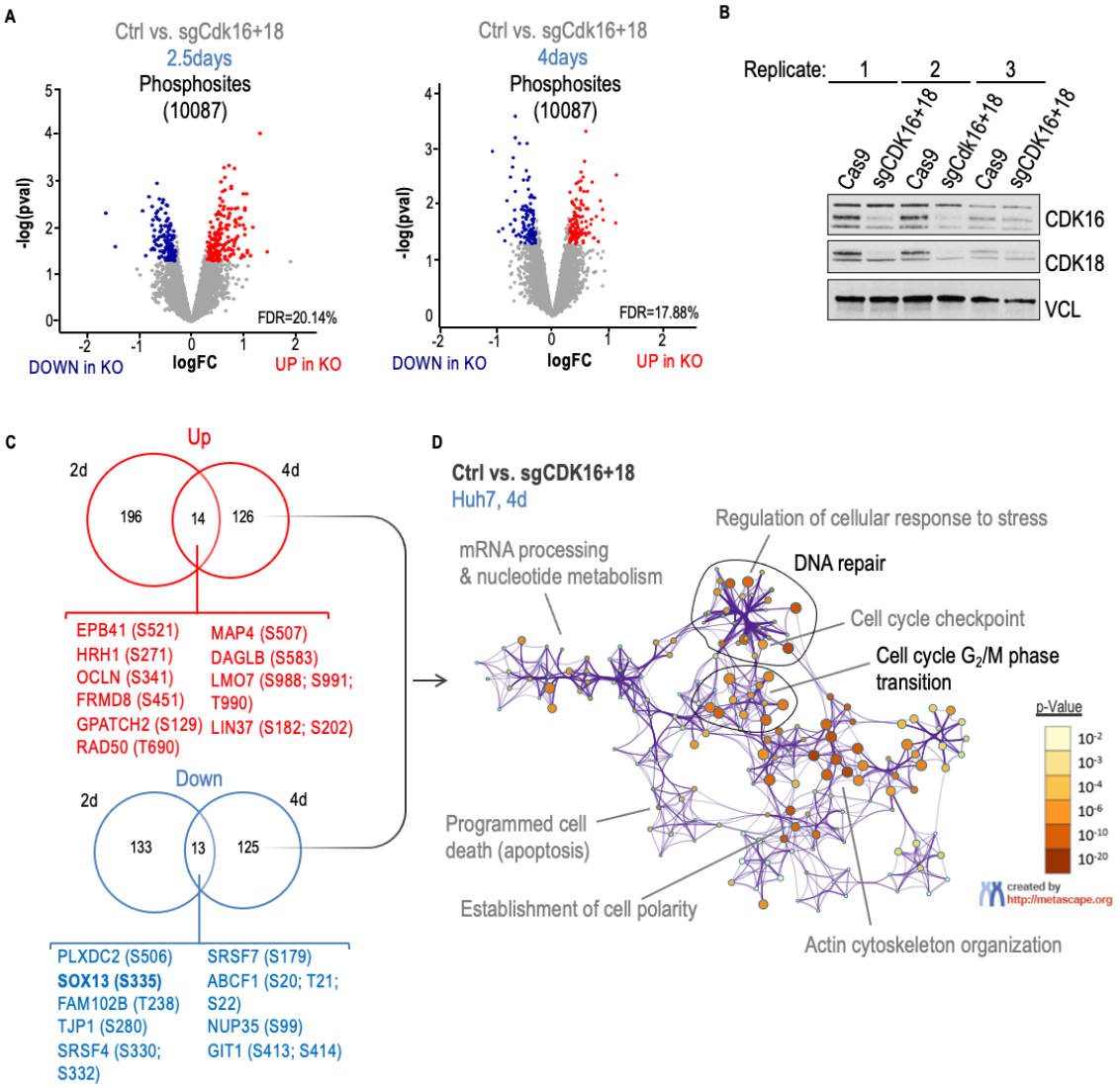

Figure 4.9. Analysis of altered phosphosites in CDK16,18 dKO Huh7 cells and associated GO categories. A) Volcano plots for deregulated phosphosites in Huh7 CDK16,18 dKO cells vs. control (EV-Cas9) after infection with lentiCRISPR. **B)** WB analysis of CDK16,18 levels in experimental samples. **C)** Venn diagram analysis of significantly up- and down-regulated phosphosites (p-adjusted value<0.05), at 2 and 4d post-infection. **D)** Graphical view of gene ontology categories (GO) for proteins with significantly up- and down-regulated phosphosites (padj <0.05) 4d post-infection; Obtained in Metascape [149]. FC: fold change.

4.4. CDK14-18 depletion induces DNA damage accumulation

4.4.1. Different contribution of PFTK- and PCTK-subfamily members to prevent DNA damage

We selected the groups to be functionally analyzed from subfamily sequence homology-based classification (PFTAIRE and PCTAIRE subfamilies) and associated phenotype observations (CDK16,18 dKO and CDK14,16 dKO). CDK14 depletion, and to a lesser extent that of CDK15, induced only a modest increase in γH2AX (**Fig.4.10a,b**). Furthermore, whereas the combination of CDK14,15 dKO did not increase in the phosphorylation of ATR and ATM and total levels of the latest in the

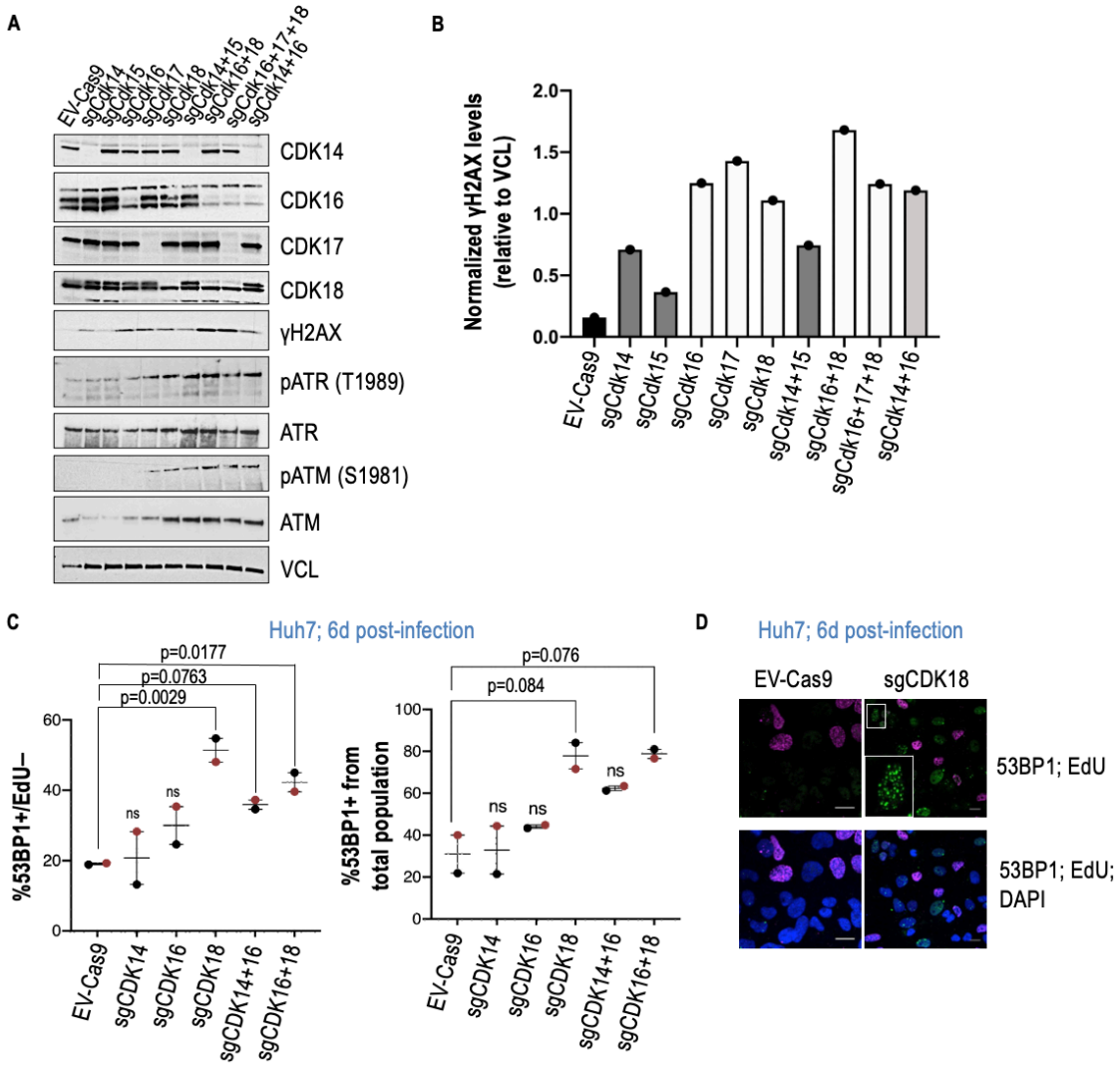

Figure 4.10. CDK14-18 depletion induces DNA damage accumulation in HCC cells. A) WB analysis of CDK14-18 KO vs. control (EV-Cas9) cells 6d after infection with lentiCRISPR-Cas9 and **B)** quantification of γH2AX levels relative to VCL loading control (n=1). CDK15 expression could not be detected by WB in this experiment (data not shown). **C)** Quantification and **D)** representative images of EdU incorporation and 53BP1 immunofluorescence in Huh7 cells 6d after infection with lentiCRISPR-Cas9 (n=2 ± SD). p-values for one-way anova are indicated unless ns (p>0.05).

dKO, an observation that can be extended to all combinations (**Fig.4.10a**). CDK16-18 single depletion was more efficient inducing DNA damage accumulation than that of CDK14-15, and CDK16,18 dKO combination elicited the most significant increase in γH2AX levels (**Fig.4.10a,b**). Interestingly, addition of CDK17 sgRNA to CDK16,18 dKO did not significantly increase DNA damage accumulation (**Fig.4.10a,b**). Furthermore, CDK14,16 dKO showed DNA damage levels comparable to CDK16 single KO, suggesting that the synergistic effects obtained with this combination might not be related to DNA repair (**Fig.4.10a,b**).

Remarkably, when we analyzed EdU incorporation and 53BP1 staining by immunofluorescence we could observe that CDK18 KO group showed an increased tendency towards accumulation of 53BP1+; EdU− cells, in contrast to individual depletion of others and to a comparable extent as that of the combinations (**Fig.4.10c,d**).

4.4.2. Compensation between CDK16 and CDK18 explain adaptation in single KOs

To further evaluate the contribution of each gene and gain better insight into the mechanisms underlying the attenuated phenotypes observed in single KOs, we tested DNA damage accumulation in our single cell clones. We infected Huh7 clones with sgRNAs targeting the alternative CDK locus, generating dKO cells in clones already adapted to single depletion (after several passages). Expression of CDK16 sgRNA in WT-Cas9 clones did not elicit any increase in γH2AX or 53BP1 markers (**Fig.4.11a-c**). However, when we depleted CDK16 in CDK18 stable KO clones, both markers showed a significant increase (**Fig.4.11a-c**). Moreover, CDK18 single depletion in WT clones induced a strong accumulation of γH2AX and 53BP1 foci (**Fig.4.11a-c**). Similarly, addition of this sgRNA to CDK16 stable KO clones significantly increased the levels of DNA damage (**Fig.4.11a-c**).

These results demonstrate that both CDK16 and CDK18 are redundant in preventing DNA damage: at least one of them is required in the analyzed HCC cells, while the other would be essential for adaptation mechanisms, likely thanks to functional redundancy. Importantly, western blot analysis of CDK14, CDK16 and CDK18 status showed that these adaptation mechanisms rely on variations in the protein levels of the alternative, putative redundant CDK (**Fig.4.11d**). However, this was only evident in the case of CDK18 KO clones, which upregulated CDK16, whereas

stable CDK16 KO clones downregulated CDK14 instead, suggesting that compensatory mechanisms and adaptation in the long term might implicate other members of the subfamily.

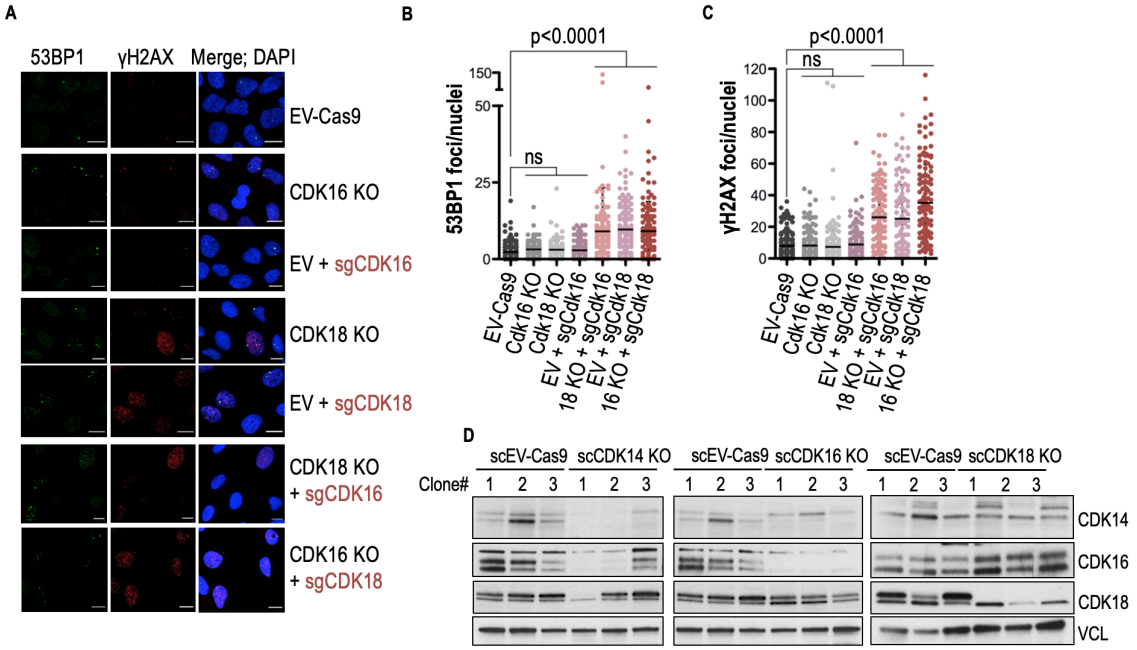

Figure 4.11. Evaluation of CDK16 and CDK18 compensatory mechanisms preventing DNA damage accumulation. A) Representative images of 53BP1 and γH2AX IF in Huh7 stable single cell clones with and without transient infection with lentiCRISPR-Cas9 for CDK16/18 depletion. **B,C)** Quantification of 53BP1 and γH2AX foci/nuclei (n=1), respectively; P-values for one-way anova are indicated, unless non-significant (p>0.05). **D)** WB analysis of CDK14,16,18 protein levels in Huh7 stable single cell (sc)-KO clones (n=3).

4.5. WNT/ß-catenin and GSK3ß signaling network as critical determinants of cell fate after CDK14-18 depletion

4.5.1. Increased MYC expression or stabilization as a counteracting mechanism after CDK16,18 depletion, precedes DNA damage accumulation

In the previous sections we show RNAseq and proteomics data descriptive of several processes underlaying reduced proliferation in HCC cell lines following CDK14-18 depletion. Beyond deficient DNA repair and DNA damage accumulation, several other significantly deregulated hallmarks and statistically relevant correlations could be reported. Perhaps the most evident and significant would be that related to *MYC*. As previously mentioned, we observed how mRNAs with significant variations in their expression levels (padj<0.05) mainly correlated with *MYC* (**Fig.4.8; Table 4.2**). Intriguingly, our data shows a shift in MYC targets from upregulation (3 days) towards downregulation (4 days) after CDK16,18 co-depletion (**Fig.4.12a**). Interestingly, this

tendency could be also observed in JHH2 cell line, which upregulated MYC targets V1, but not Myc targets V2 gene set, particularly at day 3 (**Fig.4.12a**). To better interpret these rapid changes, we performed time course analysis of FMF-treated Huh7 cells. FMF treatment induced rapid and acute MYC variations at the protein level followed by an increase in γH2AX, until a critical point of DNA damage accumulation in which MYC expression and/or stability was compromised, and cell death was induced, as indicated by PARP1 cleavage (**Fig.4.12b**). Increase in MYC was induced from the earliest time point analyzed and preceded DNA damage accumulation, consistent with a primary, critical role of MYC deregulation in our phenotypes (**Fig.4.12b,c**). Remarkably, we could observe variations in the phosphorylation status of LRP6 receptor, a known target of Cyclin Y-CDK14 complexes, coinciding with MYC increase (**Fig.4.12b**), arguing in favor of an implication of canonical Wnt signaling in the phenotype. However, we did not observe a reduction as expected from CDK14-18 inhibition, but instead the pattern of band recognition by this antibody was modified (**Fig.4.12b**).

Table 4.2. Association of genes significantly deregulated (RNAseq) with transcription factors in CDK14-18 KO cells. Genes with significant log_2foldchange (padj<0.05) in their mRNA levels were queried for association with transcription factors in Enrichr portal [142].

Gene(s) KO	Associated TFs	p-Value	Adjusted p-Value
CDK14	MYC CHEA TAF1 ENCODE MAX ENCODE MYC ENCODE	2.182e-25 2.039e-23 8.435e-20 1.091e-17	2.226e-23 1.040e-21 2.868e-18 2.782e-16
CDK16	MYC CHEA KAT2A ENCODE BCL3 ENCODE PBX3 ENCODE	0.0009220 0.002306 0.01964 0.01587	0.04702 0.05881 0.2504 0.2504
CDK18	MYC CHEA TAF1 ENCODE BRCA1 ENCODE MYC ENCODE	1.760e-12 8.728e-12 1.103e-9 1.916e-8	1.742e-10 4.320e-10 3.641e-8 4.742e-7
CDK16,18	TAF1 ENCODE MYC CHEA MYC ENCODE ATF2 ENCODE	9.890e-29 9.507e-20 1.160e-18 7.367e-18	1.019e-26 4.896e-18 3.984e-17 1.897e-16
CDK14,16	SOX2 CHEA NANOG CHEA TRIM28 CHEA TCF3 CHEA	0.00001502 0.00008999 0.001729 0.002863	0.001246 0.003734 0.04418 0.04753

Consistent to the existence of compensatory mechanisms between CDK16/18, analysis after CDK16 KO in SNU449, which expresses low levels of CDK18, showed upregulation of CDK18 as a response to increased DNA damage. Importantly, the increase in CDK18 was accompanied by DNA damage response (DDR) signaling, which reverted γH2AX accumulation at longer time points (**Fig.4.12d**). Interestingly, knockout of CDK16, but not CDK18, was followed by stabilization of ß-catenin and MYC, underpinning the existence of a crosstalk between CDK16 and WNT signaling (**Fig.4.12d**). The intensity in MYC and ß-catenin increase correlated with that of γH2AX (**Fig.4.12d**), thus supporting a direct relationship between these two events.

These results demonstrate that these cells increase MYC protein levels in response to CDK14-18 inhibition or genetic ablation. Downregulation of SOX13 phosphorylation, a known inhibitor of canonical WNT signaling, upon CDK16,18 depletion (**Fig.4.9c**), would support that the increase in MYC levels has a transcriptional origin. Nonetheless, when we analyzed SNU475 cell line, the increase in MYC was accompanied by changes in the phosphorylation status of critical residues determining MYC stability. Both control (EV-Cas9) and CDK14-18 KO cells were positive for T58 phosphorylation, whereas S62 phosphorylation, indicative of MYC stabilization, was higher in CDK16,18 dKO cells (**Fig.4.12e**). Importantly, the increase in S62 observed in CDK16,18 dKO cells correlated with the highest increase in MYC levels (**Fig.4.12e**). These results suggest the existence of a fine-tune modulation of MYC protein levels in this cell line, which is altered after CDK16,18 dKO by the accumulation of a S62-phosphorylated, stable MYC pool.

Importantly, these analyses revealed that both WNT-proficient (SNU449) and WNT-unresponsive (SNU475) cells were able to upregulate MYC in response to CDK16,18 depletion, suggesting that MYC upregulation can be partially WNT-independent. Nonetheless, WNT signaling upregulation in RNAseq data from Huh7 and JHH2, and the increase in ß-catenin levels in SNU449 cells suggest upregulation of WNT represents a counteracting mechanism of critical importance, since SNU475 is the most sensitive to CDK16,18 depletion among the cell lines analyzed in the present work, as detailed in comparative analyses in the following sections.

Upregulation of MYC and ß-catenin might have beneficial effects in these cells ranging from anti-apoptotic signaling to DNA repair. However, in the absence of CDK18, MYC-mediated unrestrained cell cycle entry could have undesired effects such as excessive origin licensing leading to replication stress, and even MYC-induced

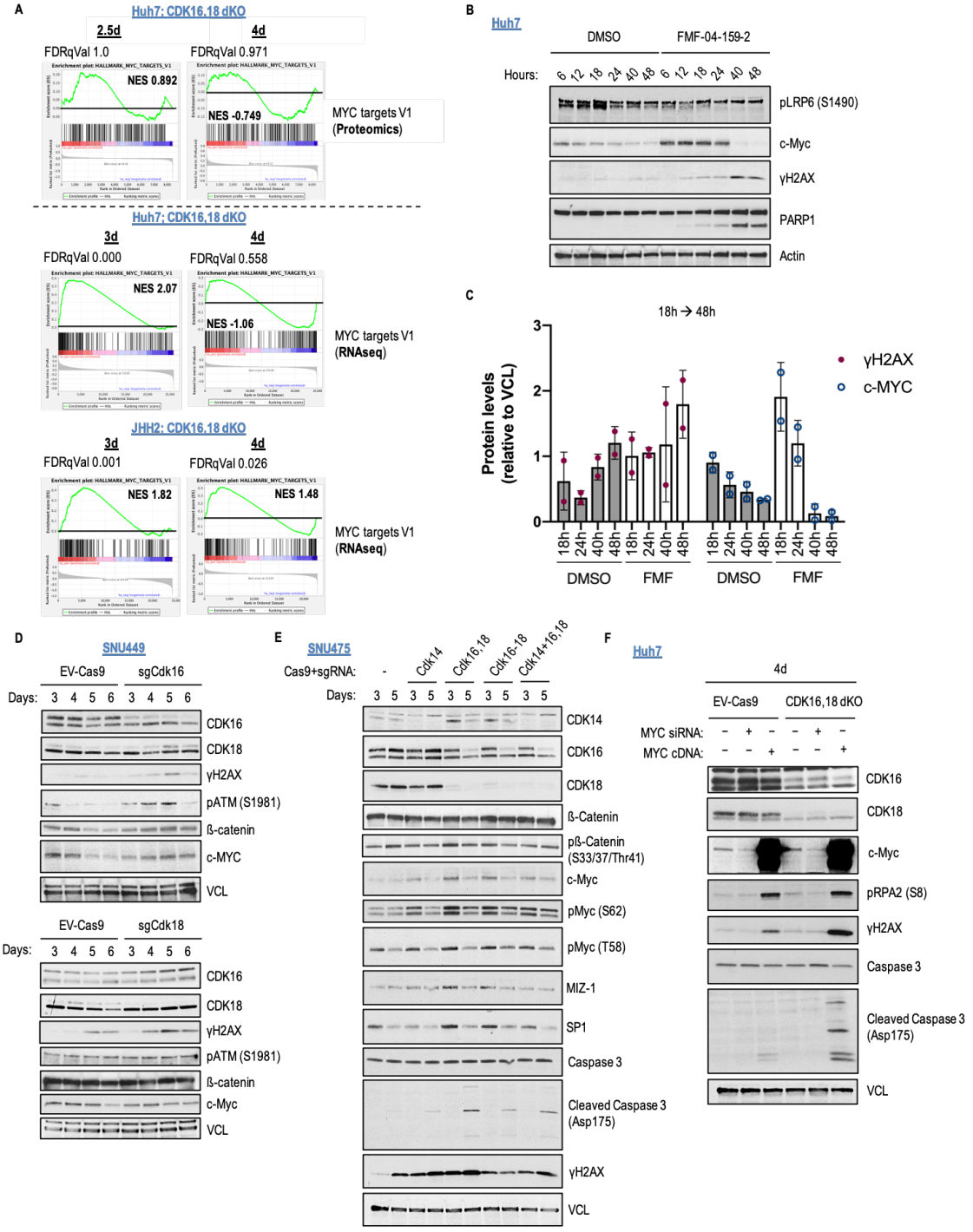

Figure 4.12. Balanced MYC increase after CDK16,18 depletion counteracts DNA damage-induced apoptosis. A) GSEA of MYC targets V1 in proteomics and RNAseq samples from CDK16,18 dKO vs. EV-Cas9 Ctrl. Huh7 and JHH2 cell lines. **B)** Time course WB analysis and **C)** quantification of DMSO- and FMF-treated Huh7 cells (n=2±SD). **D)** WB analysis of SNU449 cells infected with lentiCRISPR EV-Cas9 or CDK16/18 sgRNAs. **E)** WB analysis of SNU475 3 and 5 days after infection with indicated Cas9-sgRNA combinations. **F)** WB analysis of Huh7 cells infected with lentiCRISPR EV-Cas9 or CDK16,18 sgRNAs for 120h and transiently transfected for MYC knockdown (48h) and overexpression (24h) (n=1). siCtrl. And pcDNA3.1(+) were transfected as controls for knockdown and overexpression, respectively.

apoptosis. Since MYC transcriptional activity or its capacity to act as a repressor strongly rely on additional co-factors [150][151], we speculated that CDK14-18 depleted cells might modulate MYC upregulation by inducing the expression and/or stabilization of these genes. For example, SP1 has been shown to cooperate with MYC to promote repression of specific promoters [152][153][154], while at the same time promote DNA repair [155]. Underlying this interpretation, western blot analysis of different CDK14-18 depletion combinations in SNU475 cell line showed that SP1 was upregulated following MYC upregulation in all cases, whilst MIZ-1 was upregulated in response to CDK16,18 dKO (**Fig.4.12e**).

To add evidence to the importance of keeping balanced MYC levels in these cells, we designed an experiment that could highlight these hypothetical scenarios by knocking-down or overexpressing MYC. Remarkably, although the experiment was performed at early time points (4d), CDK16,18 dKO alone was sufficient to increase the levels of replication stress (pRPA2 S8) and DNA damage (γH2AX) compared to the basal levels carried by Huh7 cells, and the increase in pRPA2 was rescued by MYC knockdown (**Fig.4.12f**). As expected, MYC overexpression increased replication stress in both groups and induced a clear accumulation of γH2AX and cleaved caspase 3 (**Fig.4.12f**). Notably, this increase was considerably stronger in CDK16,18 dKO cells (**Fig.4.12f**), indicating that the toxicity associated to MYC overexpression had a deeper impact in the absence of CDK16,18.

Taken together, our results suggest that MYC upregulation after CDK16,18 depletion represents a counteracting mechanism, but must be kept in balance to prevent a replication stress catastrophe.

4.5.2. GSK3ß dual roles in WNT canonical pathway and apoptotic signaling link DNA repair and survival after CDK14-18 depletion

Despite initial increase in MYC levels and activity after CDK14-18 depletion, the transcriptional activation of MYC targets and the increase in MYC protein levels are severely compromised at later time points (**Fig.4.12**). This shift in the tendency of MYC level variations was independent of the final outcome of the cells (i.e. reduced DNA damage and survival or DNA damage accumulation and apoptosis induction), and was reproduced in all the cell lines analyzed. However, induction of DNA damage and cell death in these time courses had a reverse correlation with MYC levels. Hence, these results suggest MYC is induced to favor pro-survival signaling until either DNA

damage accumulation feeds any given checkpoint activation triggering cell death, or DNA repair satisfies the system and therefore makes MYC upregulation unnecessary.

Proteomic analysis of CDK16,18 dKO Huh7 cells showed upregulation of unfolded protein response related genes, and the activation of intrinsic apoptotic signaling (**Fig.4.13a**). Because GSK3ß has been shown to induce this apoptotic pathway in response to several stressors such as DNA damage or ER stress, and given its fundamental role in WNT signaling control and MYC stability regulation, we decided to use a chemical inhibitor of this multifunctional kinase to modulate the phenotypes associated to CDK14-18 inhibition. Additionally, to fully understand these hypotheses we took advantage of two inhibitors of WNT canonical signaling (**Fig4.13b**).

Treatment of Huh7 cells with WNT inhibitors or GSK3ß inhibition had little or no effect in the viability of Huh7 (**Fig.4.13c,d**). However, combination of FMF treatment with WNT inhibitors induced higher levels of cell death compared to FMF individual treatment, accompanied by increased levels of DNA damage (**Fig.4.13c,d**), thus suggesting a role of WNT signaling in DNA repair in this context. Interestingly, GSK3ß inhibition reverted DNA damage accumulation and rescued cell death, as indicated by γH2AX and PARP1 cleavage, respectively (**Fig.4.13c,d**). The rescue in these markers was observed at 12h post-FMF treatment initiation. However, this effect was attenuated at 18h and lost at 24h (**Fig.4.13d**).

Interestingly, phosphorylation of ß-catenin at S33/37/Thr41 was abolished in the presence of FMF, whilst individual GSK3ß inhibition induced an increase in this marker (**Fig4.13d**), as previously reported in mutant KRAS-independent cell lines [156]. Since this marker indicate both targeted proteasomal degradation or sequestration of ß-catenin in the membrane, this result indicates mechanisms of regulation WNT signaling pathway in these contexts. However, further characterization of ß-catenin localization and activity would be necessary to fully understand the correlation in this marker with ß-catenin function and MYC levels.

Taken together, our data suggests that canonical WNT and GSK3ß pathways mediate opposite outcomes, linking DNA repair and survival through the balanced regulation of these signaling modules.

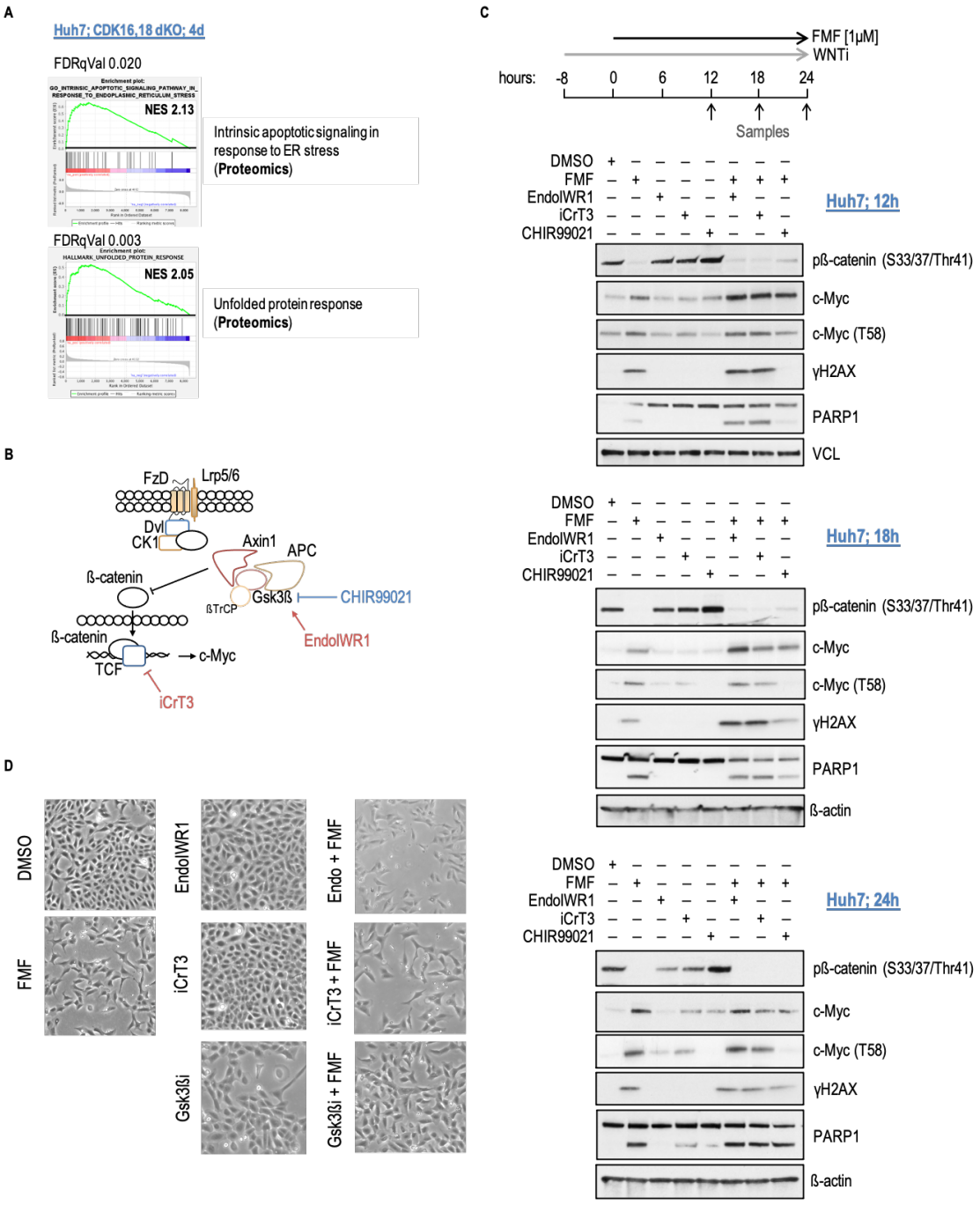

Figure 4.13. GSK3ß inhibition temporarily rescues DNA damage and cell death after CDK14-18 inhibition in HCC cells. A) Total proteome GSEA analysis of indicated hallmarks from CDK16,18 dKO vs. EV-Cas9 Ctrl. Huh7 cells, 4d post-infection. **B)** Graphical view of canonical WNT signaling pathway, and mode of action of indicated compounds. **C)** Schedule of drug administration and WB analysis of Huh7 cells treated with indicated compounds at different time points. **D)** Representative images of Huh7 cells treated with indicated compounds after 18h of FMF administration.

4.6. Resistance to CDK14-18 inhibition and combination therapeutic strategies

4.6.1. Understanding mechanisms of resistance to CDK16,18 depletion

To integrate functional analysis data into the susceptibility of different oncogenic backgrounds, we decided to compare the accumulation of DNA damage after CDK16,18 ablation in several human HCC cell lines. All cell lines showed a tendency towards increased γH2AX, with the exceptions of JHH2 and SNU449 (**Fig.4.14a,b**). Importantly, this pattern of susceptibility was phenocopied by treatment with FMF (**Fig.4.14a,b**). In SNU475 cells, the significant reduction in γH2AX levels likely represented a consequence of a stronger induction of apoptosis, as indicated by PARP1 cleavage, thus demonstrating this cell line is the most susceptible (**Fig.4.14a,b**). Moreover, FMF treatment strongly reduced, in a dose-dependent manner, the proliferation/survival of those cells that accumulated γH2AX after CDK16,18 depletion or CDK14-18 inhibition, reinforcing a critical link between DNA damage and reduced proliferation in these contexts (**Fig.4.14c,d**).

Susceptibility to CDK16,18 depletion was not dependent on MYC expression status, since all cell lines expressed MYC to comparable levels. Nevertheless, regardless a unique time point of analysis, we could observe that roughly most cell lines increased MYC upon CDK16,18 dKO (**Fig.4.14a**), consistent with our previous results.

To identify additional requirements that could correlate with resistance to CDK14-18 inhibition, we took advantage of our RNAseq data in JHH2 and Huh7 cell lines. Analysis of early events (3d) showed that E2F targets, like those of Myc, were among the most significantly deregulated hallmarks, in both Huh7 and JHH2 (**Fig.4.14e**). Nonetheless, when we examined this deregulation globally, throughout analyzed time points, we encountered important differences between the susceptible and the resistant cell line. First, JHH2 upregulated E2F targets to a greater extent at day 3 (FDRqVal=0.000; NES= 2.2). Second, at day 4 Huh7 showed acute downregulation of E2F targets at the protein level (FDRqVal=0.000; NES= -2.2) and at the mRNA level (FDRqVal= 0.587; NES= 1.06), whereas JHH2 maintained upregulated or neutral expression of most genes in this hallmark (FDRqVal= 0.063; NES= 1.53) (**Fig.4.14e**). Remarkably, when we analyzed the genes included in the core enrichment of E2F targets hallmark at day 4, we found that JHH2, but not Huh7, upregulated several genes related to DNA repair (**Fig.4.14f**,**g**).

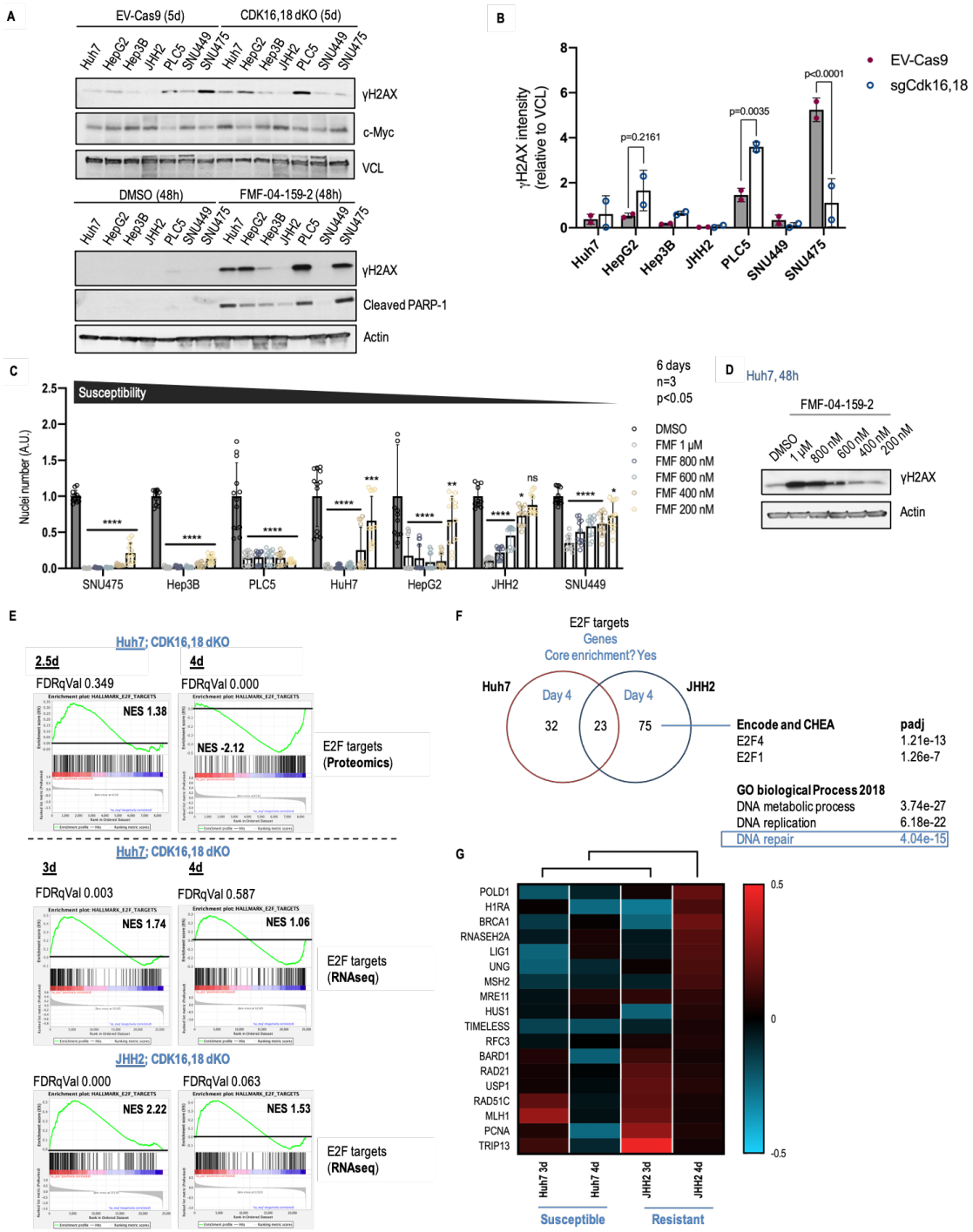

Figure 4.14. Susceptibility to DNA damage induction after CDK16,18 depletion or CDK14-18 inhibition across HCC cell lines. A) WB analysis of CDK16,18 depletion (5d) or CDK14-18 pharmacological inhibition (48h) in human HCC cell lines. **B)** Quantification of γH2AX levels relative to VCL loading control in WT and CDK16,18 dKO cells (n=2±SD). **C)** Evaluation of HCC cell line proliferation/survival after FMF-04-159-2 treatment (6d) with decreasing concentrations (n=3±SD). **D)** γH2AX levels in Huh7 after treatment with FMF-04-159-2 at indicated concentrations. **E)** GSEA analysis of E2F targets at indicated time points and cell lines, in proteomics and RNAseq samples. **F)** Venn diagram for E2F targets at day 4 in indicated cell lines. **G)** Expression profiling of E2F targets at indicated time points in Huh7 and JHH2. Two-way anova: ns p>0.05; *p<0.05; **p<0.005; ***p<0.0005; ****p<0.0001.

Since we have demonstrated that DNA damage accumulation is responsible of reduced proliferation in HCC cell lines and that JHH2 is partially resistant to DNA damage induction and reduced proliferation after CDK16,18 depletion, increased expression of DNA repair genes through E2F provides an explanation of a possible resistance mechanism. Moreover, increased MYC expression would fuel E2F activation and therefore links this data to WNT signaling, which as we have demonstrated, plays a critical role determining cell fate after CDK14-18 depletion.

4.6.2. Synthetic lethality of FMF-04-159-2 and DNA repair inhibitors

To further evaluate the therapeutic potential of CDK14-18 inhibition, we explored the synergies of FMF combination with compounds known to be DNA damage-inducing agents and most of them used in the clinic. A combination of suboptimal doses of FMF, Palbociclib and Olaparib, but not those of Cis-platin, elicited a significant increase in 53BP1 foci in Huh7 cells compared to single treatments (**Fig.4.15b**). Additionally, CDK16,18 genetic depletion synergized with Olaparib treatment inducing DNA damage (**Fig.4.15b**). Moreover, working doses of FMF (1μM) synergized with Palbociclib and Olaparib, but not with ATR inhibition (ATRi), inducing DNA damage in this cell line (**Fig.4.15c**), further supporting a critical role for ATM inducing homologous recombination (HR) in these cells. Importantly, use of FMF-R, a reversible version of CDK14-18 inhibitor, reverted DNA damage accumulation after washout (**Fig.4.15c**). These results were complemented with colony formation assays in which all combinations of suboptimal doses of the drugs increased the antiproliferative efficacy of the compounds alone, bypassing resistance to CDK14-18 inhibition (**Fig.4.15d**).

Since FMF-Olaparib synthetic lethality has been already investigated in glioblastoma cells [137], we focused our attention to Palbociclib. Analysis of RNAseq data from $HER2^{-}$ breast cancer patients showed that CDK14 was particularly upregulated in samples from patients resistant to either hormonotherapy (HT) alone or in combination with Palbociclib, compared to responders in both groups (**Fig.4.16a**), suggesting that CDK14-18 might mediate resistant to CDK4,6 inhibition.

Despite the strong impact in proliferation and survival that we had observed with FMF and Palbociclib treatments in Huh7 cells, transcriptomic analysis showed slight variations in S phase- and G2-related genes in FMF-treated cells, or recovery from acute variations in these cell cycle-related signatures at 48h in Palbociclib

treatment (**Fig.4.16b**). Interestingly, recovery in Palbociclib was abolished in the combination with FMF, suggesting that both compounds cooperate to bypass resistance mechanisms in these cells (**Fig.4.16b**). Gene enrichment analysis after 12h and 48h of

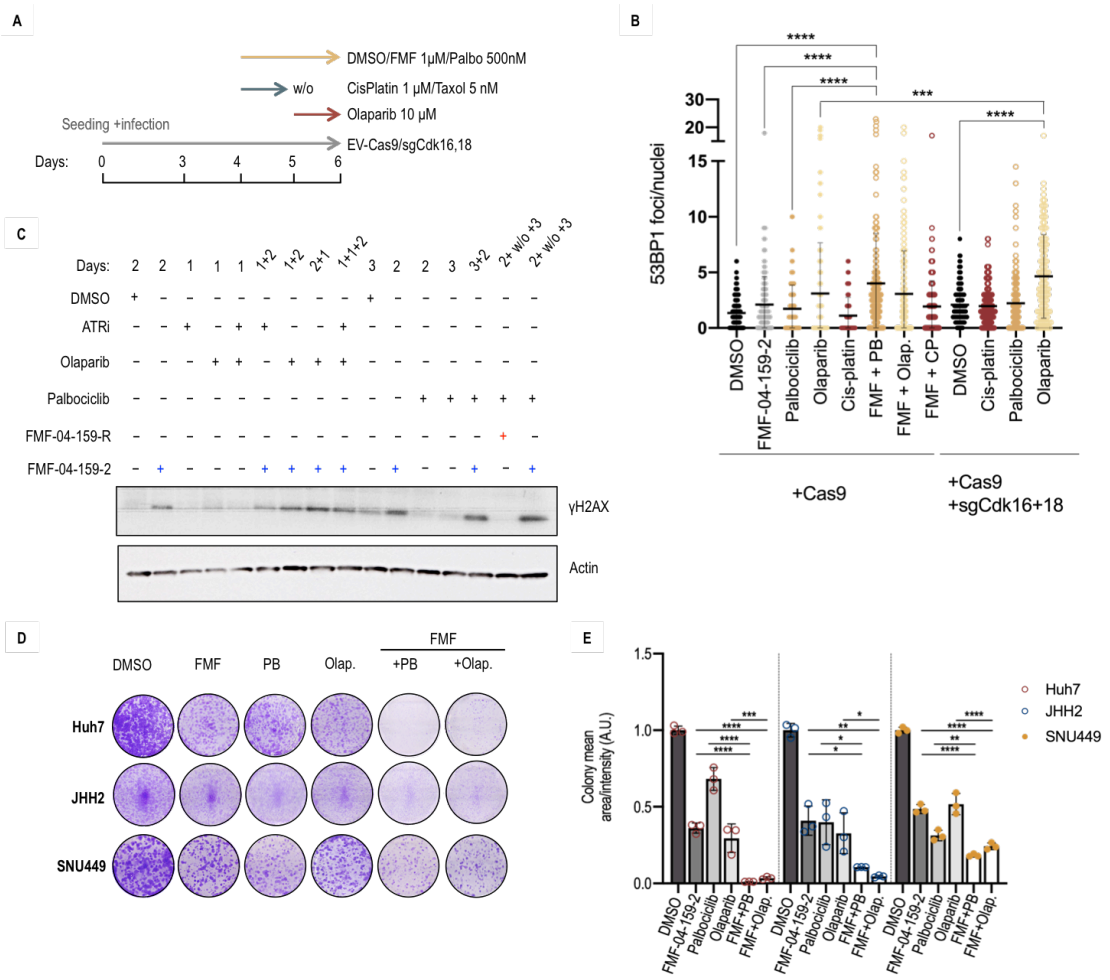

Figure 4.15. Evaluation of FMF-04-159-2 combination with DNA damage-inducing agents in HCC cell lines. A) Schedule of drug administration at indicated suboptimal doses. **B)** Quantification of 53BP1 in Huh7 treated as indicated in A), over a WT (EV-Cas9) or a CDK16,18 dKO background. **C)** γH2AX levels in Huh7 after different schedules of drug administration, with the first number corresponding to the days of FMF-04-159-2 exposure. **D)** Representative images and **E)** quantification of CF assays in HCC cell lines after 7-9d of treatment with indicated compounds (n=3±SD). Different doses of each compound were used in each cell line to achieve 50% reduction in proliferation with individual treatments. One-way anova: ns p>0.05; *p<0.05; **p<0.005; ***p<0.0005; ****p<0.0001.

FMF or Palbociclib treatment and their combination revealed that essentially, DNA repair and mTORC1 signaling signatures were robustly downregulated in the combination at 48h compared to individual treatments, whereas increase in androgen and estrogen response gene sets was attenuated in the presence of FMF (**Fig.4.16c**).

It has been reported that Palbociclib interferes with DNA repair machinery, inducing a pathway switch from HR towards NHEJ [31][157]. FMF inhibits CDK18,

implicated in ATR activation and HR signaling, and we have additionally described increased phosphorylation of NHEJ-related proteins after CDK16,18 dKO. Since Palbociclib was used at suboptimal concentrations in these experiments, we speculated that FMF and Palbociclib cooperation may arise from synergistic effects in DNA repair signaling, rather than a result of interfering with cell cycle progression, as supported by the modest variations in expression of cell cycle-related genes in individual treatments, and the increase in DNA damage observed upon the combination of both compounds (**Fig.4.16b,c**). Consistent with this hypothesis, analysis of E2F targets showed that 1) cells recovered E2F targets expression from Palbociclib treatment at 48h, whereas this recovery was abolished when FMF was present, and 2) analysis of DNA repair genes within E2F targets signature showed that FMF-treated cells sustained expression of these genes despite general downregulation of E2F- and DNA repair-related signatures, whereas combination with Palbociclib effectively prevented this putative resistance mechanism (**Fig.4.16d**).

Given that RB1 and E2F have been shown to regulate DNA repair signaling independently of each other [158][159], and because E2F transcriptional activity is controlled through RB1 phosphorylation, we also analyzed RB1 status. Surprisingly, FMF treatment induced downregulation of RB1 at the protein level at 12h (**Fig.4.16e**). Notably this effect was partially reverted after FMF washout (2h) (**Fig.4.16e**). Since FMF is a CDK14 covalent inhibitor, and CDK16-18 engagement is compromised after washout of the compound [115], this result indicates CDK16,18 are at least partially responsible of this effect. Concomitant to our previous results, 12h of FMF treatment were not sufficient to induce DNA damage. However, we could already observe induction of CHK1 phosphorylation, suggesting that RB1 degradation promotes DNA repair even before significant amounts of DNA damage are accumulated. Importantly, FMF-withdrawal also reverted CHK1 activation, suggesting that RB1 downregulation may contribute to promote DNA repair signaling (**Fig.4.16d**). Finally, we demonstrated that CDK14-18 depletion-mediated RB1 downregulation was induced by degradation, since MG132, a proteasome inhibitor, rescued this effect (**Fig.4.16c**). Importantly, MYC upregulation and RB1 downregulation would cooperate inducing unrestrained cell cycle entry, and therefore, might contribute to increase the levels of replication stress. Thus, RB1 downregulation dependency for DNA repair related genes might represent an imperfect, yet partially effective, complementary solution to MYC upregulation in the context of CDK14-18 inhibition.

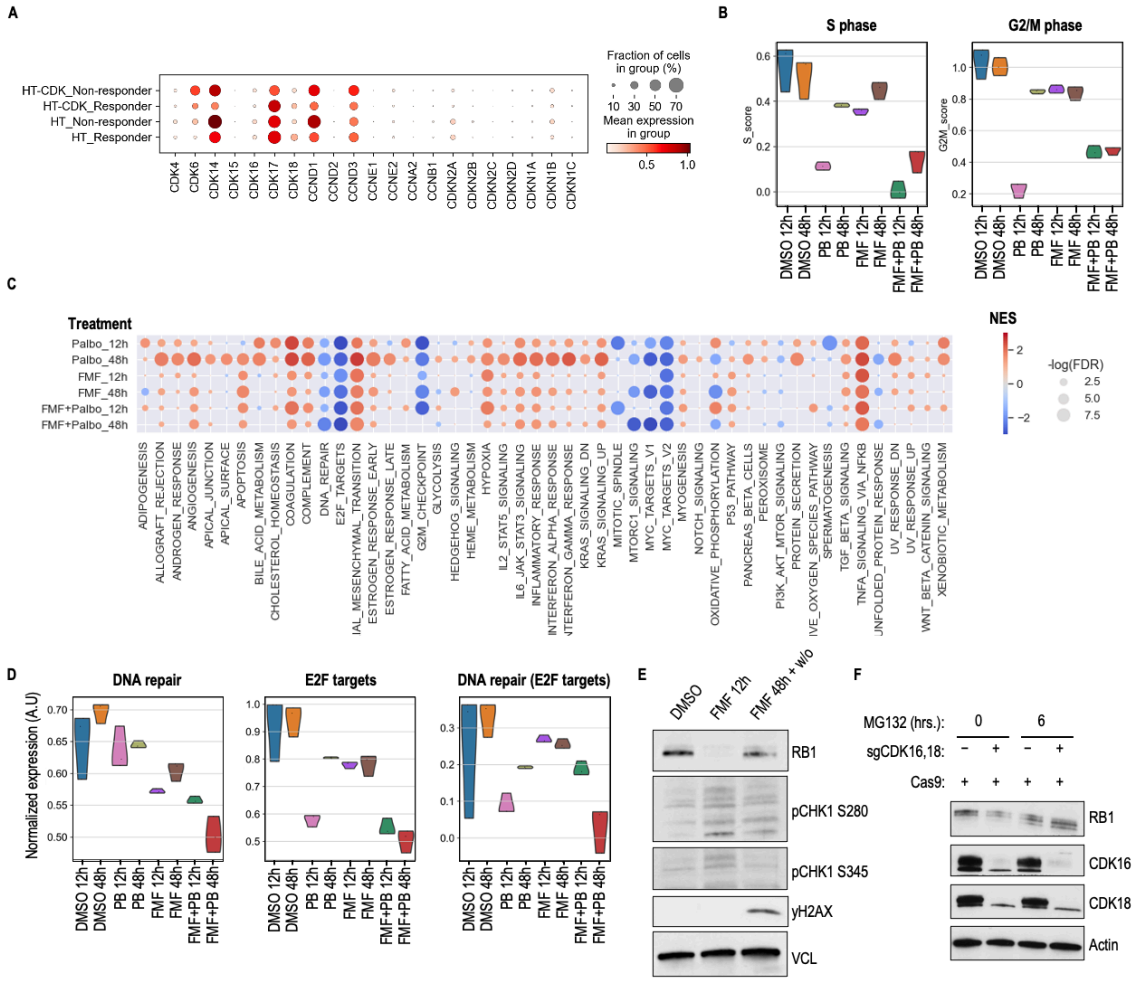

Figure 4.16. CDK14-18 inhibition cooperates with Palbociclib through transcriptional control of DNA repair genes. **A)** Enrichment of indicated genes in human samples stratified according to their response to hormonotherapy (HT) alone or in combination with Palbociclib (CDK). **B)** Violin plot for S-phase and G2/M-related gene expression in Huh7 cells treated with indicated compounds. **C)** Dot plot of GSEA analysis of FMF- and/or Palbociclib-treated Huh7 cells (12-48h). **D)** Violin plot for DNA repair and E2F targets gene sets, and DNA repair-related genes within E2F targets signature. **E)** WB analysis of Huh7 cells treated with DMSO (Ctrl.), FMF for 12h or FMF for 48h + 2h washout. **F)** WB analysis of RB1 stability after treatment with proteasome inhibitor in CDK16,18 dKO Huh7 cells.

4.7. In vivo evaluation of CDK14-18 as therapeutic targets

Breeding of *CDK14-18* mutant mice discarded fertility problems since normal litter size were obtained, and these mice developed normally and showed no major abnormalities in their adult tissues, as evidenced in histological analyses (data not shown). Additionally, 4-month-old mice did not present significant variations in blood parameters or cell populations, with the exception of total white blood cell (WBC) number, which was significantly decreased in *Cdk15(-)* and *Cdk18(-)* mice (**Fig.4.17a**),

thus, allowing to conclude that individual ablation of *CDK14-18* does not induce severe phenotypes.

To evaluate the therapeutic potential of CDK14-18 inhibition, we generated liver tumors in 6 weeks-old mice using hydrodynamic injection (HI) technique [145]. Interestingly, WB analysis of these tumors showed increased CDK16 and CDK18 expression in tumor samples compared to control animals and adjacent normal liver samples, whereas in diethylnitrosamine (DEN)-induced liver tumors these variations

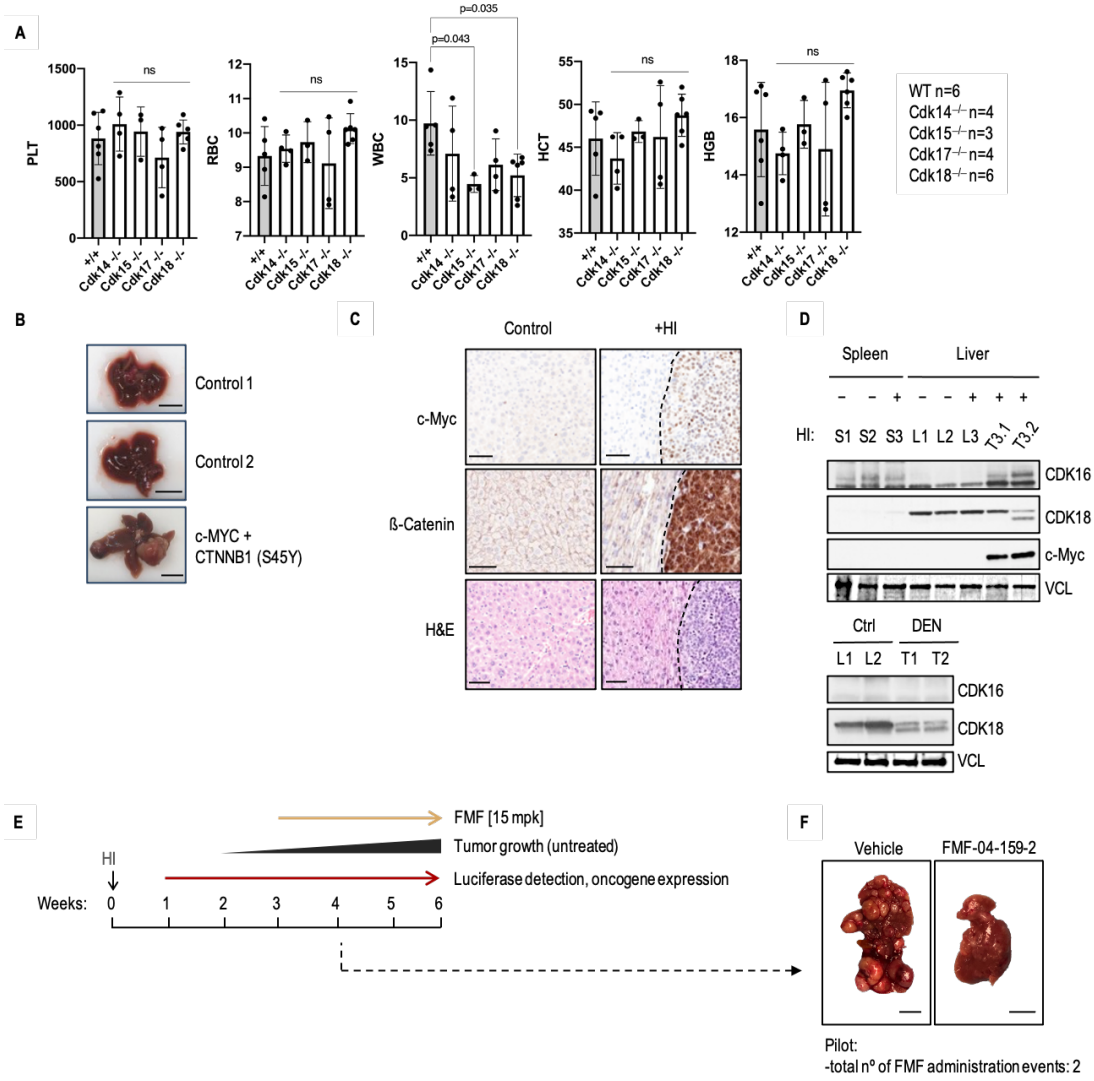

Figure 4.17. Evaluation of CDK14-18 requirement for normal tissues and therapeutic evaluation of CDK14-18 inhibition in liver tumors. A) Evaluation of blood parameters and cell populations in *CDK14-18* mutant mice. **B)** Representative pictures and **C)** corresponding IHC analysis of normal liver and HI-induced liver tumors. **D)** Comparison by WB analysis of HI- or DEN-induced liver tumors, adjacent normal liver tissue, and spleen. **E)** schedule of liver tumor generation and drug administration. **F)** Representative images of a preliminary pilot experiment (n=2), 4 weeks after HI, for the evaluation of toxicity and therapeutic potential of two rounds of FMF-04-159-2 administration. HI: hydrodynamic injection. S: spleen; L: liver; T: tumor nodule. One-way anova: ns = p>0.05.

were not observed (**Fig.4.17b-d**). Preliminary data from MYC/ß-catenin S44Y-driven tumors treated with FMF has evidenced a clear tendency towards reduction in tumor growth (n=4) (**Fig.4.17f**). We are currently evaluating the therapeutic effect in a representative cohort of animals either by FMF treatment or conditional ablation of CDK16,18.

Discussion

5.1. Identification of therapeutic targets among poorly characterized atypical kinases

5.1.1. Druggable CDKs in precision oncology: variables affecting target validation and opportunities for CDK14-18

Since their discovery in the decade of 70's, CDKs attracted scientific interest given the crucial role they exert in the regulation of cell cycle, helping to understand a plethora of biological processes [1]. Nevertheless, it took a while realizing the real scope of understanding how relevant these genes were in cell biology and human disease. Decades of studies have demonstrated that inhibition of these genes prevents tumorigenesis and cancer progression in many contexts [1][7][29], whereas overexpression of CDKs or their cognate cyclins are events typically associated to cancer development and tumor progression [7]. Importantly, restricted requirement of some of these genes at specific developmental stages and cell types make them dispensable for the viability of most adult mammalian tissues. Many reports have elegantly dissected the cell type specificity of cyclin and CDK requirement, allowing distinction of druggable CDKs based on the promiscuity of multiple cyclins to bind more than one CDK partner, and the redundant functions which several of these genes share [1][7][29]. Not surprisingly, drug-targeted inhibition of specific CDKs has resulted in a significant therapeutic effect in human cancer patients: FDA-approved CDK4,6 inhibition in patients with advanced hormone-positive breast cancer increases patient survival with tolerable levels of associated toxicity [1][7][29].

In the present work, we have characterized the requirements for CDK14-18, poorly characterized cell cycle-related CDKs, in human cancer cell line survival and proliferation. Like CDK4,6, their expression pattern is restricted in time and space, being mainly detected in well-differentiated tissues and essentially during brain development [43-51]. Therefore, we hypothesized these genes might be good candidates for targeted inhibition in cancer cells without interfering normal cell function.

In our initial CRISPR-Cas9 screenings we were able to detect susceptibilities to CDK16,18 depletion in several cancer cells from different tissue of origin (**Fig.4.4**). Mostly studied individually, uncovering a therapeutic value for CDK14-18 has been hampered by the functional redundancy and compensatory mechanisms between members of the subfamily. Sequence homology analysis reveals high levels of similarity between CDK16 and CDK18, which suggests that to obtain a significant

effect by depleting these genes paired ablation is required. Concomitantly, individual depletion of CDK16 and CDK18 did not elicit a significant phenotype, whereas only a small fraction of the cell lines analyzed was resistant to paired depletion of both genes (**Fig.4.4**).

Analysis of CDK14-18 inhibition associated toxicity in healthy tissues was still an unresolved question. CDK16 mutant mice showed that this gene was not required during embryonic development or in adult tissues, with the only exception of spermatogenesis, a process in which Cyclin-Y-like1 and CDK16 cooperate and play essential non-redundant roles [54][108][109]. CDK14, CDK15, CDK17 and CDK18 mutant mice have not been previously characterized. In the present study, characterization of these mouse models revealed these genes are dispensable for embryogenesis, adult tissue viability and fertility. Analysis of blood parameters and cell populations also revealed minor differences compared to control *wild type* mice, further supporting that these genes are dispensable in adult healthy tissues. Concomitantly, injection of FMF-04-159-2, a first-generation inhibitor of CDK14-18 [115], in healthy adult animals did not induce major abnormalities in tissues. Finally, we are currently crossing mice carrying individual KO alleles to evaluate the toxicity associated to different combinations of members of the subfamily.

5.1.2. Evidence supporting CDK14-18 as new cancer targets in hepatocellular carcinoma

HCC incidence is increasing (6th cancer type worldwide diagnosed last year, according to the NIH). Cirrhosis represents the greatest risk factor for HCC development, and hepatocellular carcinoma remains one of the most common causes of cancer-related death globally [160]. Chronic liver disease is a consequence of multiple risks factors affecting hepatocyte function and liver homeostasis, mainly chronic hepatitis B in Asia and chronic hepatitis C in Europe and the United States [161]. Incidence of HCC is higher in rich countries, which favors inclusion of additional risk variables as a result of modern lifestyle, ranging from heavy alcohol consumption, obesity, type 2 diabetes and metabolic disease to recurrent disruption of circadian rhythms (chronic jet lag) as a result of eased global interconnection and night-shift workers [162][163].

Previous reports had shown implications of CDK14 in HCC cell line migration and invasion capacity [119][120][122]. However, the requirement of CDK14-18 for

proliferation and survival had never been reported before in this tumor type. The relationship of MYC with CDK18 [137], and that of CDK14 with WNT signaling [76], also prompted us to think these CDKs may play important roles in HCC, since *MYC* amplification and mutations in WNT signaling genes are frequently associated to HCC development and progression [164][165][166]. Our results showed that CDK16,18 dKO was the most efficient combinations of CDK depletion reducing proliferation and interfering with cell cycle progression in human HCC cell lines (**Figs.4.6-4.7**), revealing mechanisms of adaptation through functional redundancy.

Additionally, we have uncovered implications of CDK16 in canonical WNT signaling. Our data also suggests that WNT signaling plays key roles in determining cell fate after CDK14-18 inhibition, as commented in detail in the following sections. These results open interesting possibilities for increasing our understanding of liver tumor biology and hence build new avenues for therapeutic opportunities through the inhibition of CDK14-18.

5.2. Deciphering CDK16,18 implications in hepatocellular carcinoma

5.2.1. CDK14-18 implications in DNA repair

From the simplest form of cell cycle machinery in yeast, to the intricate mammalian cell cycle apparatus, millions of years and mutational events generated a palette of genes required for increased functional complexity [1]. Specific CDK activity in well-defined time frames during development or under particular conditions explain the requirement of a higher number of actors, but, as the environmental challenges multicellular organisms face are comparable to those encountered by simpler eukaryotic life forms, CDK evolution can be tracked back to ancestor genes controlling similar processes. Thus, as we follow the increase in complexity of eukaryotic life, we can notice how groups of CDKs arise to control new aspects related to the development of new cell types and organs. This is particularly evident in the case of CDK14-18, which, as stated in the introduction, can be tracked to yeast if grouped as ‘’stress-related CDKs’’, but for which real homologs cannot be found until the development of a central nervous system [48].

The ancestor gene of CDK5 subfamily, Pho85, has been characterized as a ‘’multifunctional’’ signaling module essential for stress response in budding yeast. Pho85 controls aspects related to cell cycle progression, since its deletion induces G_1 delay and slow growth, and because it has been implicated in several processes at other

cell cycle phases, such as mitotic spindle establishment [167]. *Pho85Δ* strains also present morphological abnormalities and defects associated with polarity, and they are sensitive to a broad spectrum of stressors, ranging from extracellular environment sensing and response (e.g., osmolarity and nutrient starvation), to linking DNA damage checkpoints with the cell cycle [167]. CDK5 has also been implicated in stress response, playing important roles in cancer cells beyond its well established neuronal-related implications [168]. Among these, it is worth highlighting that CDK5 directly phosphorylates several DNA damage and replication stress-related actors contributing to increase DNA damage repair, such as ATM in HCC cell lines, PARP-1, STAT3 or RPA32 [168].

Closely related, poorly characterized CDK18 has also been implicated in DNA repair. As recently reported, CDK18 depletion induce S-phase accumulation and defects in replication fork dynamics in breast cancer cells [136]. Additionally, these cells have reduced ATR signaling in response to replication stress induced by hydroxyurea (HU), which can be explained by the implications of CDK18 in recruiting several components of DNA repair machinery (i.e., Rad9, Rad17 and TOPBP1)[136]. These results have been translated to glioblastoma cell lines, where CDK18 was found in complex with ATR and regulates ATR-Rad9/ATR-ETAA1 interactions, thereby promoting HR[137].

In the present work we recapitulate in HCC cell lines how CDK18 ablation induces defects in S-phase progression as evidenced in EdU incorporation experiments, and by the accumulation of cells in S/G_2 observed in cell cycle profiles from total DNA content. Co-depletion of CDK16 with CDK18, however, induced a stronger accumulation of cells in S-phase, indicating that CDK16 expression attenuates CDK18 ablation-related cell cycle defects. Our transcriptomic, proteomic and biochemical data uncovers implications of members of the subfamily and synergies never reported before. For example, we could observe that depleting PCTAIRE kinases (CDK16-18), is more efficient inducing γH2AX accumulation, but that CDK14 is also implicated in preventing DNA damage accumulation. Similarly, individual PCTAIRE kinase depletion induced an accumulation of p-ATM and p-ATR, whereas CDK14,15 dKO was required to observe similar events.

Stronger induction of DNA damage accumulation in CDK16,18 dKO cells compared to their single KO counterparts was explained with an experiment in which we took advantage of our stable single cell clones. We demonstrated how functional redundancy between these kinases allow cancer cells to bypass single depletion and

adapt to control the induction of DNA damage (**Fig.4.11**). Importantly, this experiment provides an explanation for the stronger phenotypes encountered with combined depletion but was also informative about the mechanisms of adaptation to single depletion of these genes.

Taken together, uncovering CDK14-18 implications in DNA damage supports block inhibition of several or all members of the subfamily, representing the most feasible context with a pharmacological inhibitor given their high sequence similarity in the kinase domain. On the other hand, these results dissect the individual contribution of each subfamily member helping to understand the mechanisms underlying compromised proliferation of HCC cells after their depletion. With these experiments, CDK14 also emerges as a potential cancer target in tumors in which DNA damage can be exploited as a therapeutic strategy.

5.2.2. CDK16 implications in WNT signaling

CDK18 implications in DNA repair have been manifested in the context of response to replication stress induced by HU treatment or the inhibition of PARP1 [136][137]. CDK14-18 depletion in HCC cell lines leads to DNA damage accumulation, and because we have worked with highly proliferative MYC-addicted cell lines, we hypothesized that oncogene-induced replication stress might escalate the impact of depleting these genes. Supporting this hypothesis, pathway switching from HR to NHEJ observed in Huh7 cells after CDK16,18 depletion suggests that DNA damage is a consequence of replication stress-induced DSBs, since NHEJ activation outcome is abortive and does not resolve DNA damage, but instead leads to G_2/M arrest and apoptosis (**Fig.4.13**), like previously described [169].

By using several biochemical analyses with CDK14-18 pharmacological inhibitor, and CRISPR-Cas9 mediated CDK14-18 depletion, we demonstrate that a rapid, acute increase in MYC precedes DNA damage accumulation (**Fig.4.12**). However, increased expression of MYC cofactors required to act as a transcriptional repressor suggest MYC transcriptional network is tightly regulated to avoid replication stress or induction of apoptotic cell death. MIZ-1 and SP1 implications in determining opposite, alternative outcomes for MYC-mediated cell cycle control and apoptosis [153-155][170][171], suggest their upregulation is an attempt to maintain MYC activity in balance. To fully demonstrate this possibility, we evaluated how WT and CDK16,18 dKO Huh7 cells responded to MYC overexpression and knockdown. As expected, we

show how MYC-induced replication stress and apoptotic signaling was stronger in CDK16,18 dKO cells compared to WT EV-Cas9 controls. Conversely, MYC depletion ameliorated the effect of CDK16,18 depletion, reducing p-RPA32 levels (**Fig.4.12**). This was not sufficient to revert accumulation of γH2AX, which might be explained by CDK18 deficiency. It would also explain why, as observed in other experiments, MYC upregulation is not effective for HCC cell lines to promote cell survival and DNA repair, since DSB accumulation cannot be regressed, thereby enhancing G_2/M checkpoint activation, and ultimately triggering apoptotic signaling (**Fig.4.12**).

Remarkably, a comparison of WNT-not responsive and -responsive cell lines has shown that MYC upregulation is at least partially dependent on protein stabilization, since we observed increased MYC S62 phosphorylation after CDK16,18 depletion (**Fig.4.12**). Two phosphorylation residues in MYC have been described to be critical for MYC stability. T58 phosphorylation, mediated by AXIN1 and GSK3ß, triggers proteosome-mediated MYC degradation, whereas S62 phosphorylation, mainly mediated by MAPK/ERK signaling stabilizes MYC [172][173]. Furthermore, PP2A dephosphorylates S62, which in the context of T58 phosphorylation favors MYC degradation [174][175]. In our experiments, we observed that MYC upregulation in CDK14 KO and CDK16,18 dKO SNU475 cells is accompanied by increased S62 phosphorylation (**Fig.4.12**). Increased MYC levels was observed in WNT responsive cell lines that showed upregulation of WNT-ß-catenin targets and ß-catenin protein levels, but also in SNU475 (WNT not responsive cell line), showing modest or absent changes in ß-catenin. Thus, we hypothesize that MYC upregulation is both transcription- and stabilization-dependent. Remarkably, phosphoproteome analysis of CDK16,18 dKO cells evidenced increased phosphorylation of several MAPKs and MAPK-related factors (i.e. MAPK1, MAP4K2, MAP4K4, JUN), whereas western blot analyses evidenced variations in MYC phosphorylation status, both in S62 and T58 residues, suggesting an implication of GSK3ß in these variations. Taken together our data suggests that CDK14-18 inhibition or CDK16,18 genetic depletion induce changes in WNT/MYC signaling networks, either by transcriptional activation or post-translational modification means.

The transcriptional changes associated to WNT signaling via ß-catenin and MYC in resistant and susceptible cell lines, and the clear variations in post-translational control of MYC stability, prompted us to interpret these changes as a counteracting mechanism to CDK14-18 inhibition. Moreover, the rapid, acute increase in MYC after

CDK14-18 inhibition suggested a direct implication of these kinases in WNT signaling modulation, since it preceded DNA damage accumulation. Finally, dissecting individual contribution of each gene in SNU449 cell line (**Fig.4.12**), allowed us to demonstrate that CDK16 is the critical kinase acting as a regulator of WNT signaling in these cells.

Our data also suggests that WNT signaling inhibition enhances the phenotype of CDK14-18 inhibition, inducing DNA damage and cell death. Therefore, this result supports that, at least initially, WNT ß-catenin-MYC axis mediates DNA repair and promotes survival (**Fig.4.13**). This would explain why SNU475, unresponsive to WNT stimuli, is more susceptible to CDK14-18 inhibition (**Fig.4.12 and Fig.4.14**), because while MYC can mediate survival and DNA repair, ß-catenin would enhance the latest [176][177]. Additionally, an important consideration in the interpretation of this data is the dual opposite roles that many genes related to WNT signaling have regarding cell survival or induction of apoptosis, and in particular MYC. In the absence of WNT signaling, MYC triggers apoptosis, whereas under active WNT signaling, and depending on additional cofactors, promotes cell survival and growth [81]. Therefore, this result confirms that, shortly after CDK14-18 inhibition, WNT signaling upregulation represents a counteracting mechanism, and not the ultimate cause triggering the phenotypes here reported.

On the other hand, GSK3ß inhibition had opposite effects, partially rescuing DNA damage and cell death. Moreover, CDK14-18 inhibition increased the levels of MYC T58 phosphorylation, an effect reverted by GSK3ß inhibition, thus suggesting that GSK3ß is not a direct target of CDK14-18. These experiments also suggest that GSK3ß blocks the pro-survival effect of WNT/ß-catenin and MYC and may favor pro-apoptotic signaling. If GSK3ß is inhibited, MYC and ß-catenin signaling would be initially sufficient to overcome the negative consequences of CDK14-18 inhibition, favoring DNA repair and survival. Nevertheless, the high levels of replication origin licensing, replication stress and DNA damage accumulation triggered by CDK14-18 inhibition would be strong enough to explain the temporal restriction in the beneficial effects of GSK3ß inhibition.

Additionally, CDK14-18 inhibition strongly reduces ß-catenin S33/37/Thr41 phosphorylation, suggesting increased ß-catenin stability, nuclear translocation and transcriptional activity. However, either WNT or GSK3ß inhibition increased the phosphorylation of these residues. Importantly, increased S33 phosphorylation after GSK3ß inhibition has been previously reported in mutant KRAS-independent cell lines

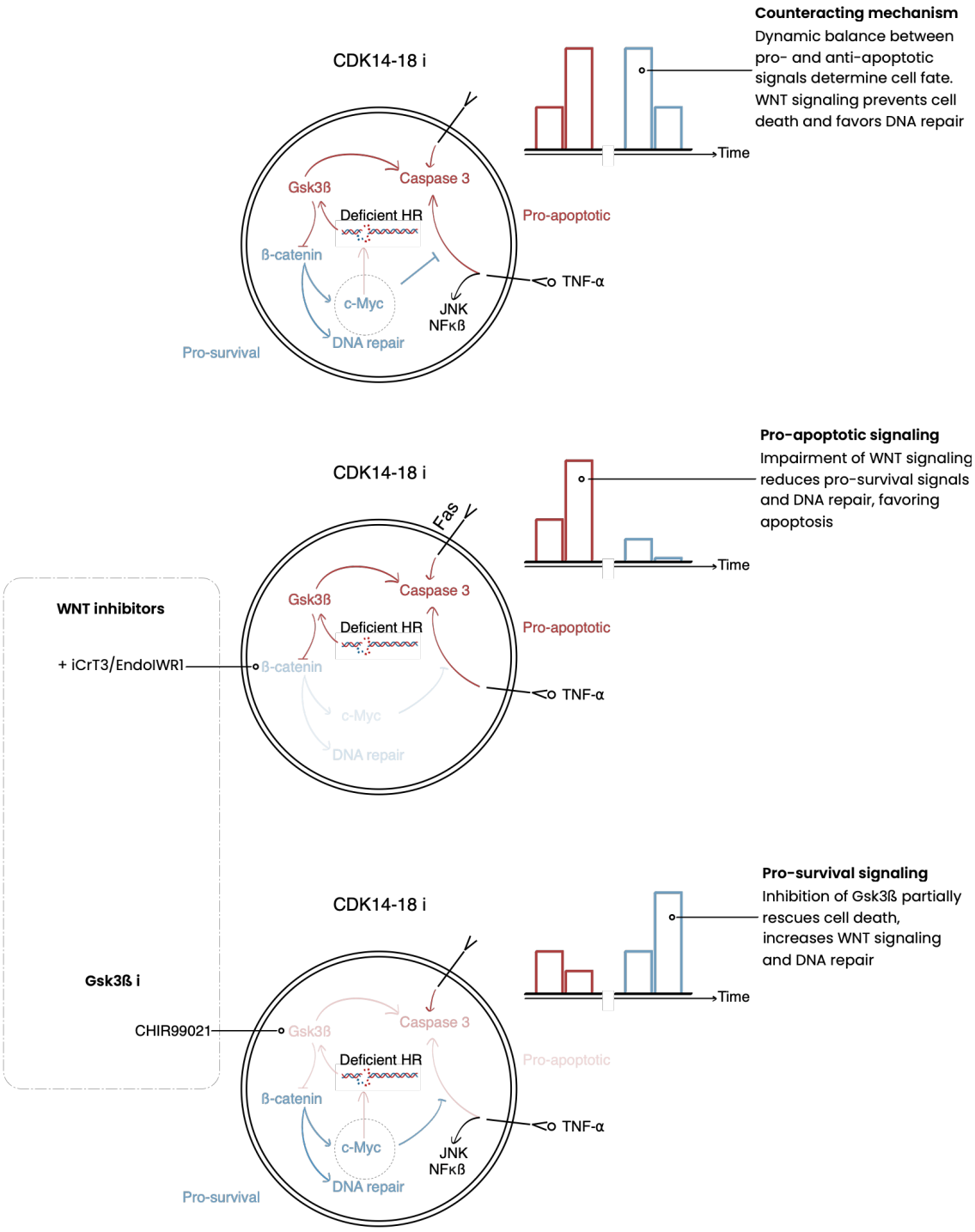

Figure 5.1. Working model for the anti-proliferative effect induced by CDK14-18 inhibition and its combination with inhibitors targeting WNT canonical pathway. Integrative model for our data emphasizing how the balance between survival and apoptosis is controlled by WNT ß-catenin-MYC axis and GSK3ß, respectively, in human HCC cells. These mechanisms underlying HCC cell response to CDK14-18 inhibition are highlighted in the context of WNT and GSK3ß inhibition, which robustly facilitate the opposite outcomes here represented.

(A549), whereas mutant KRAS-dependent tumors and cell lines (MiaPaca2) responded downregulating this residue [156]. ß-catenin S33/37/Thr41 phosphorylation is mainly mediated by GSK3ß and phosphatases [178], but the consequences of this phosphorylation are multifactorial and their interpretation would require further characterization of the biochemical alterations following CDK14-18 inhibition.

Interestingly, CDK5, closely related to CDK16, and its regulatory partner P25, have been shown to interact with ß-catenin. In mouse neuroblastoma cells, P35-CDK5 have been shown to phosphorylate ß-catenin on S191 and S246, directly controlling its activity and interaction with PIN1 [179]. Additionally, P25 interacts with AXIN1, outcompeting GSK3ß to form the destruction complex with APC, and therefore impacting ß-catenin phosphorylation at S33/37/Thr41 and thereby its activity.

A recent report has dissected the molecular mechanisms leading to male infertility *Ccnyl1* null mice [109]. Interestingly, the authors showed how CCNYL1 negatively controls GSK3ß activity in mammalian spermatozoa, to regulate WNT/STOP signaling and promote proteome stability [109]. Importantly, CCNYL1 had been previously shown to be the critical cyclin controlling CDK16 activity in murine spermatozoa [54][108]. If considered together, these reports and the present work would strongly suggest an implication of CDK16, perhaps activated by CCNYL1, in WNT signaling through GSK3ß activity control also in HCC cell lines (**Fig.5.1**).

As a result of this interpretation, our main future perspective is to identify direct CDK14,16,18 targets possibly controlling WNT signaling, to fully characterize the implications of these kinases in the phenotypes reported in the present work and deepen our insights into the therapeutic potential of CDK14-18 inhibition.

5.3. Validation of CDK14-18 as new therapeutic targets in HCC

5.3.1. Understanding resistance to CDK14-18 inhibition and synthetic lethality with FDA-approved compounds

FMF-04-159-2, has been the first generation inhibitor designed to specifically target CDK14-18 subfamily [115]. In the present work we show five important features of this compound in HCC cell lines that recapitulate the effects of genetic ablation of CDK14-18: 1) accumulation of cells at S and G_2/M phases, 2) variations in WNT signaling and MYC transcriptional activity, 3) accumulation of DNA damage 4) reduction in proliferation and survival and 5) correlation in resistance or sensitivity to CDK16,18 genetic depletion with pharmacological CDK14-18 inhibition.

FMF was extremely useful to understand the consequences of CDK14-18 inhibition, since we have demonstrated that functional redundancy is characteristic of this subfamily. Moreover, it allowed us to confirm that most of the effect is mediated by CDK16 and CDK18, since the inhibitor recapitulates all the phenotypes encountered with the genetic depletion of these two members of the subfamily.

Finally, treatment of FMF with FDA-approved compounds demonstrated the cooperation of CDK14-18 with inhibition of CDK4,6 and PARP1, since both combinations robustly suppressed HCC cell line proliferation and survival, bypassing resistance to single treatments (**Fig.4.16**).

Synergy or cooperation between CDK14-18 inhibition and Palbociclib have not been previously reported. Palbociclib (PD-0332991) efficacy for suppressing HCC cell proliferation, however, has been recently described [180]. Since Palbociclib induces G_1 arrest, but at suboptimal doses many cells are able to bypass this restriction (**Fig.4.16d**), those cells recovering from Palbociclib treatment would encounter defective DNA repair in the presence of FMF, which would explain increased DNA damage and reduced survival (**Fig.4.16**) (**Fig.5.2**).

Among the clinically relevant small molecule inhibitors evaluated in this work, it was not surprising to find significant cooperative effects precisely with those targeting HR, given the phenotypes reported here and the functions previously described for CDK18 [136][137]. As previously stated, our proteomic analysis after CDK16,18 dKO shows an enrichment in phosphosites of proteins involved in NHEJ (**Fig.4.9**). Interestingly, Palbociclib has been shown to upregulate NHEJ as a compensatory response to HR deficiency [31][157]. This would suggest a cooperative effect with the combination of FMF and Palbociclib compared to individual treatments. The downregulation of DNA repair genes in FMF-treated cells was enhanced in the presence of Palbociclib (**Fig.4.17**), suggesting that FMF and Palbociclib cooperatively compromise HR response (**Fig.5.2**).

Since MYC overexpression is frequently associated to HCC [164][165][166], and *RB1* is rarely mutated in this tumor type [180], a wide spectrum of patients could benefit from the cooperation between CDK4,6 and CDK14-18 inhibition.

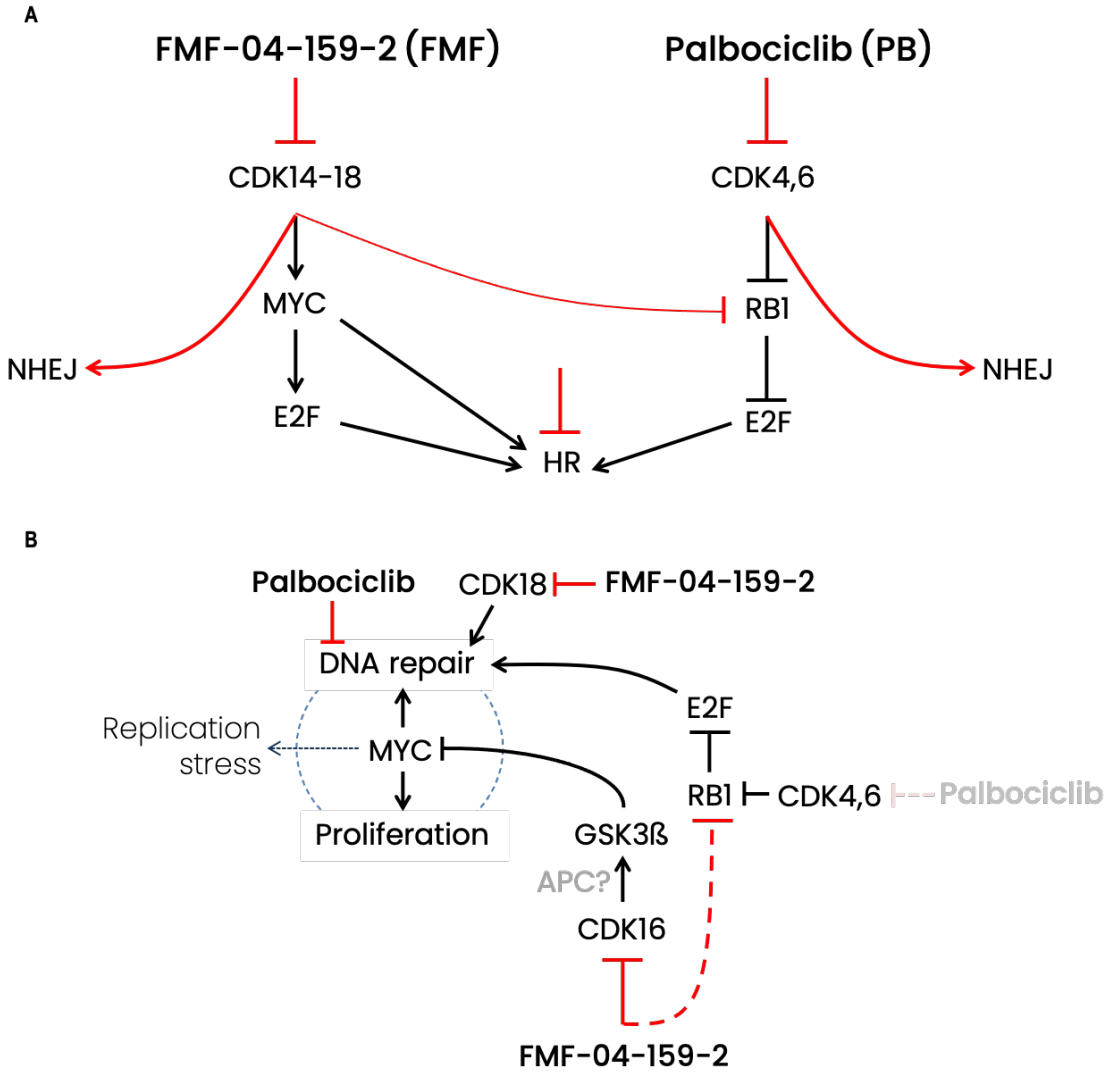

Figure 5.2. Schematic representation for proposed model of Palbociclib and FMF-04-59-2 cooperation. A) FMF-04-159-2 and Palbociclib favor NHEJ and block HR. RB1 degradation after CDK14-18 inhibition would allow HCC cells to partially bypass CDK4,6 inhibition. However, suboptimal doses of Palbociclib have been shown to interfere with HR, hindering resistance mechanisms. **B)** Proposed model for cooperative mechanisms of FMF with suboptimal doses of Palbociclib. Black lines indicate signaling cascades in untreated cancer cells. Red lines indicate the consequences of FMF or Palbociclib treatment. Color intensity reflects the potency of drug effect when used at suboptimal concentrations. HR: homologous recombination. NHEJ: non-homologous end joining.

5.3.2. Confirmation of CDK14-18 therapeutic effect in vivo: evaluation of FMF-04-159-2 in liver tumors

Analysis of *Myc* + *CTNNB1*^{Y44S}-induced liver tumors revealed that both CDK16 and CDK18 are overexpressed in tumoral samples compared to adjacent normal liver tissue or normal liver from control mice (**Fig.4.18**). This result adds evidence to MYC

and CDK16,18 positive correlation. Furthermore, it suggests that both genes play important roles in WNT-driven HCC, since DEN-induced tumors did not show that increase in protein levels (**Fig.4.18**). Further studies will allow us to explore the therapeutic possibilities in other oncogenic backgrounds (e.g., MYC + TP53 deletion) representative of the most common scenarios found in human patients.

In the present work we have set up the conditions to evaluate the therapeutic potential of pharmacological CDK14-18 inhibition in liver tumors. Our preliminary data suggest that inhibition of CDK14-18 has antitumoral effect, since treated mice had significantly lower proportion of tumor nodules (**Fig.4.18**). Remarkably, these effects were mediated without compromised viability of normal healthy cells, since these mice remained viable throughout the experiment and their blood parameters were similar to those of the controls. Our future goal is to increase the number of treated mice to validate, with statistical support, these observations. Additionally, we have planned to perform similar experiments with our genetic models for the conditional ablation of CDK14-18 to demonstrate target specificity using the appropriate genetic models.

Conclusions

1. Clinical data analysis shows that alterations CDK14-18 expression associate to liver tumors and the prognosis of hepatocellular carcinoma (HCC) patients.
2. Human HCC cell lines are susceptible to different combinations of CDK14-18 depletion. Overlapping roles and cooperation in different signaling pathways, and high sequence homology that allows functional redundancy between members of the subfamily, explain that individual ablation of CDK14-18 can be bypassed by cancer cells trough compensatory mechanisms.
3. CDK14, CDK16 and CDK18 induce cell cycle defects principally associated to increase S phase entry, resulting in replication stress-induced endogenous DNA damage accumulation.
4. CDK16 regulates WNT signaling and cooperates with CDK18-mediated DNA repair to control replication stress and promote HCC cell line proliferation and viability.
5. Pharmacological inhibition of CDK14-18 cooperates with FDA-approved drugs, Palbociclib and Olaparib, leading to reduced expression of DNA repair genes and altered DNA damage response.
6. In vivo evaluation of CDK14-18 mutant mice and the effect of a chemical inhibitor, demonstrates individual ablation or inhibition of these genes does not compromise mice viability, whereas preliminary data in MYC-induced liver tumors suggests their pharmacological inhibition reduces tumor growth.

References

[1] M. Malumbres, "Cyclin-dependent kinases," *Genome Biol.*, vol. 15, no. 6, 2014.

[2] T. Evans, E. T. Rosenthal, J. Youngblom, D. Distel, and T. Hunt, "Cyclin: A protein specified by maternal mRNA in sea urchin eggs that is destroyed at each cleavage division," *Cell*, vol. 33, no. 2, Jun. 1983.

[3] A. W. Murray and M. W. Kirschner, "Cyclin synthesis drives the early embryonic cell cycle," *Nature*, vol. 339, no. 6222, May 1989.

[4] A. W. Murray, M. J. Solomon, and M. W. Kirschner, "The role of cyclin synthesis and degradation in the control of maturation promoting factor activity," *Nature*, vol. 339, no. 6222, May 1989.

[5] L. H. Hartwell, J. Culotti, and B. Reid, "Genetic Control of the Cell-Division Cycle in Yeast, I. Detection of Mutants," *Proc. Natl. Acad. Sci.*, vol. 66, no. 2, Jun. 1970.

[6] P. Nurse, P. Thuriaux, and K. Nasmyth, "Genetic control of the cell division cycle in the fission yeast Schizosaccharomyces pombe," *Mol. Gen. Genet. MGG*, vol. 146, no. 2, Jan. 1976.

[7] D. Martínez-Alonso and M. Malumbres, "Mammalian cell cycle cyclins," *Semin. Cell Dev. Biol.*, vol. 107, Nov. 2020.

[8] E. Quandt, M. P. C. Ribeiro, and J. Clotet, "Atypical cyclins: the extended family portrait," *Cell. Mol. Life Sci.*, vol. 77, no. 2, Jan. 2020.

[9] C. J. Sherr, "Mammalian G1 cyclins," *Cell*, vol. 73, no. 6, Jun. 1993.

[10] G. Tchakarska and B. Sola, "The double dealing of cyclin D1," *Cell Cycle*, vol. 19, no. 2, Jan. 2020.

[11] D. Desai, H. C. Wessling, R. P. Fisher, and D. O. Morgan, "Effects of phosphorylation by CAK on cyclin binding by CDC2 and CDK2.," *Mol. Cell. Biol.*, vol. 15, no. 1, Jan. 1995.

[12] T. Lei *et al.*, "Cyclin K regulates prereplicative complex assembly to promote mammalian cell proliferation," *Nat. Commun.*, vol. 9, no. 1, Dec. 2018.

[13] M. M. Magiera, E. Gueydon, and E. Schwob, "DNA replication and spindle checkpoints cooperate during S phase to delay mitosis and preserve genome integrity," *J. Cell Biol.*, vol. 204, no. 2, Jan. 2014.

[14] I. García-Cao *et al.*, "'Super p53' mice exhibit enhanced DNA damage response, are tumor resistant and age normally," *EMBO J.*, vol. 21, no. 22, Nov. 2002.

[15] S. Goldstone, S. Pavey, A. Forrest, J. Sinnamon, and B. Gabrielli, "Cdc25-dependent activation of cyclin A/cdk2 is blocked in G2 phase arrested cells

independently of ATM/ATR," *Oncogene*, vol. 20, no. 8, Feb. 2001.

[16] R. Y. C. Poon, "Cell Cycle Control: A System of Interlinking Oscillators," 2016.

[17] L. K. Teixeira and S. I. Reed, "Cyclin E Deregulation and Genomic Instability," 2017.

[18] H.-J. Nam and J. M. van Deursen, "Cyclin B2 and p53 control proper timing of centrosome separation," *Nat. Cell Biol.*, vol. 16, no. 6, Jun. 2014.

[19] P. Gutiérrez-Escribano and P. Nurse, "A single cyclin–CDK complex is sufficient for both mitotic and meiotic progression in fission yeast," *Nat. Commun.*, vol. 6, no. 1, Nov. 2015.

[20] D. Santamaría *et al.*, "Cdk1 is sufficient to drive the mammalian cell cycle," *Nature*, vol. 448, no. 7155, Aug. 2007.

[21] M. A. Ciemerych, "Development of mice expressing a single D-type cyclin," *Genes Dev.*, vol. 16, no. 24, Dec. 2002.

[22] T. Parisi, "Cyclins E1 and E2 are required for endoreplication in placental trophoblast giant cells," *EMBO J.*, vol. 22, no. 18, Sep. 2003.

[23] Y. Geng *et al.*, "Cyclin E Ablation in the Mouse," *Cell*, vol. 114, no. 4, Aug. 2003.

[24] K. Kozar *et al.*, "Mouse Development and Cell Proliferation in the Absence of D-Cyclins," *Cell*, vol. 118, no. 4, Aug. 2004.

[25] M. Brandeis *et al.*, "Cyclin B2-null mice develop normally and are fertile whereas cyclin B1-null mice die in utero," *Proc. Natl. Acad. Sci.*, vol. 95, no. 8, Apr. 1998.

[26] E. A. Musgrove, C. E. Caldon, J. Barraclough, A. Stone, and R. L. Sutherland, "Cyclin D as a therapeutic target in cancer," *Nat. Rev. Cancer*, vol. 11, no. 8, Aug. 2011.

[27] T. Yoshida, S. Tanaka, A. Mogi, Y. Shitara, and H. Kuwano, "The clinical significance of Cyclin B1 and Wee1 expression innon-small-cell lung cancer," *Ann. Oncol.*, vol. 15, no. 2, Feb. 2004.

[28] L. M. Spring, S. A. Wander, F. Andre, B. Moy, N. C. Turner, and A. Bardia, "Cyclin-dependent kinase 4 and 6 inhibitors for hormone receptor-positive breast cancer: past, present, and future," *Lancet*, vol. 395, no. 10226, Mar. 2020.

[29] U. Asghar, A. K. Witkiewicz, N. C. Turner, and E. S. Knudsen, "The history and future of targeting cyclin-dependent kinases in cancer therapy," *Nat. Rev. Drug Discov.*, vol. 14, no. 2, Feb. 2015.

[30] M. Malumbres and M. Barbacid, “To cycle or not to cycle: a critical decision in cancer,” *Nat. Rev. Cancer*, vol. 1, no. 3, Dec. 2001.

[31] B. Salvador-Barbero *et al.*, “CDK4/6 Inhibitors Impair Recovery from Cytotoxic Chemotherapy in Pancreatic Adenocarcinoma,” *Cancer Cell*, vol. 37, no. 3, Mar. 2020.

[32] K. Kozar and P. Sicinski, “Cell Cycle Progression without Cyclin D-CDK4 and Cyclin D-CDK6 Complexes,” *Cell Cycle*, vol. 4, no. 3, Mar. 2005.

[33] M. Malumbres *et al.*, “Mammalian Cells Cycle without the D-Type Cyclin-Dependent Kinases Cdk4 and Cdk6,” *Cell*, vol. 118, no. 4, Aug. 2004.

[34] A. Axtman, D. Drewry, and C. Wells, “CDK16: the pick of the understudied PCTAIRE kinases,” *Nat. Rev. Drug Discov.*, vol. 18, no. 7, Jul. 2019.

[35] T. Yanagi and S. Matsuzawa, “PCTAIRE1/PCTK1/CDK16: a new oncotarget?,” *Cell Cycle*, vol. 14, no. 4, Feb. 2015.

[36] R. de O. Pepino, F. Coelho, T. A. B. Janku, D. P. Alencar, W. F. de Azevedo Jr, and F. Canduri, “Overview of PCTK3/CDK18: A Cyclin-Dependent Kinase Involved in Specific Functions in Post-Mitotic Cells,” *Curr. Med. Chem.*, vol. 28, Mar. 2021.

[37] S. Philip, M. Kumarasiri, T. Teo, M. Yu, and S. Wang, “Cyclin-Dependent Kinase 8: A New Hope in Targeted Cancer Therapy?,” *J. Med. Chem.*, vol. 61, no. 12, Jun. 2018.

[38] F. Morales and A. Giordano, “Overview of CDK9 as a target in cancer research,” *Cell Cycle*, vol. 15, no. 4, Feb. 2016.

[39] G. Y. L. Lui, C. Grandori, and C. J. Kemp, “CDK12: an emerging therapeutic target for cancer,” *J. Clin. Pathol.*, vol. 71, no. 11, Nov. 2018.

[40] V. Quereda *et al.*, “Therapeutic Targeting of CDK12/CDK13 in Triple-Negative Breast Cancer,” *Cancer Cell*, vol. 36, no. 5, Nov. 2019.

[41] S. R. Vora *et al.*, “CDK 4/6 Inhibitors Sensitize PIK3CA Mutant Breast Cancer to PI3K Inhibitors,” *Cancer Cell*, vol. 26, no. 1, Jul. 2014.

[42] M. Meyerson *et al.*, “A family of human cdc2-related protein kinases.,” *EMBO J.*, vol. 11, no. 8, Aug. 1992.

[43] T. Okuda, Cleveland JL, and Downing JR, “PCTAIRE-1 and PCTAIRE-3, two members of a novel cdc2/CDC28-related protein kinase gene family,” *Oncogene*, vol. 7, no. 11, pp. 2249–2258, 1992.

[44] T. Hirose, T. Tamaru, N. Okumura, K. Nagai, and M. Okada, “PCTAIRE 2, A

Cdc2-Related Serine/Threonine Kinase, is Predominantly Expressed in Terminally Differentiated Neurons," *Eur. J. Biochem.*, vol. 249, no. 2, Oct. 1997.

[45] K. Sauer, K. Weigmann, S. Sigrist, and C. F. Lehner, "Novel members of the cdc2-related kinase family in Drosophila: cdk4/6, cdk5, PFTAIRE, and PITSLRE kinase.," *Mol. Biol. Cell*, vol. 7, no. 11, Nov. 1996.

[46] M. A. Lazzaro, P. R. Albert, and J.-P. Julien, "A Novel cdc2-Related Protein Kinase Expressed in the Nervous System," *J. Neurochem.*, vol. 69, no. 1, Nov. 2002.

[47] V. Besset, K. Rhee, and D. Wolgemuth, "The identification and characterization of expression of Pftaire-1, a novel Cdk family member, suggest its function in the mouse testis and nervous system," *Mol. Reprod. Dev.*, vol. 50, no. 1, pp. 18–29, Dec. 1998.

[48] P. Mikolcevic, J. Rainer, and S. Geley, "Orphan kinases turn eccentric," *Cell Cycle*, vol. 11, no. 20, Oct. 2012.

[49] C. A. Stanyon *et al.*, "A Drosophila protein-interaction map centered on cell-cycle regulators," *Genome Biol.*, vol. 5, no. 12, Dec. 2004.

[50] D. Liu and R. L. Finley, "Cyclin Y Is a Novel Conserved Cyclin Essential for Development in Drosophila," *Genetics*, vol. 184, no. 4, Apr. 2010.

[51] D. Liu, S. Guest, and R. L. Finley, "Why Cyclin Y? A highly conserved cyclin with essential functions," *Fly (Austin).*, vol. 4, no. 4, Oct. 2010.

[52] P. Di Tommaso *et al.*, "T-Coffee: a web server for the multiple sequence alignment of protein and RNA sequences using structural information and homology extension," *Nucleic Acids Res.*, vol. 39, no. suppl, Jul. 2011.

[53] C.-Y. Ou *et al.*, "Two Cyclin-Dependent Kinase Pathways Are Essential for Polarized Trafficking of Presynaptic Components," *Cell*, vol. 141, no. 5, May 2010.

[54] P. Mikolcevic *et al.*, "Cyclin-Dependent Kinase 16/PCTAIRE Kinase 1 Is Activated by Cyclin Y and Is Essential for Spermatogenesis," *Mol. Cell. Biol.*, vol. 32, no. 4, Feb. 2012.

[55] Besset V, Rhee K, and Wolgemuth DJ, "The cellular distribution and kinase activity of the Cdk family member Pctaire1 in the adult mouse brain and testis suggest functions in differentiation," *Cell Growth Differ.*, vol. 10, no. 3, pp. 173–181, Mar. 1999.

[56] K. Rhee and D. J. Wolgemuth, "Cdk family genes are expressed not only in

dividing but also in terminally differentiated mouse germ cells, suggesting their possible function during both cell division and differentiation," *Dev. Dyn.*, vol. 204, no. 4, Dec. 1995.

[57] Charrase S, Carena I, Hagmann J, Woods-Cook K, and Ferrari S, "PCTAIRE-1: characterization, subcellular distribution, and cell cycle-dependent kinase activity," *Cell Growth Differ.*, vol. 10, no. 9, pp. 611–620, Sep. 1999.

[58] T. Yang and J. Chen, "Identification and cellular localization of human PFTAIRE1," *Gene*, vol. 267, no. 2, Apr. 2001.

[59] M. Jiang, Y. Gao, T. Yang, X. Zhu, and J. Chen, "Cyclin Y, a novel membrane-associated cyclin, interacts with PFTK1," *FEBS Lett.*, vol. 583, no. 13, Jul. 2009.

[60] A. Asada, N. Yamamoto, M. Gohda, T. Saito, N. Hayashi, and S. Hisanaga, "Myristoylation of p39 and p35 is a determinant of cytoplasmic or nuclear localization of active cycline-dependent kinase 5 complexes," *J. Neurochem.*, vol. 106, no. 3, Aug. 2008.

[61] A. Z. Herskovits and P. Davies, "The regulation of tau phosphorylation by PCTAIRE 3: Implications for the pathogenesis of Alzheimer's disease," *Neurobiol. Dis.*, vol. 23, no. 2, Aug. 2006.

[62] T. Hirose, M. Kawabuchi, T. Tamaru, N. Okumura, K. Nagai, and M. Okada, "Identification of tudor repeat associator with PCTAIRE 2 (Trap)," *Eur. J. Biochem.*, vol. 267, no. 7, Apr. 2000.

[63] K. Cheng, Z. Li, W.-Y. Fu, J. H. Wang, A. K. Y. Fu, and N. Y. Ip, "Pctaire1 Interacts with p35 and Is a Novel Substrate for Cdk5/p35," *J. Biol. Chem.*, vol. 277, no. 35, Aug. 2002.

[64] S. N. Shehata *et al.*, "Analysis of substrate specificity and cyclin Y binding of PCTAIRE-1 kinase," *Cell. Signal.*, vol. 24, no. 11, Nov. 2012.

[65] Y. Gao, M. Jiang, T. Yang, J. Ni, and J. Chen, "A Cdc2-related protein kinase hPFTAIRE1 from human brain interacting with 14-3-3 proteins," *Cell Res.*, vol. 16, no. 6, Jun. 2006.

[66] S. Li, M. Jiang, W. Wang, and J. Chen, "14-3-3 Binding to Cyclin Y contributes to cyclin Y/CDK14 association," *Acta Biochim. Biophys. Sin. (Shanghai).*, vol. 46, no. 4, Apr. 2014.

[67] S. N. Shehata *et al.*, "Cyclin Y phosphorylation- and 14-3-3-binding-dependent activation of PCTAIRE-1/CDK16," *Biochem. J.*, vol. 469, no. 3, Aug. 2015.

[68] M. Dohmen *et al.*, "AMPK-dependent activation of the Cyclin Y/CDK16

complex controls autophagy," *Nat. Commun.*, vol. 11, no. 1, Dec. 2020.

[69] Grasser R, Gannon J, Poon RYC, Dubois T, Aitken A, and Hunt T, "Regulation of the CDK-related protein kinase PCTAIRE-1 and its possible role in neurite outgrowth in Neuro-2A cells," *J. Cell Sci.*, vol. 115, no. 17, pp. 3479–3490, Sep. 2002.

[70] F. Sladeczek, J. H. Camonis, A.-F. Burnol, and F. Le Bouffant, "The Cdk-like protein PCTAIRE-1 from mouse brain associates with p11 and 14-3-3 proteins," *Mol. Gen. Genet. MGG*, vol. 254, no. 5, May 1997.

[71] S. Matsuda *et al.*, "PCTAIRE Kinase 3/Cyclin-dependent Kinase 18 Is Activated through Association with Cyclin A and/or Phosphorylation by Protein Kinase A," *J. Biol. Chem.*, vol. 289, no. 26, Jun. 2014.

[72] A. R. Cole, "PCTK Proteins: The Forgotten Brain Kinases?," *Neurosignals*, vol. 17, no. 4, 2009.

[73] S. Li, W. Song, M. Jiang, L. Zeng, X. Zhu, and J. Chen, "Phosphorylation of cyclin Y by CDK14 induces its ubiquitination and degradation," *FEBS Lett.*, vol. 588, no. 11, May 2014.

[74] K. Sato *et al.*, "Regulation of membrane association and kinase activity of Cdk5–p35 by phosphorylation of p35," *J. Neurosci. Res.*, vol. 85, no. 14, Nov. 2007.

[75] G. N. Patrick, P. Zhou, Y. T. Kwon, P. M. Howley, and L.-H. Tsai, "p35, the Neuronal-specific Activator of Cyclin-dependent Kinase 5 (Cdk5) Is Degraded by the Ubiquitin-Proteasome Pathway," *J. Biol. Chem.*, vol. 273, no. 37, Sep. 1998.

[76] G. Davidson *et al.*, "Cell Cycle Control of Wnt Receptor Activation," *Dev. Cell*, vol. 17, no. 6, Dec. 2009.

[77] H. Clevers, "Wnt/β-Catenin Signaling in Development and Disease," *Cell*, vol. 127, no. 3, Nov. 2006.

[78] P. C. Salinas, "Retrograde signalling at the synapse: a role for Wnt proteins," *Biochem. Soc. Trans.*, vol. 33, no. 6, Dec. 2005.

[79] S. Benhamouche *et al.*, "Apc Tumor Suppressor Gene Is the 'Zonation-Keeper' of Mouse Liver," *Dev. Cell*, vol. 10, no. 6, Jun. 2006.

[80] S. Bahmanyar *et al.*, "Beta-Catenin is a Nek2 substrate involved in centrosome separation," *Genes Dev.*, vol. 22, no. 1, Jan. 2008.

[81] Z. You *et al.*, "Wnt signaling promotes oncogenic transformation by inhibiting c-Myc–induced apoptosis," *J. Cell Biol.*, vol. 157, no. 3, Apr. 2002.

[82] T. Zhan, N. Rindtorff, and M. Boutros, "Wnt signaling in cancer," *Oncogene*, vol. 36, no. 11, Mar. 2017.

[83] W.-Q. Fang *et al.*, "Cdk5-Mediated Phosphorylation of Axin Directs Axon Formation during Cerebral Cortex Development," *J. Neurosci.*, vol. 31, no. 38, Sep. 2011.

[84] Y. Wen *et al.*, "Interplay between Cyclin-Dependent Kinase 5 and Glycogen Synthase Kinase 3 Mediated by Neuregulin Signaling Leads to Differential Effects on Tau Phosphorylation and Amyloid Precursor Protein Processing," *J. Neurosci.*, vol. 28, no. 10, Mar. 2008.

[85] H.-M. Chow *et al.*, "CDK5 activator protein p25 preferentially binds and activates GSK3β," *Proc. Natl. Acad. Sci.*, vol. 111, no. 45, Nov. 2014.

[86] S. Kesavapany *et al.*, "p35/cdk5 binds and phosphorylates β-catenin and regulates β-catenin/presenilin-1 interaction," *Eur. J. Neurosci.*, vol. 13, no. 2, Jan. 2001.

[87] S. Hernández-Ortega *et al.*, "Phosphoregulation of the oncogenic protein regulator of cytokinesis 1 (PRC1) by the atypical CDK16/CCNY complex," *Exp. Mol. Med.*, vol. 51, no. 4, Apr. 2019.

[88] M. Leonardi, E. Perna, S. Tronnolone, D. Colecchia, and M. Chiariello, "Activated kinase screening identifies the IKBKE oncogene as a positive regulator of autophagy," *Autophagy*, vol. 15, no. 2, Feb. 2019.

[89] A. S. L. Wong *et al.*, "Cdk5-mediated phosphorylation of endophilin B1 is required for induced autophagy in models of Parkinson's disease," *Nat. Cell Biol.*, vol. 13, no. 5, May 2011.

[90] W.-Y. Fu, K. Cheng, A. K. Y. Fu, and N. Y. Ip, "Cyclin-dependent kinase 5-dependent phosphorylation of Pctaire1 regulates dendrite development," *Neuroscience*, vol. 180, Apr. 2011.

[91] M. H. Mokalled, A. Johnson, Y. Kim, J. Oh, and E. N. Olson, "Myocardin-related transcription factors regulate the Cdk5/Pctaire1 kinase cascade to control neurite outgrowth, neuronal migration and brain development," *Development*, vol. 137, no. 14, Jul. 2010.

[92] S. N. Shehata *et al.*, "Identification of novel PCTAIRE-1/CDK16 substrates using a chemical genetic screen," *Cell. Signal.*, vol. 59, Jul. 2019.

[93] H. Hu *et al.*, "X-exome sequencing of 405 unresolved families identifies seven novel intellectual disability genes," *Mol. Psychiatry*, vol. 21, no. 1, Jan. 2016.

[94] F. Le Bouffant, J. Capdevielle, J.-C. Guillemot, and F. Sladeczek, "Characterization of brain PCTAIRE-1 kinase immunoreactivity and its interactions with p11 and 14-3-3 proteins," *Eur. J. Biochem.*, vol. 257, no. 1, Oct. 1998.

[95] Y. Liu, K. Cheng, K. Gong, A. K. Y. Fu, and N. Y. Ip, "Pctaire1 phosphorylates N-ethylmaleimide-sensitive fusion protein: Implications in the regulation of its hexamerization and exocytosis," *J. Biol. Chem.*, vol. 281, no. 15, pp. 9852–9858, 2006.

[96] K. J. Palmer, "PCTAIRE protein kinases interact directly with the COPII complex and modulate secretory cargo transport," *J. Cell Sci.*, vol. 118, no. 17, Sep. 2005.

[97] X. Tang *et al.*, "An RNA interference-based screen identifies MAP4K4/NIK as a negative regulator of PPARγ, adipogenesis, and insulin-responsive hexose transport," *Proc. Natl. Acad. Sci.*, vol. 103, no. 7, Feb. 2006.

[98] A. Dema *et al.*, "Cyclin-Dependent Kinase 18 Controls Trafficking of Aquaporin-2 and Its Abundance through Ubiquitin Ligase STUB1, Which Functions as an AKAP," *Cells*, vol. 9, no. 3, Mar. 2020.

[99] R. Dhavan and L.-H. Tsai, "A decade of CDK5," *Nat. Rev. Mol. Cell Biol.*, vol. 2, no. 10, Oct. 2001.

[100] N. Cortés, L. Guzmán-Martínez, V. Andrade, A. González, and R. B. Maccioni, "CDK5: A Unique CDK and Its Multiple Roles in the Nervous System," *J. Alzheimer's Dis.*, vol. 68, no. 3, Apr. 2019.

[101] A. Brenna *et al.*, "Cyclin-dependent kinase 5 (CDK5) regulates the circadian clock," *Elife*, vol. 8, Nov. 2019.

[102] K. Shimizu, A. Uematsu, Y. Imai, and T. Sawasaki, "Pctaire1/Cdk16 promotes skeletal myogenesis by inducing myoblast migration and fusion," *FEBS Lett.*, vol. 588, no. 17, Aug. 2014.

[103] Y. Pan *et al.*, "Cyclin-dependent Kinase 18 Promotes Oligodendrocyte Precursor Cell Differentiation through Activating the Extracellular Signal-Regulated Kinase Signaling Pathway," *Neurosci. Bull.*, vol. 35, no. 5, Oct. 2019.

[104] D. Chaput, L. Kirouac, S. M. Stevens, and J. Padmanabhan, "Potential role of PCTAIRE-2, PCTAIRE-3 and P-Histone H4 in amyloid precursor protein-dependent Alzheimer pathology," *Oncotarget*, vol. 7, no. 8, Feb. 2016.

[105] F. Le Bouffant, P. Le Minter, E. Traiffort, M. Ruat, and F. Sladeczek, "Multiple

Subcellular Localizations of PCTAIRE-1 in Brain," *Mol. Cell. Neurosci.*, vol. 16, no. 4, Oct. 2000.

[106] F. Shu *et al.*, "Functional characterization of human PFTK1 as a cyclin-dependent kinase," *Proc. Natl. Acad. Sci.*, vol. 104, no. 22, May 2007.

[107] J.-F. Rual *et al.*, "Towards a proteome-scale map of the human protein–protein interaction network," *Nature*, vol. 437, no. 7062, Oct. 2005.

[108] Z. Zi *et al.*, "CCNYL1, but Not CCNY, Cooperates with CDK16 to Regulate Spermatogenesis in Mouse," *PLOS Genet.*, vol. 11, no. 8, Aug. 2015.

[109] S. Koch, S. P. Acebron, J. Herbst, G. Hatiboglu, and C. Niehrs, "Post-transcriptional Wnt Signaling Governs Epididymal Sperm Maturation," *Cell*, vol. 163, no. 5, Nov. 2015.

[110] L. Zeng *et al.*, "Essential Roles of Cyclin Y-Like 1 and Cyclin Y in Dividing Wnt-Responsive Mammary Stem/Progenitor Cells," *PLOS Genet.*, vol. 12, no. 5, May 2016.

[111] W. An, Z. Zhang, L. Zeng, Y. Yang, X. Zhu, and J. Wu, "Cyclin Y Is Involved in the Regulation of Adipogenesis and Lipid Production," *PLoS One*, vol. 10, no. 7, Jul. 2015.

[112] T. Tanaka *et al.*, "Neuronal Cyclin-Dependent Kinase 5 Activity Is Critical for Survival," *J. Neurosci.*, vol. 21, no. 2, Jan. 2001.

[113] A. Kumazawa *et al.*, "Cyclin-dependent kinase 5 is required for normal cerebellar development," *Mol. Cell. Neurosci.*, vol. 52, Jan. 2013.

[114] Y. Yang *et al.*, "Cyclin dependent kinase 5 is required for the normal development of oligodendrocytes and myelin formation," *Dev. Biol.*, vol. 378, no. 2, Jun. 2013.

[115] F. M. Ferguson *et al.*, "Discovery of Covalent CDK14 Inhibitors with Pan-TAIRE Family Specificity," *Cell Chem. Biol.*, vol. 26, no. 6, Jun. 2019.

[116] S. E. Dixon-Clarke *et al.*, "Structure and inhibitor specificity of the PCTAIRE-family kinase CDK16," *Biochem. J.*, vol. 474, no. 5, Mar. 2017.

[117] A. A. Antolin, M. Ameratunga, U. Banerji, P. A. Clarke, P. Workman, and B. Al-Lazikani, "The kinase polypharmacology landscape of clinical PARP inhibitors," *Sci. Rep.*, vol. 10, no. 1, Dec. 2020.

[118] R. Charmet *et al.*, "Novel risk genes identified in a genome-wide association study for coronary artery disease in patients with type 1 diabetes," *Cardiovasc. Diabetol.*, vol. 17, no. 1, Dec. 2018.

[119] E. Y.-T. Pang *et al.*, "Identification of PFTAIRE protein kinase 1, a novel cell division cycle-2 related gene, in the motile phenotype of hepatocellular carcinoma cells," *Hepatology*, vol. 46, no. 2, Aug. 2007.

[120] W. K. C. Leung *et al.*, "A novel interplay between oncogenic PFTK1 protein kinase and tumor suppressor TAGLN2 in the control of liver cancer cell motility," *Oncogene*, vol. 30, no. 44, Nov. 2011.

[121] S. Matsuda, K. Kawamoto, K. Miyamoto, A. Tsuji, and K. Yuasa, "PCTK3/CDK18 regulates cell migration and adhesion by negatively modulating FAK activity," *Sci. Rep.*, vol. 7, no. 1, Apr. 2017.

[122] W. K. C. Leung, A. K. K. Ching, and N. Wong, "Phosphorylation of Caldesmon by PFTAIRE1 kinase promotes actin binding and formation of stress fibers," *Mol. Cell. Biochem.*, vol. 350, no. 1–2, Apr. 2011.

[123] L. Yang *et al.*, "PFTK1 Promotes Gastric Cancer Progression by Regulating Proliferation, Migration and Invasion," *PLoS One*, vol. 10, no. 10, Oct. 2015.

[124] S. Li, X. Dai, K. Gong, K. Song, F. Tai, and J. Shi, "PA28α/β Promote Breast Cancer Cell Invasion and Metastasis via Down-Regulation of CDK15," *Front. Oncol.*, vol. 9, Nov. 2019.

[125] M. H. Park, S. Y. Kim, Y. J. Kim, and Y.-H. Chung, "ALS2CR7 (CDK15) attenuates TRAIL induced apoptosis by inducing phosphorylation of survivin Thr34," *Biochem. Biophys. Res. Commun.*, vol. 450, no. 1, Jul. 2014.

[126] T. Yanagi, R. Shi, P. Aza-Blanc, J. C. Reed, and S. Matsuzawa, "PCTAIRE1-Knockdown Sensitizes Cancer Cells to TNF Family Cytokines," *PLoS One*, vol. 10, no. 3, Mar. 2015.

[127] S. Bhalla, H. Kaur, A. Dhall, and G. P. S. Raghava, "Prediction and Analysis of Skin Cancer Progression using Genomics Profiles of Patients," *Sci. Rep.*, vol. 9, no. 1, Dec. 2019.

[128] M. Phadke *et al.*, "Dabrafenib inhibits the growth of BRAF-WT cancers through CDK16 and NEK9 inhibition," *Mol. Oncol.*, vol. 12, no. 1, Jan. 2018.

[129] T. Yanagi, M. Krajewska, S. Matsuzawa, and J. C. Reed, "PCTAIRE1 Phosphorylates p27 and Regulates Mitosis in Cancer Cells," *Cancer Res.*, vol. 74, no. 20, Oct. 2014.

[130] T. Yanagi, J. C. Reed, and S. Matsuzawa, "PCTAIRE1 regulates p27 stability, apoptosis and tumor growth in malignant melanoma," *Oncoscience*, vol. 1, no. 10, Oct. 2014.

[131] J. Xie *et al.*, "CDK16 Phosphorylates and Degrades p53 to Promote Radioresistance and Predicts Prognosis in Lung Cancer," *Theranostics*, vol. 8, no. 3, 2018.

[132] J. W.-C. CHANG *et al.*, "Transcriptomic Analysis in Liquid Biopsy Identifies Circulating PCTAIRE-1 mRNA as a Biomarker in NSCLC," *Cancer Genomics - Proteomics*, vol. 17, no. 1, Dec. 2020.

[133] J. Xie *et al.*, "CDK16 Phosphorylates and Degrades p53 to Promote Radioresistance and Predicts Prognosis in Lung Cancer," *Theranostics*, vol. 8, no. 3, pp. 650–662, 2018.

[134] G. Barone *et al.*, "The relationship of CDK18 expression in breast cancer to clinicopathological parameters and therapeutic response," *Oncotarget*, vol. 9, no. 50, Jun. 2018.

[135] U. Naumann *et al.*, "PCTAIRE3: a putative mediator of growth arrest and death induced by CTS-1, a dominant-positive p53-derived synthetic tumor suppressor, in human malignant glioma cells," *Cancer Gene Ther.*, vol. 13, no. 5, May 2006.

[136] G. Barone *et al.*, "Human CDK18 promotes replication stress signaling and genome stability," *Nucleic Acids Res.*, vol. 44, no. 18, Oct. 2016.

[137] J.-F. Ning *et al.*, "Myc targeted CDK18 promotes ATR and homologous recombination to mediate PARP inhibitor resistance in glioblastoma," *Nat. Commun.*, vol. 10, no. 1, Dec. 2019.

[138] P. Ćwiek *et al.*, "RNA interference screening identifies a novel role for PCTK1/CDK16 in medulloblastoma with c-Myc amplification," *Oncotarget*, vol. 6, no. 1, Jan. 2015.

[139] K. Labun, T. G. Montague, M. Krause, Y. N. Torres Cleuren, H. Tjeldnes, and E. Valen, "CHOPCHOP v3: expanding the CRISPR web toolbox beyond genome editing," *Nucleic Acids Res.*, vol. 47, no. W1, Jul. 2019.

[140] L. Vouillot, A. Thélie, and N. Pollet, "Comparison of T7E1 and Surveyor Mismatch Cleavage Assays to Detect Mutations Triggered by Engineered Nucleases," *G3 Genes|Genomes|Genetics*, vol. 5, no. 3, Mar. 2015.

[141] O. Menyhárt, Á. Nagy, and B. Győrffy, "Determining consistent prognostic biomarkers of overall survival and vascular invasion in hepatocellular carcinoma," *R. Soc. Open Sci.*, vol. 5, no. 12, Dec. 2018.

[142] E. Y. Chen *et al.*, "Enrichr: interactive and collaborative HTML5 gene list enrichment analysis tool," *BMC Bioinformatics*, vol. 14, no. 1, 2013.

[143] D. W. Huang, B. T. Sherman, and R. A. Lempicki, "Systematic and integrative analysis of large gene lists using DAVID bioinformatics resources," *Nat. Protoc.*, vol. 4, no. 1, Jan. 2009.

[144] D. W. Huang, B. T. Sherman, and R. A. Lempicki, "Bioinformatics enrichment tools: paths toward the comprehensive functional analysis of large gene lists," *Nucleic Acids Res.*, vol. 37, no. 1, Jan. 2009.

[145] X. Chen and D. F. Calvisi, "Hydrodynamic Transfection for Generation of Novel Mouse Models for Liver Cancer Research," *Am. J. Pathol.*, vol. 184, no. 4, Apr. 2014.

[146] E. Cerami *et al.*, "The cBio Cancer Genomics Portal: An Open Platform for Exploring Multidimensional Cancer Genomics Data: Figure 1.," *Cancer Discov.*, vol. 2, no. 5, May 2012.

[147] J. Gao *et al.*, "Integrative Analysis of Complex Cancer Genomics and Clinical Profiles Using the cBioPortal," *Sci. Signal.*, vol. 6, no. 269, Apr. 2013.

[148] H. J. Melichar *et al.*, "Regulation of γδ Versus αß T Lymphocyte Differentiation by the Transcription Factor SOX13," *Science (80-.).*, vol. 315, no. 5809, Jan. 2007.

[149] Y. Zhou *et al.*, "Metascape provides a biologist-oriented resource for the analysis of systems-level datasets," *Nat. Commun.*, vol. 10, no. 1, Dec. 2019.

[150] L. García-Gutiérrez, M. D. Delgado, and J. León, "MYC Oncogene Contributions to Release of Cell Cycle Brakes," *Genes (Basel).*, vol. 10, no. 3, Mar. 2019.

[151] M. Wanzel, S. Herold, and M. Eilers, "Transcriptional repression by Myc," *Trends Cell Biol.*, vol. 13, no. 3, Mar. 2003.

[152] A. L. Gartel and K. Shchors, "Mechanisms of c-myc-mediated transcriptional repression of growth arrest genes," *Exp. Cell Res.*, vol. 283, no. 1, Feb. 2003.

[153] A. L. Gartel *et al.*, "Myc represses the p21(WAF1/CIP1) promoter and interacts with Sp1/Sp3," *Proc. Natl. Acad. Sci.*, vol. 98, no. 8, Apr. 2001.

[154] H. Liu *et al.*, "Transcriptional regulation of BRD7 expression by Sp1 and c-Myc," *BMC Mol. Biol.*, vol. 9, no. 1, 2008.

[155] K. Beishline and J. Azizkhan-Clifford, "Sp1 and the 'hallmarks of cancer,'" *FEBS J.*, vol. 282, no. 2, Jan. 2015.

[156] A. Kazi *et al.*, "GSK3 suppression upregulates β-catenin and c-Myc to abrogate KRas-dependent tumors," *Nat. Commun.*, vol. 9, no. 1, Dec. 2018.

[157] J. L. Dean, A. K. McClendon, and E. S. Knudsen, "Modification of the DNA Damage Response by Therapeutic CDK4/6 Inhibition," *J. Biol. Chem.*, vol. 287, no. 34, Aug. 2012.

[158] P. H. Huang, R. Cook, G. Zoumpoulidou, M. T. Luczynski, and S. Mittnacht, "Retinoblastoma family proteins: New players in DNA repair by non-homologous end-joining," *Mol. Cell. Oncol.*, vol. 3, no. 2, Mar. 2016.

[159] X. Pei, E. Du, Z. Sheng, and W. Du, "Rb family-independent activating E2F increases genome stability, promotes homologous recombination, and decreases non-homologous end joining," *Mech. Dev.*, vol. 162, Jun. 2020.

[160] J. Hartke, M. Johnson, and M. Ghabril, "The diagnosis and treatment of hepatocellular carcinoma," *Semin. Diagn. Pathol.*, vol. 34, no. 2, Mar. 2017.

[161] A. Suriawinata and S. N. Thung, "Molecular Signature of Early Hepatocellular Carcinoma," *Oncology*, vol. 78, no. 1, 2010.

[162] N. Ganne-Carrié and P. Nahon, "Hepatocellular carcinoma in the setting of alcohol-related liver disease," *J. Hepatol.*, vol. 70, no. 2, Feb. 2019.

[163] N. M. Kettner *et al.*, "Circadian Homeostasis of Liver Metabolism Suppresses Hepatocarcinogenesis," *Cancer Cell*, vol. 30, no. 6, Dec. 2016.

[164] M.-F. Yuen, P.-C. Wu, V. C.-H. Lai, J. Y.-N. Lau, and C.-L. Lai, "Expression of c-Myc, c-Fos, and c-Jun in hepatocellular carcinoma," *Cancer*, vol. 91, no. 1, Jan. 2001.

[165] C.-P. Lin, C.-R. Liu, C.-N. Lee, T.-S. Chan, and H. E. Liu, "Targeting c-Myc as a novel approach for hepatocellular carcinoma," *World J. Hepatol.*, vol. 2, no. 1, 2010.

[166] S. P. Monga, "β-Catenin Signaling and Roles in Liver Homeostasis, Injury, and Tumorigenesis," *Gastroenterology*, vol. 148, no. 7, Jun. 2015.

[167] D. Huang, H. Friesen, and B. Andrews, "Pho85, a multifunctional cyclin-dependent protein kinase in budding yeast," *Mol. Microbiol.*, vol. 66, no. 2, Oct. 2007.

[168] S. Sharma and P. Sicinski, "A kinase of many talents: non-neuronal functions of CDK5 in development and disease," *Open Biol.*, vol. 10, no. 1, Jan. 2020.

[169] A. Kurosawa *et al.*, "DNA Ligase IV and Artemis Act Cooperatively to Suppress Homologous Recombination in Human Cells: Implications for DNA Double-Strand Break Repair," *PLoS One*, vol. 8, no. 8, Aug. 2013.

[170] J. H. Patel and S. B. McMahon, "Targeting of Miz-1 Is Essential for Myc-

mediated Apoptosis," *J. Biol. Chem.*, vol. 281, no. 6, Feb. 2006.

[171] M. Bédard, L. Maltais, M. Montagne, and P. Lavigne, "Miz-1 and Max compete to engage c-Myc: implication for the mechanism of inhibition of c-Myc transcriptional activity by Miz-1," *Proteins Struct. Funct. Bioinforma.*, vol. 85, no. 2, Feb. 2017.

[172] H. K. Arnold *et al.*, "The Axin1 scaffold protein promotes formation of a degradation complex for c-Myc," *EMBO J.*, vol. 28, no. 5, Mar. 2009.

[173] R. Sears, "Multiple Ras-dependent phosphorylation pathways regulate Myc protein stability," *Genes Dev.*, vol. 14, no. 19, Oct. 2000.

[174] H. K. Arnold and R. C. Sears, "Protein Phosphatase 2A Regulatory Subunit B56α Associates with c-Myc and Negatively Regulates c-Myc Accumulation," *Mol. Cell. Biol.*, vol. 26, no. 7, Apr. 2006.

[175] H. K. Arnold and R. C. Sears, "A tumor suppressor role for PP2A-B56α through negative regulation of c-Myc and other key oncoproteins," *Cancer Metastasis Rev.*, vol. 27, no. 2, Jun. 2008.

[176] L. A. Serebryannyy, A. Yemelyanov, C. J. Gottardi, and P. de Lanerolle, "Nuclear α-catenin mediates the DNA damage response via β-catenin and nuclear actin," *J. Cell Sci.*, vol. 130, no. 10, May 2017.

[177] A. Karimaian, M. Majidinia, H. Bannazadeh Baghi, and B. Yousefi, "The crosstalk between Wnt/β-catenin signaling pathway with DNA damage response and oxidative stress: Implications in cancer therapy," *DNA Repair (Amst).*, vol. 51, Mar. 2017.

[178] E. Sadot *et al.*, "Regulation of S33/S37 phosphorylated β-catenin in normal and transformed cells," *J. Cell Sci.*, vol. 115, no. 13, Jul. 2002.

[179] J. P. Muñoz, C. H. Huichalaf, D. Orellana, and R. B. Maccioni, "cdk5 modulates β- and δ-catenin/Pin1 interactions in neuronal cells," *J. Cell. Biochem.*, vol. 100, no. 3, Feb. 2007.

[180] J. Bollard *et al.*, "Palbociclib (PD-0332991), a selective CDK4/6 inhibitor, restricts tumour growth in preclinical models of hepatocellular carcinoma," *Gut*, vol. 66, no. 7, Jul. 2017.

Annex

Annex 1.1

List of publications (2016-2021)

1. **D. Martínez-Alonso** and M. Malumbres, "Mammalian cell cycle cyclins," *Semin. Cell Dev. Biol.*, vol. 107, Nov. 2020.
2. **D. Martínez-Alonso**, L.R. López, S. Wakahashi, J. González-Martínez, G. de Cárcer, S. Ortega, J. Muñoz, N.S. Gray, A. Lujambio, M. Malumbres. "CDK14-18 inhibition suppresses hepatocellular carcinoma progression through cooperative alterations in WNT and DNA repair signaling''. *Manuscript in preparation*. 2021.
3. J. González-Martínez, A.W. Cwetsch, **D. Martínez-Alonso**, L.R. López-Sainz, J. Almagro, J. Gómez, M. Pérez, D. Megías, J. Boskovic, J. Gilabert-Juan, O. Graña-Castro, A. Pierani, S. Ortega and M. Malumbres. ''Deficient adaptation to centrosome duplication defects as a cause of microcephaly and subcortical heterotopias''. *Under revision in JCI insight*. 2021
4. B. Sanz-Castillo, B. Hurtado, A. El Bakkali, D. Hermida, B. Salvador-Barbero, **D. Martínez-Alonso**, J. González-Martínez, C. Santiveri, R. Campos-Olivas, P. Ximénez, J. Muñoz, M. Álvarez-Fernández, M. Malumbres. "A cell cycle kinase-phosphatase module restrains PI3K-Akt activity in an mTORC1 dependent manner", *bioRxiv*. Nov 2020. *Under revision in Mol. Cell.*

Annex 1.2

Disclaimer

Cover page credit:

Image of Barcelona city map was obtained from Reddit social media. It was originally posted by ''daniskarma'' user in ''r/dataisbeautiful'' as original content, for which I acknowledge here its creator.

This image has not been used with professional purposes here or anywhere else. This image has been used with artistical purposes in the present thesis manuscript. I properly informed its creator for this usage.

Cover page was designed by Ana Sánchez Martínez

contact: ana20sanmar@gmail.com.